IDENTIFICATION AND CHARACTERIZATION OF A NOVEL TRANSCRIPTION FACTOR THAT REGULATES *NCF2* EXPRESSION VIA THE TNF-α RESPONSIVE REGION

by

Mary Cloud Bosworth Ammons Anderson

A dissertation submitted in partial fulfillment
of the requirements for the degree

of

Doctor of Philosophy

In

Veterinary Molecular Biology

MONTANA STATE UNIVERSITY
Bozeman, Montana

November 2007

APPROVAL

of a dissertation submitted by

Mary Cloud Bosworth Ammons Anderson

This dissertation has been read by each member of the dissertation committee and has been found to be satisfactory regarding content, English usage, format, citations, bibliographic style, and consistency, and is ready for submission to the Division of Graduate Education.

Approved for the Department of Veterinary Molecular Biology

Dr. Mark T. Quinn

Approved for the Division of Graduate Education

Dr. Carl A. Fox

STATEMENT OF PERMISSION TO USE

In presenting this dissertation in partial fulfillment of the requirements for a doctoral degree at Montana State University-Bozeman, I agree that the Library shall make it available to borrowers under the rules of the Library. I further agree that copying of this dissertation is allowable only for scholarly purposes, consistent with "fair use" as prescribed in the U.S. Copyright Law. Requests for extensive copying or reproduction of this dissertation should be referred to ProQuest Information and Learning, 300 North Zeeb Road, Ann Arbor, Michigan 48106, to whom I have granted "the exclusive right to reproduce and distribute my dissertation in and from microfilm along with the non-exclusive right to reproduce and distribute my abstract in any format in whole or in part."

Mary Cloud Bosworth Ammons Anderson

November 2007

ACKNOWLEDGEMENTS

I would first and foremost like to thank my parents. All the fundamentally valuable characteristics that have carried me through the process of my doctoral work were planted by my parents in each of us kids from the very first. I would like to thank them for never saying I could not do anything to which I put my mind. I would like to thank them for teaching me patience, humility, and, above all, intellectual curiosity. Without their solid foundation I would never have reached this goal.

I would also like to thank my advisor Dr. Mark Quinn for giving me the opportunity to pursue my doctorate in his lab. Although guidance and support from Dr. Quinn was essential to my success, I am also grateful for his help in cultivating my intellectual independence and personal self-reliance. I would also like to thank the Quinn lab regulars who provided not only vital technical guidance, but also moral support and an indisspensible sense of humor.

Thanks are due to my committee who always sought to challenge me to greater scientific analysis and creativity. I would especially like to thank Dr. Kathrine Gauss, an exceptional scientific purist, for not only guiding me through my doctoral work, but also for being a friend when I needed it.

Finally, I must thank my husband Brock, to whom I could always come home and count on being met at the door with infinite sanity.

TABLE OF CONTENTS

TABLE OF CONTENTS (CONTINUED)

TABLE OF CONTENTS (CONTINUED)

LIST OF TABLES

LIST OF FIGURES

LIST OF FIGURES (CONTINUED)

Figure Page

LIST OF FIGURES (CONTINUED)

ABSTRACT

The multicomponent NADPH oxidase is an essential enzyme complex found in professional phagocytic cells that mediates innate immune defence against multiple pathogens through the production of reactive oxygen species. The vital and functionally limiting cytosolic component of the NADPH oxidase, $p67^{phox}$, is transcriptionally regulated by TNF-α at the TNF-α Responsive Region (TRR) in the intragenic region of *Neutrophil Cytosolic Factor 2* (*NCF2*), the gene which codes for $p67^{phox}$. The aim of this dissertation is to identify and charaterize the factor(s) that binds the TRR and regulates *NCF2* expression in response to TNF-α. Using the TRR as bait in a yeast one-hybrid screen, we identified Pleomorphic Adenoma Gene-Like 2 (PLAGL2) as a candidate regulator of *NCF2* expression. *In vitro* and *in vivo* analysis confirmed that PLAGL2 binds to the TRR in *NCF2* and that endogenous PLAGL2 binding is enhanced in the presence of TNF-α. Knock-down of endogenous PLAGL2 expression inhibited TNF-α-mediated *NCF2* expression, $p67^{phox}$ expression, and subsequent superoxide production. Characterization of PLAGL2 binding to the *NCF2* TRR identified the essential core sequence which is recognized by zinc fingers six and seven of PLAGL2. Using PLAGL2 as bait in a yeast two-hybrid screen, we identified ubiquitin protein ligase (E2I), positive cofactor 2 (PC2,) four and a half LIM domain 3 (FHL3), and chromodomain helicase DNA binding protein 3 (CHD3) as putative PLAGL2 binding partners. *In vitro* and *in vivo* analysis confirmed that PLAGL2 binds $PC2_{434\text{-}748}$, FHL3, and CHD3 via interactions mediated through unique and overlapping domains of PLAGL2. In conclusion, we have identified a novel regulator of *NCF2* transcription and have further characterized the features of PLAGL2 binding and recognition of the TRR sequence in the intragenic region of *NCF2*. Finally, through identification of PLAGL2 binding partners, we have begun to determine a model by which PLAGL2 regulates transcription in a context dependent manner.

PROFESSIONAL PHAGOCYTES AND THE NADPH OXIDASE

Professional Phagocytes and the Innate Immune System

Polymorphonuclear and Mononuclear Professional Phagocytes

The innate immune system is evolutionarily conserved and represents the first responders of the immune system. The cells of the innate immune system are able to defend the host against pathogens ranging from bacteria to viruses to fungi, and mediate an inflammatory response for quick killing and clearance of many infections. Additionally, the innate immune system appears to mediate the subsequent activation of the adaptive immune response [1]. Professional phagocytes, including neutrophils, monocytes, and macrophages, represent the defensive cells of the immune system that use phagocytosis to defend against invasive pathogens. These cells are critical to the inflammatory response. Although phagocytes possess a number of anti-pathogenic mechanisms, all phagocytes utilize their ability to engulf and destroy pathogens in host defense. Phagocytosis is also perfomed by non-professional phagocytes such as endothelial and epithelial cells [2].

Granulocytes are a type of white blood cell characterized by the presence of cytoplasmic granules. Neutrophils are professional phagocytic granulocytes whose main physiologic and pathogenic activities include adherence, degranulation and release of inflammatory mediators, and phagocytosis (reviewed in [3]). The most abundant of the professional phagocytes, neutrophils circulate at a concentration ten to twenty times that of monocytes and represent about ninety-five percent of the total body granulocytes. At the site of inflammation, neutrophils are the first innate immune cell recruited and

predominate in their response over monocytes; however, neutrophils also have a very short lifespan. By six to eight hours, most circulating neutrophils are destroyed, and isolated neutrophils can be expected to live only about twenty-four hours in culture [4]. Indeed, over 10^{11} neutrophils are removed from the body every day, primarily through apoptosis [5]. Activation of the neutrophil also activates programmed cell death though apoptosis. This short lifespan is likely the primary means of regulating these hyperactive immune cells, and multiple extracellular agents such as cytokines can determine not only whether a neutrophil will be activated and mature, but also whether a neutrophil survives or undergoes apoptosis. Furthermore, pathogens can capitalize on neutrophil apoptosis to evade the immune system. For example, when *Leishmania major* infects neutrophils, the pathogen uses phophatidylserine externalization, which is recognized by phagocytosing macrophages. *Leishmania major* is then able to infect invade their primary host cell, the macrophage [6]. Finally, recent work studying programmed cell death in neutrophils identified another anti-microbial mechanismin which cell death results in the formation of extra cellular traps that capture and kill microorganisms [7].

Phagocytosis is one of the primary means by which neutrophils exert their antimicrobial and antifungal effect on invading pathogens, however the antimicrobial content in granules also play an essential role in immune defense. Phagocyte anti-pathogenic efficiency depends on both the generation of reactive oxygen species via the assembly and activation of the nicotinamide adenine dinucleotide phosphate-oxidase (NADPH oxidase) and the release of anti-microbial factors stored in cytoplasmic granules. There are three types of cytoplasmic granules found in neutrophils (reviewed in [8]). The first type, called specific or secondary granules, contain lactoferrin enzyme and

cathelicidin peptide. The second type, called the azurophilic or primary granules, contain myeloperoxidase, bactericidal/permeability increasing protein, defensins, and the serine proteases neutrophil elastase and cathepsin G. The third type, called the tertiary granules, contain cathepsin and gelatinase. These two means of immune defense are interrelated, as the neutrophil phagosome acquires its antimicrobial effects through fusion with secretory vesicles and granules. The secretory vesicles carry the intracellular, membrane-attached components of the NADPH oxidase. In order for the phagosome to completely mature, acidification must occur on the luminal side [9], although the neutrophil phagosome is initially alkaline before becoming acidic. This is in contrast to the phagosome of the macrophage, indicating that the environment and hence the activity of the neutrophil phagosome may have unique functions from that of the macrophage phagosome.

Although they constitute only about five to ten percent of the peripheral blood leukocytes, monocytes play a key role in innate immunity. Monocytes/macrophages are derived of a common myeloid precursor as neutrophils in the bone marrow [10], and monocytes/macrophages exhibit much greater heterogeneity in form and function [11] (Figure 1.1). Whereas the primary function of phagocytosis in neutrophils is immune clearance of pathogens or infected cells, monocytes and the more differentiated macrophages utilize phagocytosis for a variety of functions. Monocytes primarily remain in the circulation until proinflammatory, metabolic, and/or immune stimuli recruit them to peripheral sites where they differentiate into macrophages or dendritic cells [12] (Figure 1.1).

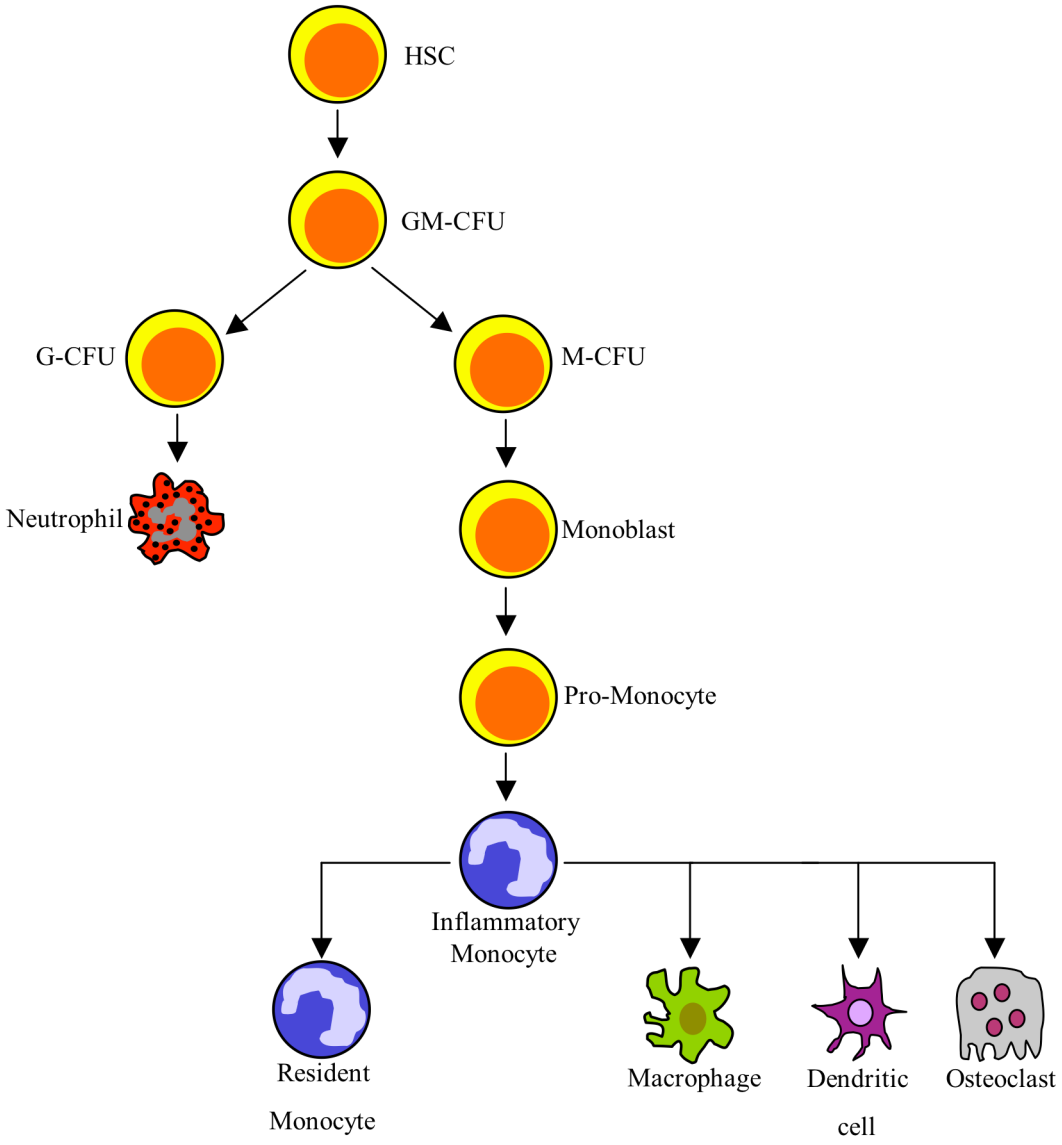

Figure 1.1: Schematic of phagocytic cell differentiation. Although generated from a common myeloid precursor, heterogeneity among cell types is demonstrated through context dependent cell differentiation into specific capacities. Acronyms of cells identified are as follows: haematopoietic stem cell (HSC), granulocyte/macrophage colony forming unit (GM-CFU), macrophage colony-forming unit (M-CFU), and granulocyte colony-forming unit (G-CFU). Adapted from Reference [11].

The observed heterogeneity of tissue macrophages demonstrates the various functions in which macrophages have specialized phagocytosis. For example, osteoclasts use phagocytosis to continually remodel bone tissue [13], and alveolar macrophages clear microorganisms, viruses, and environmental particles by phagocytosis [14-16]. As an essential component of autoimmunity regulation, thymic macrophages in germinal centers use phagocytosis to clear apoptotic lymphocytes [17]. Finally, macrophages are important antigen presenting cells and thus mediate pathogen killing both directly through phagocytosis and indirectly by mediating the adaptive immune response.

Primary Defects in Professional Phagocytes

Although primary defects in professional phagocytes are uncommon in the general population, they are typified by severity of infection and require aggressive, life-long management. Neutropenia is characterized by low neutrophil counts of less then 1000 neutrophils per microliter and can range from moderate to severe. Reduced numbers of neutrophils can result from a myriad of causes such as drug effects, infection, autoimmunity, congenital disorders, and malignancy [18]. Examples of primary neutrophil disorders associated with neutropenia include Chediak-Higashi syndrome [19] and glycogen storage disease type Ib [20] and are characterized by chronic infections.

More common than neutropenia are primary disorders of neutrophils that result in functional abnormalities. Chronic granulomatous disease (CGD) is a functional disorder of neutrophils resulting from the inability to produce superoxide and presenting clinically as chronic bacterial and fungal infections [21]. Other diseases of neutrophil function include leukocyte adhesion deficiency (LAD), myeloperoxidase deficiency, specific

granule deficiency, Papillon-Lefevre syndrome, Gaucher's disease, and Hyper-IgE syndrome, and all result in multiple clinical pathologies dominated by susceptibility to infection [22].

Known primary defects in macrophages predominantly result in functional defects of intracellular pathogen killing. Commonly referred to as disorders with Mendelian susceptibility to mycobacteria because they present with mycobacterial infections in offspring with a Mendelian pattern of inheritance, infection with this pathogen dominates defects of macrophage function. Indeed, NADPH oxidase defects in monocytes/macrophages of chronic granulomatous disease patients result in a predisposition for mycobacterial infection in macrophages [23] and the characteristic granulomas of CGD consist primarily of monocytes and macrophages with phagocytosed, but intact bacteria [21]. Other macrophage disorders with mycobacterial susceptibility include anhidrotic ectodermal dysplasia with immunodeficiency (EDA-ID), defects in the gamma interferon receptor complex, defects in signal transducer and activator of transcription 1 (STAT1), and defects in interleukin-12 (IL-12) and its receptor [22].

Inflammatory Disorders and Professional Phagocytes

There is also a growing body of evidence that professional phagocytes play an important role in mediating multiple inflammatory disorders. In this case, it is likely that the innate immune cells are themselves functioning correctly with an inappropriate response. The damage to the host may result in potential agitation of a secondary pathology. Pathology associated with chronic granulomatous disease indicates that

aberrant regulation of inflammation also contributes to the clinical aspects of this disease. For example, when CGD mice (lacking a functional phagocytic oxidase) were infected with *Aspergillus fumigatus*, clinical manifestations included not only impaired microbial killing, but also abnormalities in the inflammatory response [24]. Resolution of inflammation requires efficient clearance of apoptotic neutrophils, a process that is impaired in patients with chronic granulomatous disease (CGD) [25]. The resulting persistence in inflammation is due to neutrophil resistance to apoptosis and defective production of the anti-inflammatory prostaglandin D (PGD) (2). Additionally, those macrophages still functional in polymorphonuclear leukocyte (PMN) clearance are also defective in PGD (2) production [26]. Therefore in CGD patients, persistent and chronic inflammation results in secondary pathologies, such as non-infectiously induced and inflammation mediated colitis [27].

A classical example of an inflammatory disorder is rheumatoid arthritis (RA) (Figure 1.2). Professional phagocytes mediate unique and overlapping pathologies in RA and often exacerbate each other through the inflammatory process. A multitude of dysfunctions contribute to the pathology of RA, including aberrant chemokine ligand and receptor expression, cell adhesion, cytokine expression, bone tissue remodeling, and angiogenesis (Figure 1.2). Many of these detrimental dysfunctions are mediated by synovial monocytes/macrophages. The inflammatory activity of these cells is functionally correct, although inappropriate. For example, integrins are essential to monocyte adhesion and migration; however, in RA enhanced integrin expression mediates excessive monocyte migration into the synovium [28]. Furthermore, engagment of chemokine receptors CCR1 and CCR2 mediate further monocyte recruitment to the joint,

while the chemokine receptors CCR3 and CCR5 mediate retention of monocytes within the joint [29] (Figure 1.2). Synovial macrophages are then triggered to express pro-inflammatory cytokines IL-1 and tumor necrosis factor-α (TNF-α) through contact mediated stimulation by T lymphocytes [30, 31] and then recruit neutrophils via chemokine expression [32] (Figure 1.2). Additionally, synovial macrophages contribute to RA by mediating angiogenesis via chemokine [33] and growth factor expression (for example vascular endothelial growth factor [VEGF]), which is enhanced in inflammatory disease [34]. Finally, osteoclasts mediate bone homeostasis and remodeling in the joint; however, synovial macrophage stimulation via TNF-α and IL-1 results in bone reabsorption by osteoclasts [35].

RA has been predominantly considered a T cell and macrophage driven process early on, neutrophils appear to be primarily responsible for inflicting host damage during RA progression through the activity of serine- and metallo-proteases and the production of reactive oxygen species [3]. Synovial fluid from RA patients contains soluble antibody aggregates that have been implicated in activating synovial neutrophils and GM-CSF primed neutrophils from healthy individuals [36] (Figure 1.2). In fact, in patients with active RA disease, over thirty milliliters of synovial fluid has been extracted and shown to contain over $5x10^9$ neutrophils, nearly 100 times the average blood concentration of neutrophils [37]. TNF-α appears to play an important role in RA disease pathology, since *in vitro* cartilage damage is mediated by TNF-α [38]. Increased activity of the oxidase is associated with increased arthritic severity [39], suggesting that the oxidase could be the primary cause of host tissue damage.

In RA, the traditional view has been that TNF-α expression results in uncontrolled inflammation and hence damage to the host tissue. However, it is arguable that the mechanism behind the disease pathology of RA may be founded in the ability of TNF-α to exert an effect over the capacity of neutrophils to undergo apoptosis. TNF-α has traditionally been regarded to induce neutrophil programmed cell death; however, TNF-α has also been shown to promote neutrophil survival [40, 41]. Whether TNF-α promotes neutrophil apoptosis or cell death may depend on the environmental context, as TNF-α mediated neutrophil survival appears to depend on cross-talk with the phosphoinositide 3-kinase (PI3K) pathway and production of IL-8 [42]. Therefore, not only excessive inflammation but also dysregulation of apoptosis might be at the root of the pathology of RA. If inflammation were not limited by apoptosis then the oxidase would continue to contribute to host tissue damage, resulting in chronic clinical manifestations of the disease. In support of this, RA joints contain a significantly increased level of TNF-α [37], and anti-TNF-α antibody has shown dramatic therapeutic effects. The therapeutic effects might be mediated both through inhibition of inflammation and inhibition of survival signals. Further, the injection of apoptotic leukocytes into the joints of mice before the induction of experimental complex-mediated arthritis (ICA), a murine model of RA, was shown to be protective, as uptake of apoptotic leukocytes by synovial lining macrophages significantly reduced the subsequent chemotaxis of neutrophils, thus limiting the damage to host tissue [43]. Therefore disregulation of neutrophil apotosis contributes to RA damage and may be exacerbated through survival signaling initiated by TNF-α.

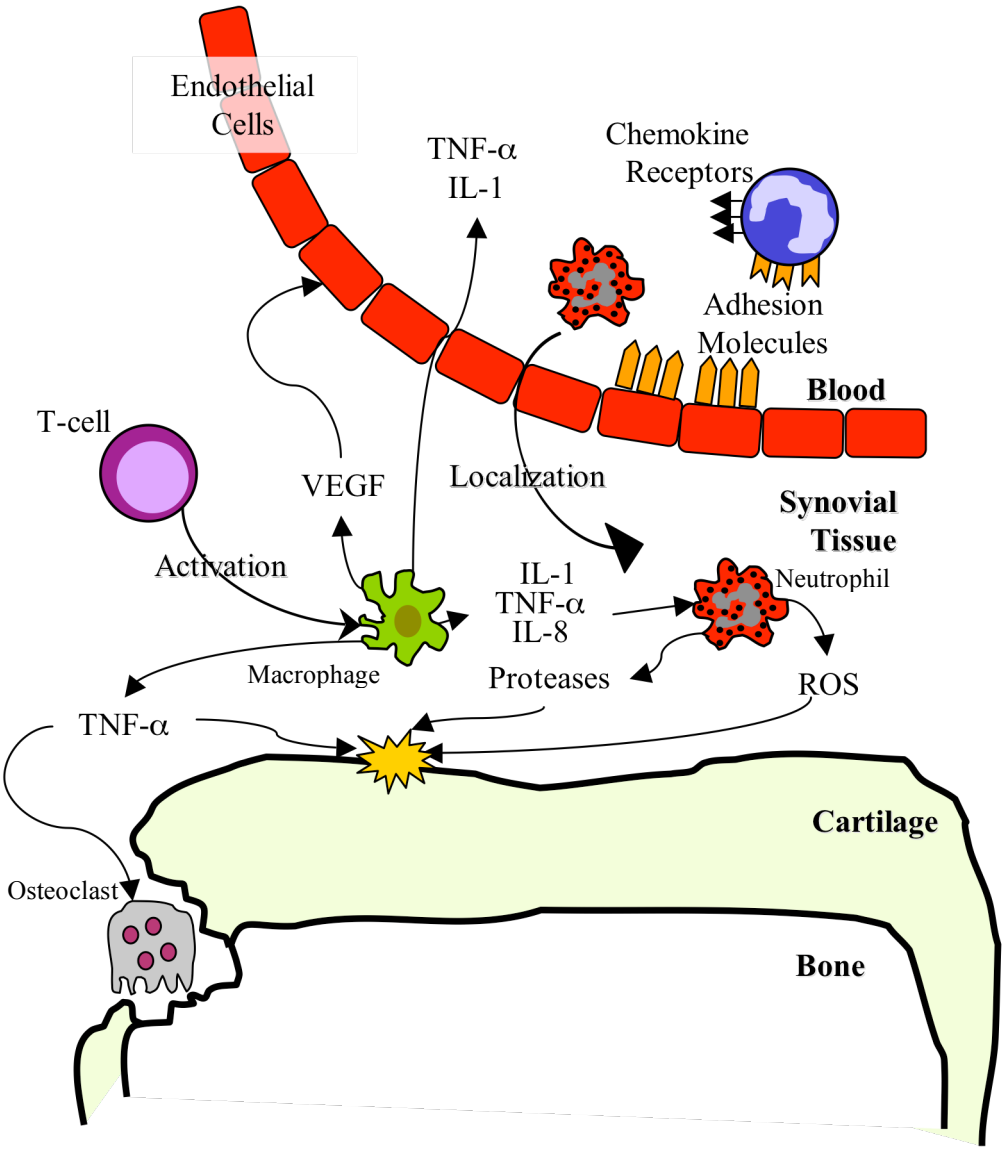

Figure 1.2: Schematic of phagocytic cell damage during the pathological progression of rheumatoid arthritis. Damage to the joint is mediated through recruitment of inflammatory cells to the synovium where activation results in the release of multiple factors that mediate damage to the cartilage and bone. See text for details.

Aberrant inflammatory activity by professional phagocytes appears to be important in mediating a variety of other pathological conditions. For example, in acute respiratory distress syndrome, mortality is the result of multiple organ dysfunction syndrome (MODS). Therapies aimed at modulating neutrophil inflammatory activation

by use of prostaglandin and complement inhibitors have shown some encouraging promise [44]. Brain inflammation also contributes to pathologies both acute and chronic. In Alzheimer's disease, alterations in the systemic immune response and immune cell infiltration into the brain may modulate clinical disease manifestations [45]. Brain inflammation may also have a role in neurogenesis through induction of TNF-α, but may also prove detrimental when TNF-α is induced during infection, hemorrhage, and aging [46].

Chronic inflammation plays a pivotal role in vascular pathologies associated with chronic obesity and is mediated both by the resident macrophages and by cross talk between macrophages and adipocytes through the activity of the NADPH oxidase. Obesity has become epidemic in the United States and is characterized by enlargement of adipocytes in the adipose tissue. As the adipocytes increase in size, the tissue produces proinflammatory cytokines, including TNF-α [47]. Global array studies have shown that the onset of obesity turns on genes primarily associated with macrophages [48, 49]. Additionally, a higher concentration of macrophages are found in the adipose tissue of obese people when compared to slim people. Further, obese mice genetically predisposed to diabetes showed gradual increases in macrophage inflammatory gene activity [50], indicating that increased proinflammatory activity may enhance the detrimental disease states resulting from chronic obesity. Obesity is marked by chronic immune activation and low-grade inflammation [51]. This may be the result of perivascular fat cells expressing pro-inflammatory factors such as monocyte chemoatractant protein-1 (MCP-1), causing macrophages to populate the arterial wall and enhancing vascular inflammation [52] Additionally, cross talk between resident macrophages and adipocytes

may result in defective insulin signaling in macrophages, which in turn makes macrophages more susceptible to apoptosis and less able to mediate phagocytic clearance of the atherosclerotic lesion [53]. Regardless of how macrophages mediate obesity-associated vascular disease, they certainly play a central role in atherosclerosis and are a major component of the atherosclerotic lesions [54]. Finally, low-density lipoprotein (LDL) oxidation by arterial wall macrophages is a key event in early atherosclerosis requiring the active NADPH oxidase [55], and unregulated uptake of oxidized LDL by macrophages results in foam cell formation [56], characteristic of disease progression.

Other Pathologies Mediated by Professional Phagocytes

Professional phagocytes are also implicated in autoimmunity. For example, systemic necrotizing vasculitide is an autoimmune disease marked by the presence of anti-neutrophil cytoplasmic antibodies (ANCA) found in the sera of patients. The target of these antibodies appears to be neutrophil granule proteins [57], suggesting that excessive degranulation might result in self-recognition of the contents of the granule by the adaptive immune system. The importance of apoptotic clearance is demonstrated by defects in components of the complement system that result in induction of systemic lupus erythmatosus with delayed clearance by resident macrophages [58]. Recent work suggests that apoptotic clearance of neutrophils itself may not be dysfunctional in the case of autoimmunity, but rather phagocytes are unable to respond to characteristic signals that induce phagocytosis [59].

Finally, recent evidence has emerged implicating professional phagocytes in neoplastic transformation and tumor persistence through pro-tumorgenic activities such

as angiogenesis, lymphanogenesis, tumor cell migration, metastasis, and immune suppression [60]. Activation of the inflammatory response has been shown to play an essential role in full transformation and tumor progression [61]. Additionally, neutrophils have been found in brain tumors [3]. Whether this is the result of failed attempts to kill the tumor mass by these professional phagocytes or whether these immune cells actually contribute to the disease has yet to be determined; however, high levels of TNF-α have been found in the supernatant of human colon cancer cell cultures, suggesting a role for immune cells in the actual disease pathology. Furthermore, cancer associated inflammation has also been shown to mediate tissue remodeling and angiogenesis in the presence of proinflammatory cytokines, TNF-α and IL-1 [62]. Finally, apoptotic cell phagocytosis by macrophages results in a blunted immune response to growing tumor mass [63]. On the other hand, professional phagocytes themselves are not immune to transformation as demonstrated by both chronic and acute forms of myeloid leukemias [64].

The NADPH Oxidase

The NADPH oxidase is a multi-component enzyme complex essential to the antimicrobial capacity of the innate immune system. The oxidase is highly evolutionarily conserved and can be found in fish, insects, and even plants [65]. The phagocytic oxidase functions as a microbial killer both by the direct means of oxidative products and by the indirect means of oxidant-mediated liberation of antimicrobial proteases [66]. The indirect means of microbial killing via liberation of proteases is dependent, in part, on the increased intraphagasomal pH caused by activity of the oxidase. Electron transfer from

NADPH to molecular oxygen forms the oxidative product of the NADPH oxidase burst, superoxide anion. Superoxide is then converted to more potent microbicidal oxidants that participate in downstream antimicrobial activities (Figure 1.3). The known essential components of the phagocytic oxidase include the transmembrane flavocytochrome$_{b558}$ (consisting of the two components gp91^{phox} [also called Nox2] and p22^{phox}), and the cytosolic components p47^{phox} and p67^{phox}. Known accessory components include the small G-coupled protein Rac (1 or 2) and the p40^{phox}. Activation of the oxidase is dependent on the functional recruitment and assembly of the cytosolic components with the transmembrane component.

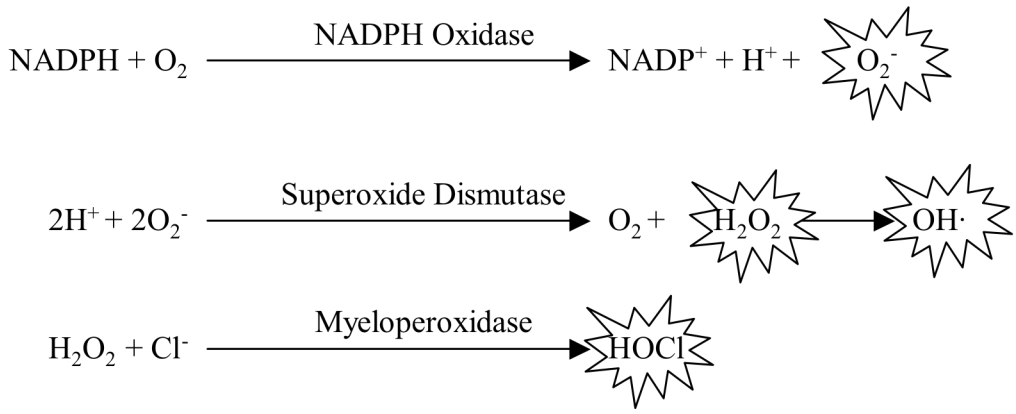

Figure 1.3: Generation of potent microbicidal oxidants. The NADPH oxidase generates superoxide from oxygen and NADPH. Superoxide is then converted to hydrogen peroxide either by spontaneous or superoxide dismutase (SOD) dismutation. Hydrogen peroxide can then convert to hydroxyl radical and thus downstream microbicidal oxidants or can be converted to hypochlorous acid by myeloperoxidase (MPO) [67].

Components of the NADPH Oxidase

Each of the components of the phagocytic NADPH oxidase performs unique and complementary functions in oxidase activation, and these functions are reflected in the structural domains of each protein. The heterodimeric flavocytochrome b was originally

identified when Segal, et al. [68] observed a non-mitrochondrial cytochrome b in phagocytic granules. The transmembrane proteins, gp91^{phox} and p22^{phox}, form a heterodimeric unit with two closely spaced hemes [69]. Recent evidence suggests that one heme is coordinated by gp91^{phox} alone, while the second heme is coordinated between gp91^{phox} and p22^{phox} and may act to enhance association between the two components [70]. Gp91^{phox} contains a flavin adenine dinucleotide (FAD)-binding moiety, identifying the dimer unit as a flavocytochrome b [71]. Oxidation of NADPH is essential to the function of the oxidase, and binding of NADPH is likely mediated through a NADPH-binding moiety in gp91^{phox} [72]. Therefore, the flavocytochrome b likely mediates the sequential transfer of two electrons from NADPH via the FAD to two hemes then on to oxygen to create two molecules of superoxide per each NADPH utilized by the active NADPH oxidase. Despite the fact that flavocytochrome b appears to contain all the essential components necessary for the production of superoxide, it is not sufficient and requires the association of other NADPH oxidase components.

The remaining phagocytic NADPH oxidase components are cytosolic and only associate with the membrane components when the oxidase is activated. Rac is maintained in an inactive state in the cytosol and dimerizes with a guanine nucleotide exchange protein (GDI) [73] and, upon activation, dissociates from GDI and translocates to the membrane independent of the other cytosolic factors [74]. Rac likely mediates oxidase assembly by indirectly activating p47^{phox} via phosphorylation [75] and through its interactions with p67^{phox} [76] and the flavocytochrome [77] (Figure 1.4).

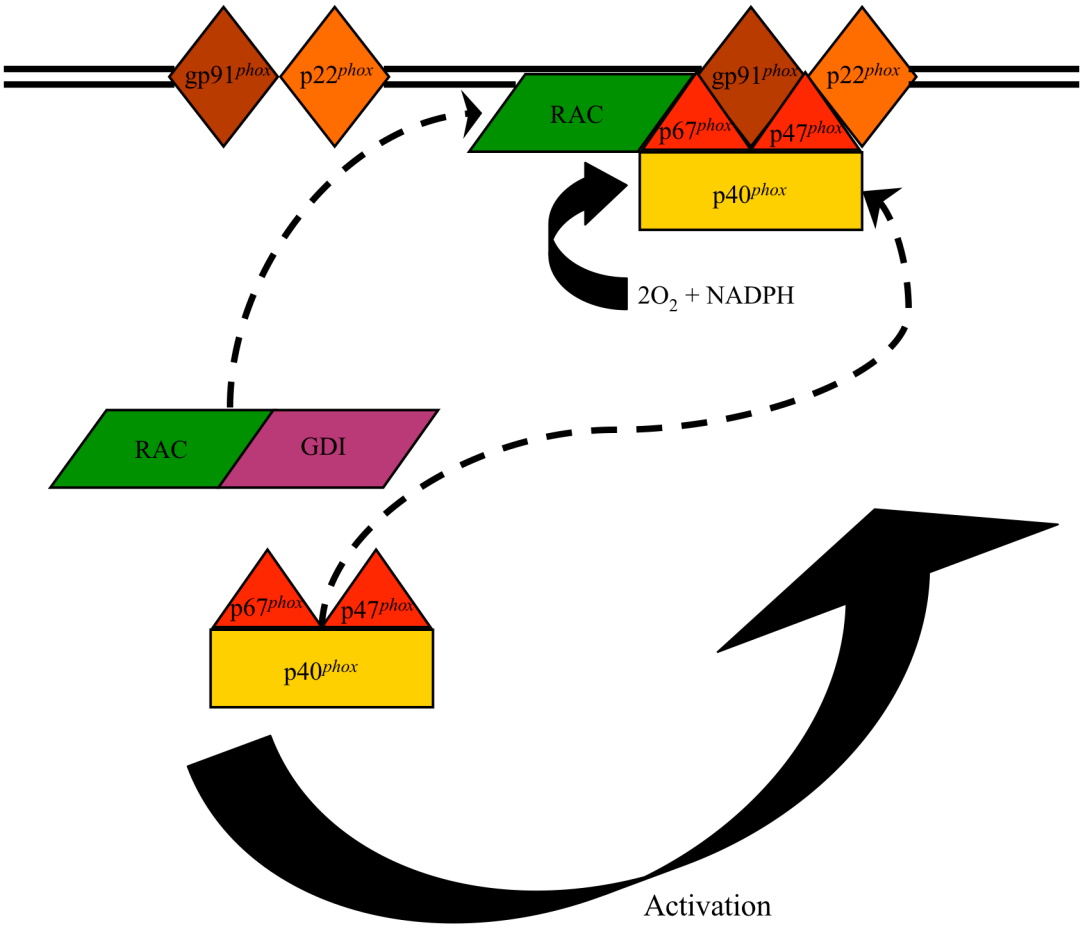

Figure 1.4: Schematic of NADPH oxidase assembly. Upon activation, cytosolic components localize to the membrane and bind to membrane-associated components. Conformational changes and activation mediates conversion of NADPH and oxygen from the cytosol to generate superoxide. Adapted from Reference [22].

Prior to activation, $p47^{phox}$, $p67^{phox}$, and $p40^{phox}$ are in a complex together in the cytosol [78]; however, $p47^{phox}$ can also be found in free form in the cytosol [79]. $P47^{phox}$ contains a number of interesting regulatory domains including an N-terminal phox homology domain, two SH3 domains, a cationic/autoinhibitory domain, and a C-terminal proline-rich domain [80] (Figure 1.5). Analysis of the function of these domains suggests that, upon oxidase activation, $p47^{phox}$ mediates both $p67^{phox}$ translocation and electron

transfer from the flavocytochrome b FAD domain to a heme [81]. Another component of the cytosolic complex is $p40^{phox}$, which also contains an SH3 domain as well as an N-terminal PX domain and a C-terminal PC domain [82] (Figure 1.5). The PC motif is a novel motif consisting of a phox homology domain and a domain with homology to the yeast Cdc24p protein. This domain likely mediates protein-protein interactions with $p67^{phox}$ at its PB1 domain, which contains a phox homology domain and a domain with homology to the yeast Blem1p protein [82]. $P40^{phox}$ likely mediates the stabilization of the phox cytosolic complex and enhances the translocation of the complex upon activation [83].

The final component of the cytosolic complex, $p67^{phox}$, is a 526 amino acid protein with four tetratricopeptide repeat (TPR) motifs, two SH3 domains, the PB1 domain, an activation domain, and one proline rich region (Figure 1.5). The interdependence of structure on function has been elucidated through mutational analysis. The first twenty-two and last sixteen amino acids are not required for oxidase activation [65]. TPR motifs consist of tandom repeat sequences in a protein often mediating protein-protein interaction. In $p67^{phox}$ the TPR motif appears to be involved in the binding of Rac1 or Rac2, which binds to $p67^{phox}$ via Rac's Switch 1 domain [76]. NADPH-dialdehyde binding studies indicate that $p67^{phox}$ directly binds NADPH [84], suggesting that $p67^{phox}$ is involved in the transfer of electrons from NADPH by the oxidase. In further analysis, deletion of the amino acids 199-210 identified an activation domain that regulates the electron transfer from NADPH to the FAD contained in the flavocytochrome b [74]. Biochemical approaches for detecting redox intermediates have provided evidence that $p67^{phox}$ indeed facilitates this electron transfer [81]. Finally, the

SH3 domains mediate complex interaction with p47^{phox} and p40^{phox}. Deletion of either SH3 domain results in a dramatic reduction of NADPH oxidase activity and decreased membrane translocation [85]. Meaurement of oxidase assembly and activation by atomic force microscopy using a microscale cantilever deflection which is detected by laser on the nanoscale level has shown that of all the cytosolic components, p67^{phox} plays the most critical role in oxidase assembly and activation, indicating that p67^{phox} is the limiting component of the activated oxidase [86].

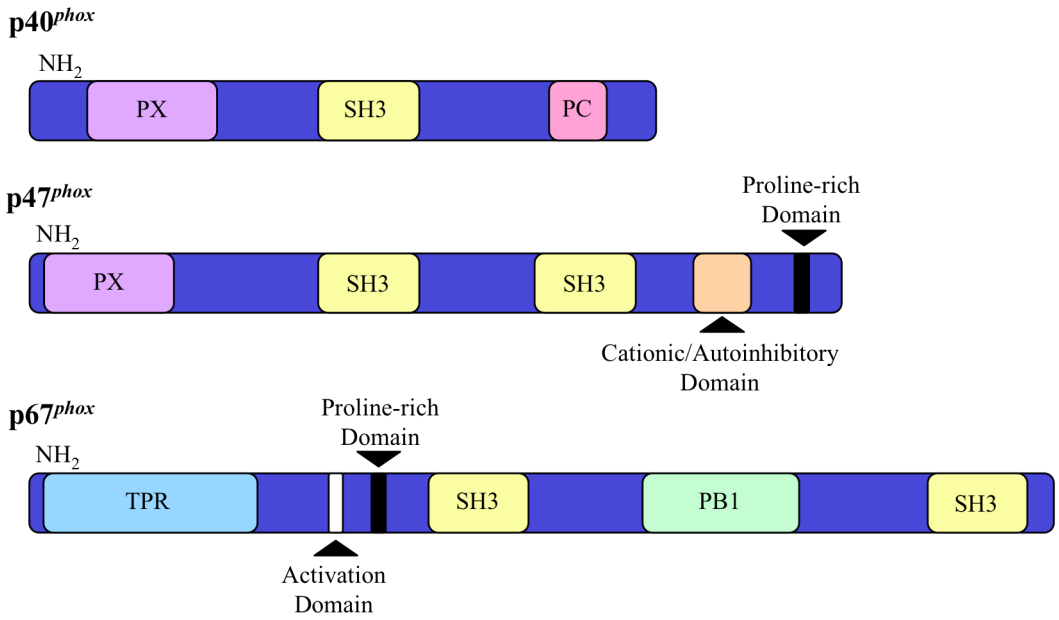

Figure 1.5: Schematic of NADPH oxidase cytosolic components. Major functional domains are indicated. See text for details. Modified from Reference [80].

Activation and Functional Implications of the NADPH Oxidase

Activation of the oxidase is itself a well controlled and regulated mechanism. Cell-free system studies first suggested that only gp91^{phox}, p22^{phox}, and p67^{phox} were essential to the functional oxidase *in vitro*; however, the assembly is clearly more

complicated *in vivo*, and the activated oxidase appears to also require $p47^{phox}$ and Rac2 (in humans) or Rac1 (in other species) to be functional [87]. When inactive, $p47^{phox}$ is in a closed formation involving binding between the C-terminal proline rich region of $p47^{phox}$ and the C-terminal SH3 domain of $p67^{phox}$ [78] (Figure 1.4). The flavocytochrome is also in a state of conformational inactivity that inhibits electron transfer [88].

Upon activation, $p47^{phox}$ is phosphorylated, resulting in a conformational change that exposes the SH3 domains, polybasic region, and PX domain and neutralizes the cationic/autoinhibitory domain [89] (Figure 1.5). Despite conformational changes, $p67^{phox}$ and $p47^{phox}$ remain in contact as they translocate to the membrane. Here $p67^{phox}$ binds to the assembling oxidase in a $p47^{phox}$-dependent manner [90]. When $p67^{phox}$ binds to flavocytochrome b, the cationic region of $p47^{phox}$ is exposed, allowing $p47^{phox}$ to bind with high affinity to the flavocytochrome via this exposed region [91]. Rac translocates independently, and then mediates $p67^{phox}$ binding to flavocytochrome b via the interaction of the switch region on Rac and the N-terminal TPR motif on $p67^{phox}$ [92]. Rac also mediates the disruption of the interaction between $p67^{phox}$ and $p40^{phox}$, thus enhancing the binding capacity of $p67^{phox}$ to the assembling oxidase [93]. Finally, the binding of $p67^{phox}$ and $p47^{phox}$ to flavocytochrome b induces a conformational change that allows for electron transfer [86] (Figure 1.4).

Functional assembly of the oxidase occurs at both the plasma membrane and intracellularly in the membrane of specific granules [94], and translocation studies indicate that this assembly on the cytoplasmic face of the membrane is the critical feature of oxidase activation [87]. While constitutive interactions are required to maintain the complex, the oxidase is likely undergoing continuous deactivation, and the activity of the

oxidase depends on the relative rates of activation and deactivation [65]. It is quite probable that the relative rates of activation and deactivation are dependent on the extracellular environment and signals transduced into the cell. Indicative of the extracellular effect on activity, receptor mediated oxidase activity lasts only about five minutes, while receptor independent activation lasts much longer [65].

It is important to note that the function of the oxidase likely extends beyond the mere production of superoxide. New model systems and more advanced means of detection have indicated that the NADPH oxidase role within the cell may be significantly more extensive than suggested by the traditional and perhaps simplistic view of the oxidase. For example, the oxidase has significant effects on the intracellular free calcium within the neutrophil. This is pertinent, as free cytosolic calcium has substantial effects on the activity and activation of the neutrophil. The electrogenic capacity of the neutrophil exerts an effect on calcium influx into the cell and thus limits the pro-inflammatory effects of free cytosolic calcium within the neutrophil. Thus, reduced oxidase activity is associated with high levels of calcium influx and with hyper responsive degranulation [37].

Chronic Granulomatous Disease: a Disorder of the NADPH Oxidase

The potent antimicrobial capacity of the phagocytic NADPH oxidase is essential to the health of the host as is most clearly demonstrated by the effects of chronic granulomatous disease (CGD), clinically characterized by the lack of a functional NADPH oxidase. Defects in the components of the NADPH oxidase result in recurrent, life-threatening bacterial and fungal infections. This results in an abnormally exuberant

inflammatory response, which in turn leads to granuloma formation. Although CGD affects approximately one in two hundred thousand people, it is severely debilitating [3]. CGD can result from a number of genetic mutations, including misense mutations in $p22^{phox}$ [95], mutations resulting in the loss of phosphorylation of $p47^{phox}$ [96], and mutations in $p67^{phox}$ and Rac2 [97]. However, mutations in $gp91^{phox}$ are the most common mutations resulting in CGD [21]. Only five percent of CGD cases are the result of an autosomal mutation in $p67^{phox}$ [97]. Interestingly, in this form of CGD, the level of mRNA expression for $p67^{phox}$ is normal, but no protein is expressed [66]. Experimental treatment of CGD has involved adenovirus-mediated gene transfer into macrophages; however, gene therapy has made little recent progress [98]. Another type of treatment that has proven efficacious is priming of CGD patients with IFN-γ, TNF-α, IL-1β, IL-6, and/or GM-CSF, thereby eliciting an improved oxidative burst [99].

Other Pathologies Mediated by the NADPH Oxidase

From wound healing to RA, the oxidase or products derived from the oxidase have been implicated in a multitude of inflammatory diseases. The extent and variety of disease pathologies associated with oxidase activity suggests a more pervasive role for the oxidase than just the traditional antimicrobial role. In support of this hypothesis, a growing number of homologs to the phagocyte oxidase are being identified and characterized. So far homologs have been found for $gp91^{phox}$ (also called Nox2) and are identified as Nox1-Nox5 and Duox1-Duox2, for $p47^{phox}$ and identified as $p41^{nox}$ or NOXO1, and for $p67^{phox}$ and identified as $p51^{nox}$ or NOXA1 [100]. While these studies are still in their infancy, it is important to note that the potentially pervasive function of

the oxidase may contribute to many more disease pathologies and physiological functions than might have been conceived even a short decade ago. For example, reactive oxygen species are the key element in the poor wound healing response that leads to excess collagen accumulation in the wound [101]. Reactive oxygen species accelerate the aging process *in vivo*, and cells cultured with reactive oxygen species exhibit accelerated signs of aging [102]. Hydrogen peroxide, a downstream product of superoxide, is increased in the exhaled air of cystic fibrosis patients and is decreased with the treatment of antibiotics [103]. Additionally, hydrogen peroxide causes the secretion of matrix metalloproteases, causing lens opacification and cataract formation [104]. Acute lung inflammation and acute respiratory distress syndrome also have a phagocyte component. Using the toxic metal gadolinium trichloride ($GdCl_3$), which inhibits neutrophil infiltration and macrophage activation, in conjunction with NADPH oxidase knock out mice, *in vivo* and *in vitro* evidence suggested that LPS induced lung injury is mediated by oxidase production of free radicals [105].

Parkinson's disease has been associated with inflammation and nervous system damage may be the result of an active NADPH oxidase. Not only has chronic inflammation been shown to increase the risk for developing Parkinson's disease, but also microglia have been shown to be capable of producing reactive oxygen species. In the Parkinson's disease mouse model induced by MPTP (1-methyl 4-phenyl 1,2,3,6-tetrahydropyridin) neurotoxicity, $gp91^{phox}$ is shown to be upregulated in the substantia nigra. This upregulation has also been found in the substantia nigra of Parkinson's disease patients. Additionally, $gp91^{phox}$ knock-out mice lacking a functional oxiase

displayed less cell death in the sibstantia nigra when compared to litter mates and had attenuated neurotoxicity resulting from MPTP treatment [106].

Cardiovascular disease is one of the greatest killers in our society and in this field there is also substantial and relevant research correlating pathology with the active oxidase. In reperfusion injury persistently elevated levels of TNF-α after a myocardial infarction identifies patients at an increased risk of recurrent coronary attacks [107], suggesting that chronic inflammation may contribute to further tissue damage. In hypertension, superoxide exerts numerous effects on vasculature. For example, superoxide can interfere with NO-dependent vasodilatation [108] and participates in endothelium-dependent constriction [109]. Mouse models for hypertension have also contributed to a greater understanding of the oxidase contribution to cardiovascular disease. Angiotensin II (AngII) is used to induce high blood pressure in mouse models. *In vivo*, oxidase derived superoxide has been implicated in AngII induced high blood pressure [65]. Further, *in vitro* studies have shown that AngII stimulates the production of superoxide by neutrophils [110]. Finally, use of chimeric peptides to interfere with the oxidase assembly in *vivo* provides direct evidence for oxidase involvement in AngII induced hypertension, including causing the upregulation of the essential oxidase components [111]. This suggests that hypertension mediated in part by regulation of the components of the oxidase.

Oxidase activity has also been implicated in multiple cancer studies. While multiple cancer lines have been shown to constitutively release large amounts of reactive oxygen species [112], studies both *in vivo* and with primary cells have also implicated activity of the oxidase in contributing to cancer formation. For example, Nox1 (a

homolog to gp91^{phox}) over expression in murine fibroblast cells (NIH3T3 cells) induced cell transformation, and, when injected into nude mice, induced the formation of highly vascularized tumors [113]. Proinflammatory responses might be contributing to cancer disease pathology. An example of inflammatory mediation of cancer development is the TNF-α polymorphism found in non-Hodgkin's lymphoma [114].

Non-phagocytic oxidases also appear to have an important role in disease pathology [100]. Beyond pathogen killing, superoxide has been shown to mediate cellular stress responses by altering cell function, adhesion, proliferation, and motility [115]. Additionally, fibroblasts have been shown to manufacture superoxide in response to growth factors, while endothelial cells produce superoxide in response to sheer stress. The potential function of superoxide production as a means of signaling is further supported by the finding that carotid body uses superoxide producing oxidase for sensing oxygen levels [65].

Increasingly, evidence also points to the important role phagocytic oxidase component homologs play in disease pathology. For example, the homolog Nox4 has been shown to function as an oxygen sensing mechanism that regulates the production of erythropoietin [116], suggesting that hypoxic conditions may stimulate downstream regulation by the oxidase. Nox1 expression is enhanced in a rat model of diabetes [117] and Nox4 expression is enhanced in artherosclerotic plaques [118] and in coronary artery disease [119]. The potential for an extensive and systemic oxidase impact is suggested by the finding that another homolog Duox is involved in the iodination of thyroid hormone, as mutations in Duox2 can be found in congenital hypothyroidism [66]. Further

investigation of these homologs will extend and advance the current understanding of the potential roles performed by the oxidase.

Transcriptional Regulation in Professional Phagocytes

Neutrophils have been historically treated as transcriptionally inert, however recent studies that have addressed transcriptional regulation and specifically global array studies have indicated that neutrophils are actually quite transcriptionally active. Before the use of global arrays a small number of studies found specific upregulation of transcripts in neutrophils. These studies included upregulation of heat shock proteins [120], phagocytic receptors [121], $gp91^{phox}$ and $p22^{phox}$ [122, 123], and TNF-α [124].

A series of studies have since used global arrays to indicate the large number of transcripts that change in the neutrophil depending upon activation and environment. For example, an early expression microarray using live *E. coli*, LPS, and fMLF found that, compared to previous findings, more chromatin-binding genes and translocation regulators and less metabolic and vesicle transport genes were upregulated in mature neutrophils [125]. This supports the hypothesis that neutrophils are not only transcriptionally active, but that transcription regulation of transcription factors is also occuring. Further, a study showed that during receptor-mediated phagocytosis, the resolution of inflammation is mediated, in part, by gene expression [126]. Another study compared global gene expression profiles between neutrophils exposed to pathogenic bacteria versus neutrophils exposed to non-pathogenic bacteria [127]. This group found that exposure to both pathogenic and non-pathogenic bacteria induced the expression of genes that delay apoptosis such as BCL2A1 and IER3, a p53 responsive factor that

protects from apoptosis induced by TNF-α and FasL. Additionally, they found that over forty percent of the immediate-early genes, upregulated within two hours after activation, were transcription factors. Particularly interesting was the finding that non-pathogenic, but not pathogenic, bacteria down regulated the expression of the phox genes including *NCF2*, the gene that codes for $p67^{phix}$.

Regulation of the NADPH oxidase genes in professional phagocytes occurs both during differentiation and in response to environmental mediators. In differentiating granulocytes and promyelocytic cells, fluctuating expression of the oxidase components $gp91^{phox}$, $p67^{phox}$, and $p47^{phox}$ indicates that these factors are regulated during differentiation [128]. Although *CYBA*, the gene that codes for $p22^{phox}$, is expressed in many cell types, it does not appear to be regulated by differentiation [69]. Additionally, $p40^{phox}$ does not appear to be regulated during differentiation, although it is expressed in immature myeloid cells [129]. Finally, $p67^{phox}$ is the last oxidase component expressed during differentiation, and its expression correlates with oxidase activity [128].

Transcriptional regulation of oxidase factors has also been demonstrated in response to cytokines [130, 131]. While *CYBB*, *NCF1*, and *NCF2* expression is induced by IFNγ, this cytokine appears to have no effect on expression of the other component of the flavocytochrome, $p22^{phox}$, which is encoded by *CYBA* [123, 130, 132], although one recent study in mesangial cells did suggest IFN-γ may enhance expression of *CYBA* and the corresponding $p22^{phox}$ protein [133]. Although Newburger, *et al.* [122] showed that *in vitro* treatment with TNF-α induced both *CYBB* and *CYBA* expression, recent studies *in vivo* have contradicted this finding, as *CYBA* message was unresponsive to TNF-α [134].

Finally, *CYBB*, *NCF1*, and *NCF2* expression responds to treatment with TNF-α *in vivo* [134].

Regulatory factors have been identified that mediate transcription of the genes encoding various oxidase components (Table 1.1). For *CYBB*, the gene that codes for gp91^{phox}, Ets factors have been shown to be essential during differentiation. For example, the myeloid specific Ets factors PU.1 and Elf-1 bind and regulate the *CYBB* intragenic region [135] in conjunction with the HAF-1 complex [136]. Additionally, PU.1 has been shown to bind and regulate the intragenic region of *NCF1*, the gene that codes for p47^{phox} [137]. Although not directly established *in vivo*, PU.1 has also been suggested to bind and regulate the expression of *NCF4*, the gene that codes for p40^{phox} [138]. Five PU.1 elements have been identified in the 5'UTR of *NCF2*, the gene that codes for p67^{phox}, and three have been shown to bind PU.1 (Figure 1.6) [130, 139, 140]. In contrast to the PU.1 elements shown to regulate expression of *CYBB*, *NCF1*, and *NCF4*, at least one of the PU.1 sites does not appear to be necessary for basal transcription of *NCF2* [137]. Additionally, binding elements for AP-1 and SP1/3 have been identified in the intragenic region of *NCF2* (Figure 1.6) [139, 140]. The AP-1 element is located within the intergenic region of *NCF2* and has been shown to be essential for basal transcription [139, 140]. Although, luciferase assays with the SP1/3 site mutated have about a third of the expression of the wild type [139], the binding element is located upstream of exon 1 and does not correlate with the majority of expressed sequence tags (ESTs) in the public database.

Finally, repression of transcription occurs in the regulatory region of *CYBB* by CDP [141] and SATB1 [142], which interfere with the binding of factors that activate

transcription. In addition, the homeodomain transcription factor HOXA10 has been shown to repress transcription of both *CYBB* and *NCF2* [143, 144]. HOXA10 transcription repression of *NCF2* is mediated through a binding element -600 to -637 basepairs upstream of the translation start site, upstream of exon 1, and repression is dependent on histone deacetylase activity (Figure 1.6). Furthermore, repression of *NCF2* transcription by HOXA10 is negatively regulated by IFN-γ-dependent tyrosine phosphorylation [144]. However, subsequent work by the same group identified HOXA10 to be bifunctional and may activate or repress transcription during myeloid differentiation in a context dependent manner [145]. The common transcriptional regulatory elements found in these 5' UTRs suggests transcription may be an essential element of oxidase regulation.

Table 1.1: Transcription Factors Regulating the NADPH Oxidase (based on [80])

Protein	Gene	Factor
$p22^{phox}$	*CYBA*	Unknown
$p40^{phox}$	*NCF4*	PU.1
$p47^{phox}$	*NCF1*	PU.1
$p67^{phox}$	*NCF2*	PU.1
		IRF-1
		ISCBP
		AP-1
		Sp1
		HOXA10
$gp91^{phox}$	*CYBB*	PU.1
		Elf-1
		IRF-1
		ICSBP
		YY1
		CDP
		CP1
		HOXA10
		SATB1
		GATA-3

It is possible that transcript stability may play an essential role in regulation of the NADPH oxidase component. A comprehensive analysis of transcription regulation verses transcript stabilization would identify whether changes in gene regulation are the result message transcription or stability. This remains an open question with regard to the components of the NADPH oxidase.

Transcriptional regulation in phagocytes also depends on transcription factor regulation. For example, redox regulation occurs via phosphorylation sites in AP-1 [101]. Further, reactive oxygen species can induce the activation of ERK, JNK, p38MAPK, and PI3/Akt cascades [146, 147], all essential regulators of gene expression in granulocytic cells. As with all signal transduction pathways, the activation or deactivation of transcription factors in a feedback mechanism by downstream products of the oxidase are complicated and sometimes contradictory. For example, treatment of various cell types with hydrogen peroxide can stimulate NF-κB DNA binding, while other studies indicate hydrogen peroxide inhibits DNA binding by Sp1, a transcription factor that works in association with the NF-κB factor RelA [101].

Multiple disease pathologies result from aberrant transcription factor regulation. For example, prolonged infection with *A. phagocytophila* can down regulate *CYBB* message [148] and Rac2 message [149]. Further, a bacterial factor from *Listeria* called YopJ/P can trigger apoptosis in phagocytes via NF-κB [150], suggesting that some pathogens can interfere with and determine the outcome of endogenous signal transduction pathways. In specific granule deficiency, a congenital disorder similar to CGD in that pathology is marked by frequent and severe bacterial infections [151], the loss of specific granules and defensins is the result of a mutation in the CCAAT/enhancer

binding protein epsilon (C/EBP-ε) transcription factor [152]. In Familial Mediteranian Fever, recurrent inflammatory episodes marked by neutrophil influx into the serosa and synovium result from a mutation in a putative transcription factor [153]. Chronic disease pathologies include the upregulation of the oxidase genes occurs during atherosclerosis [118], hypertension [154], and restenosis [155]. Finally, treatment has also proven efficacious by targeting transcription regulation. For example, glucocorticoid drugs act to specifically repress inflammatory genes in phagocytic cells [156].

TNF-α Regulation of Phagocyte Transcription

TNF-α: A Multipurpose Cytokine

The cytokine TNF-α is produced by many cells and has long been known to exert an effect on phagocytes in response to inflammation and infection [157]. Neutrophils are very responsive to the influences of this cytokine, and neutrophils from TNF-α treated subjects have an enhanced oxidative burst and degranulation [158]. While TNF-α can inhibit tumor growth through caspase activation and apoptosis [159], it has a proliferative effect, leading to increased numbers of monocytes, neutrophils, and macrophages in response to chronic and acute inflammation [160]. Additionally, TNF-α can act in an autocrine manner, and both neutrophils and macrophages express TNF-α mRNA. This cytokine exerts its effect through either the p75 receptor or the p55 receptor, although p75 is more commonly found on myeloid cells; whereas, p55 is found more commonly on epitheliod cells. Finally, the effects of TNF-α are abolished by the myeloid cell through the shedding of these receptors via the activity of elastase [3].

Aberrant TNF-α signaling has been associated with a number of diseases. *Salmonella* infection constitutes the second most common bacterial infection in CGD patients and the inability for the host to fight *Salmonella* infection is mediated by the pathogen itself. TNF-α signaling mediates the delivery of oxygen radicals to the *Salmonella*-containing phagosome. By unknown means, *Salmonella* targets the TNF-α signaling pathway with SPI2-secreted effecter proteins [161] interfering with host defence against the pathogen. Perhaps the *Salmonella* target is a regulator of the oxidase downstream of TNF-α signaling; however, identification of the factors downstream of TNF-α has proven to be very complicated. To illustrate the complexity of this signal in the cell, one can look at a global proteome analysis of the TNF-α/NF-κB signalzome. Using this approach, numerous newly observed modulators of the TNF-α/NF-κB pathway were detected, and 680 non-redundant protein hits were identified at least twice and mapped into an interacting proteome (see http://tnf.cellzome.com for the map) [162].

TNF-α Regulation of the NADPH Oxidase Component p67^{phox}

TNF-α exerts a regulatory effect on the transcription of p67^{phox} in both bone marrow derived macrophages and myeloid-like cells [163, 164]; however *NCF2* has a complex mechanism of transcription regulation. Although the location of the translation start site is fairly well established (Figure 1.6) [130, 140, 165, 166], where and how transcription is initiated remains an interesting question. The gene coding for p67^{phox} was initially cloned from a lamda-ZAP library derived from the myeloid cell line HL60s [165]. Although the translation start site was identified, this paper only reported a short region of the 5'UTR that was unlikely to contain enough sequence for transcription

initiation. Later work on *NCF2* identified an additional upstream non-coding exon and intronic sequence in the 5'UTR; however exon/intron characterization was performed on a single clone from a lambda-phage library derived from human placenta and therefore may not reflect the true site of transcription initiation [166].

Rather than clarifying the location of transcription initiation, later work suggested an even more complicated map of transcription initiation in the 5'UTR of *NCF2*. Using primer extention, Eklund, *et al.* [130], identified four sites of transcription initiation. Only one of those sites initiates upstream of exon 1 as identified by Kenny, *et al*. [166], and is only found in cells treated with intereron gamma (IFN-γ). The remaining three sites are all located in the intragenic region between exon 1 and exon 2. The transcription initiation site closest to the translation start site falls one basepair different than the start identified by Leto, *et al*. [165]; however, this site is also too close to the translation start site and likely does not reflect a true site of transcription initiation. Whether the remaining two transcription initiation start sites are real remains to be determined; however, a search of the public EST databases returns not a single EST in proximity to these transcription start sites, suggesting that these are not bonified sites of transcription initiation. Eklund, *et al*. [130] might have biased their results by using only a single monocyte-like cell line, U937. Perhaps transcription initiation is unique in this cell type and thus too rare to detect in a general search of the EST databases. It is also possible that the integrity of the mRNA was compromised.

Primer extention and 5'RACE are very similar methods except that primer extention presents data as a product in a gel and 5'RACE presents data as a sequence product. Gauss, *et al.* [167], perfomed 5'RACE on a number of myloid and monocytic

cell lines and human primary monocytes and neutrophils to acertain the transcriptional start site for *NCF2*. Four transcription start sites were identified: one upstream of exon 1 (designated exon 1) and the rest in intron 1 (designated intron 1a, 1b, and 1c). In comparison to the transcription start sites identified by Ecklund, *et al*. [130], only the start sites upstream of exon 1 are close enough in proximity to be considered identified by both groups. When transcription is initiated from exon 1, the mRNA product always has intron 1 spliced out. Indeed, a search of the EST database finds no EST sequences that include both exon 1 and intron 1. There are EST sequences that correspond to a splice product initiating transcription at exon 1; however, those sequences appear very rarely in the database suggesting that transcription intiation from exon 1 occurs very rarely. These rare EST transcripts do initiate at or near the transcription start site identified by Gauss, *et al.* [167] suggesting that the exon 1 transcription start site is rare but real (Figure 1.6). Indeed, exon 1 transcription intiation was common only in MonoMac6 cells and was absent in HL60s and neutrophils [167].

In addition to the transcription start site identified upstream of exon 1, three transcription start sites were identified within intron 1 (designated intron 1a, intron 1b, and intron 1c) [167]. Transcription intiation at both intron 1a and intron 1b is supported by a search of the public EST database. Of one hundred ESTs searched, nearly a quarter of the sequences were found to cluster around intron 1a. Interestingly, all of the EST sequences found to cluster around intron 1a were derived originally from either sinovial tissue from rheumatoid arthritis patients or from neutrophils. EST clustering was also found around intron 1b and these sequences were derived from a more heterogenous cell population. In addition, intron 1b was the most abundant transcript found by 5'RACE

[167]. It is therefore likely that intron 1a and intron 1b are true sites of transcription initiation; however, initiation at intron 1c is not supported in the EST database (Figure 1.6). As suggested by Gauss, *et al*. [167], this site of transcription initiation may have been identified due to secondary structure at this site in the intron that resulted in inhibition of the reverse transcriptase and thus termination of the sequence prematurely. A probe of the EST database also identified two clusters initiating around -183 basepairs and -273 basepairs upstream on the translation start site in intron 1. As it is not likely that these transcripts are initiating from exon 1 and neither primer extention nor 5'RACE identified start sites near these clusters, there may well be additional transcriptional start sites in intron 1 that have yet to be identified (Figure 1.6). By combining the information found in the EST databases with the previously identified transcription start sites, it is likely that transcription is initiated from *NCF2* at multiple sites, and that site choice is mediated in a context dependent manner.

While TNF-α does regulate *NCF2* transcription, it is not clear whether regulation occurs through transcript intiation at different sites or through some other mechansism of transcription regulation or mRNA stability. A TNF-α responsive region (TRR) has been mapped to the intragenic region between exon 1 and exon 2 of *NCF2* and is defined as -56 to -16 basepairs upstream of the translational start site (Figure 1.6). Using luciferase-reporter constructs for mapping, this enhancer element was found to be necessary for the upregulation of luciferase expression in response to TNF-α when cotransfected with c-Fos and c-Jun. Although transcription is mediated from this region, it remains unclear the mechanism of regulation. Identification of multiple transcription start sites suggests that TNF-α may mediate enhanced *NCF2* transcription by either initiating at different

transcrption start sites or by activating enhancing factors or both. Intitiation at different transcription start sites may result in more efficiently translated message or might enhance stability of message. When exon 1 and intron 1 transcripts are compared for stability, it appears neither has the advantage. Exon 1 transcripts do appear to transcribe more readily; however it is unlikely that transcription is initiated at exon 1 when cells are treated with TNF-α since the TRR would then flank the intron 1/exon 2 splice site. Indeed, TNF-α treatment appears to have no effect on exon 1 transcript intitiation [167].

TNF-α may mediate transcription upregulation through DNA-binding factors. The *NCF2* intragenic region between exon 1 and exon 2 contains three functional PU.1 (a myeloid-specific transcription factor) binding sites; however, only one of these sites interacts with cell extract and is not necessary for basal transcriptional activity [140]. Signaling through AP-1 has been shown to be important in cells simulated with TNF-α, acting through the Jun N-terminal kinase (JNK) pathway [168]. Recognition of an AP-1 site in the intragenic region suggested that AP-1 might regulate from this site (Figure 1.6); however, mutation of this site did not ablate the TNF-α response. DNAse footprinting showed that factor(s) bind both the AP-1 site and the TRR in the intragenic of *NCF2*. Interestingly, using a TRR competitor unprotected both the AP-1 site and the TRR of the intragenic region; whereas, competition with an AP-1 binding site competitor only unprotected the AP-1 site. Further mutation of the AP-1 site confirmed that this was indeed the site being protected. While this indicates that AP-1 is indeed binding the intragenic region, it also indicates that AP-1 binding is also mediated by interaction with some factor(s) binding the TRR [131]. Interestingly, TNF-α upregulates *NCF2*

expression only when cotransfected with the AP-1 factors c-Fos and c-Jun, suggesting that AP-1 regulates *NCF2* transcription from the intragenic region in intron 1 [140].

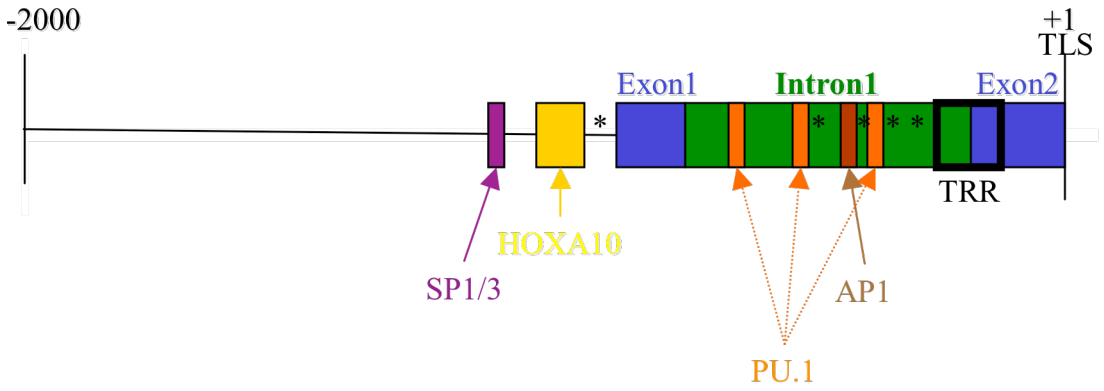

Figure 1.6: Schematic of *NCF2* 5'UTR. Putative transcription factor binding sites are identified. The TNF-α Transcription Response element (TRR) is identified. Putative transcription start sites are identified (*). See text for details. Modified from reference [131].

TNF-α dependent activation is commonly mediated through AP-1 and NF-κB [169, 170], and NF-κB can be activated by both TNF-α and reactive oxygen species [171, 172]. TNF-α can also mediate transcriptional activation through the JNK and p38 MAPK pathways [173]; however, use of pharmacological inhibitors identified the NF-κB pathway, but not the JNK or p38 MAPK pathways as the transcriptional pathway through which TNF-α enhances the expression of *NCF1, NCF2,* and *CYBB*, which in turn correlated with upregulation of superoxide production [134]. A search for NF-κB elements in the 5'UTRs of *NCF1* and *NCF2* identified one putative binding element ustream of the translation start site [134]; however, further studies are needed to confirm function. These sequences varied by two nucleotide differences when compared to the NF-κB element identified to be responsive to IFN-γ in the murine *CYBB* gene, and need

to be functionally confirmed [174]. Thus, these data suggest that the TNF-α-dependent response of the NADPH oxidase is regulated at the transcriptional level.

Summary

In summary, the phagocytic oxidase has emerged as not only an essential component of the innate imme system, but also as an important contributor to multiple pathologies both acute and chronic. Furthermore, recently identified non-phagocytic oxidase functions greatly increase the potential for oxidase utility and the potential capacity to damage the host. As the limiting component of the functional NADPH oxidase, $p67^{phox}$ regulation correlates directly with regulation of superoxide production. *NCF2*, the gene that codes for $p67^{phox}$, is transcriptionally regulated by TNF-α through the NF-κB pathway. Although there is a growing body of evidence addressing transcriptional regulation of *NCF2*, the factor(s) required for the TNF-α responsive upregulation of *NCF2* remains to be determined.

Hypothesis

It is the intention of this dissertation to continue characterization of the transcriptional regulation of the NADPH oxidase. More specifically, this dissertation intends to address the TNF-α responsive region in the intragenic region of the NADPH oxidase used as a site of transcriptional regulation by myeloid cells. Therefore, we hypothesize that the TNF-α responsive region (TRR) is bound by a transcription factor(s) responsible for the transcriptional regulation of the *NCF2* in response to TNF-α. To address this hypothesis, chapter two aims to identify a factor that binds and regulates the

TRR in the intragenic region of *NCF2*. In chapter three, this dissertation aims to characterize the binding features of the factor identified in chapter two. Finally, in chapter four this dissertation aims to characterize the potential upstream factors that interact with the factor identified in chapter two and therefore may subsequently regulate the TNF-α-dependent transcriptional regulation of *NCF2*.

BINDING OF PLEOMORPHIC ADENOMA GENE-LIKE 2 TO THE TNF-α RESPONSIVE REGION OF THE *NCF2* INTRAGENIC REGION REGULATES P67^{PHOX} EXPRESSION AND NADPH OXIDASE ACTIVITY

Introduction

The NADPH oxidase is a multi-component, enzyme complex consisting of both membrane-bound and cytosolic components and is found in all phagocytic leukocytes, such as monocytes and neutrophils, where it plays an essential role in host defense against pathogens [100]. Activation of the NADPH oxidase catalyzes electron transfer from NADPH to molecular oxygen, resulting in the production of superoxide anion (O_2^-) [175]. While O_2^- is in itself not highly microbicidal, conversion of O_2^- into more toxic reactive oxidants, such as hydrogen peroxide and hypochlorous acid, is required for pathogen killing [67].

The essential NADPH oxidase components include a membrane bound flavocytochrome b_{558}, which is a heterodimer of gp91^{phox} and p22^{phox}, and the cytosolic proteins p47^{phox}, p67^{phox}, and p40^{phox} [80]. Additionally, activation of the NADPH oxidase requires the small GTPase Rac(1/2) [176]. Cell-free NADPH oxidase assays suggest flavocytochrome b_{558} and p67^{phox} are sufficient for a functional oxidase; however, *in vivo* the system is clearly more complicated [177]. Although the specific role of p67^{phox} in enzyme function is still being determined, it has been proposed that p67^{phox} is an NADPH-binding protein [84], and Dang *et al*. [178] subsequently showed that p67^{phox} was able to directly bind NADPH. In addition, several groups have shown that p67^{phox} binding to flavocytochrome b_{558} induces conformational changes in flavocytochrome

b_{558}, resulting in initiation of electron flow [86, 179, 180]. The physiological importance of $p67^{phox}$ in NADPH oxidase function is demonstrated by certain forms of chronic granulomatous disease (CGD), which are due to autosomal mutations in *NCF2* [165]. Patients with CGD have an inactive NADPH oxidase, making them susceptible to recurrent bacterial and fungal infections (reviewed in [181]).

Regulation of $p67^{phox}$ expression appears distinct from other *phox* proteins, as $p67^{phox}$ is the last *phox* protein to be expressed during cellular differentiation, and its expression correlates the closest with the acquisition of oxidase activity [128]. Thus, it has been proposed that $p67^{phox}$ may be the rate-limiting cofactor in NADPH oxidase activation [86, 182, 183]. A number of studies indicate that cytokines and inflammatory mediators can modulate the level of expression of several oxidase proteins, including $p67^{phox}$, in mature neutrophils and monocyte/macrophages via transcriptional regulation [122, 184, 185], and the identification of an increasing number of transcription factors involved in the regulation of NADPH oxidase gene expression demonstrates the complexity of this process, (review [129]). To fully understand NADPH oxidase regulation, the identification of the complete repertoire of regulatory factors and characterization of the mechanisms whereby they regulate the NADPH oxidase is essential.

We recently mapped a TNF-α-responsive region (TRR) in the *NCF2* intragenic region and showed that the TRR was essential for TNF-α-induced up-regulation of $p67^{phox}$ [131]. Although the TRR contained no apparent consensus binding sites for currently known transcription factors, DNase footprinting analysis demonstrated binding of nuclear factors to the *NCF2* intragenic region in the region of the TRR [131]. In the

present studies, we used the *NCF2* TRR sequence in a yeast one-hybrid screen to identify transcription factors involved in *NCF2* regulation. We identified a zinc-finger transcription factor, Pleomorphic Adenoma Gene-Like 2 (PLAGL2), as an important regulatory factor that binds the *NCF2* TRR and regulates *NCF2* gene expression in response to TNF-α.

Materials and Methods

Materials

Human TNF-α was from Research Diagnostics, Inc. (Flanders, NJ). Anti-TFIIB antibody was from Active Motif (Carlsbad, CA). 3-amino-1,2,4,-triazole (3-AT) was purchased from Sigma Chemical Co. (St. Louis, MO). Yeast SD minimal base medium and amino acid supplements were from BD Biosciences (San Jose, CA). Unless otherwise noted, all oligomers and primers were from Integrated DNA Technologies (Coralville, IA). Anti-SUMO1 antibodies were from Abcam, Inc. (Cambridge, MA). TrueBlot secondary immunoblot antibodies (anti-rabbit or anti-mouse IgG) were from *e*Bioscience (San Diego, CA). Alkaline phosphatase-conjugated and horseradish peroxidase-conjugated goat anti-rabbit secondary antibodies were from BioRad (Hercules, CA).

Cell Culture

MonoMac1 cells were grown in RPMI 1640 medium supplemented with 10% fetal bovine serum (FBS), penicillin/streptomycin, non-essential amino acids, and sodium pyruvate. HL60 cells were maintained in Dulbecco's modified Eagles medium (DMEM)

supplemented with 10% FBS, penicillin/streptomycin, non-essential amino acids, and sodium pyruvate.

Neutrophils and monocytes were purified from human blood collected from healthy donors in accordance with a protocol approved by the Institutional Review Board at Montana State University. Neutrophils were purified using dextran sedimentation, followed by Histopaque 1077 gradient separation and hypotonic lysis of red blood cells, as described previously [131]. Monocytes were isolated by density gradient centrifugation using OptiPrep medium (Greiner BioOne, Longwood, FL) [131, 186]. Purified neutrophils and monocytes were suspended at 10^5 and 10^7 cells/ml, respectively, in RPMI 1640 supplemented with 10% fetal bovine serum.

Yeast One-Hybrid Assay

The Matchmaker one-hybrid system (Clontech, Mountain View, CA) was used according to the manufacturer's protocol with some modifications. The TRR sequence between -56 and -16 basepairs upstream of the *NCF2* ATG start site was self-ligated to obtain a triplicate sequence. The triplicate TRR was inserted into the TOPO4 Blunt end vector (Invitrogen, Carlsbad, CA), excised with *EcoR1*, and ligated into the bait vectors pHISi, pHIS-1, and pLacZi. Recombinant plasmids were linearized with *Xho1* for pHISi(TRR) and pHIS-1(TRR) and *Nco1* for pLacZi(TRR). Linearized plasmids were integrated into the genome of yeast strain Y187, combining each of the HIS reporter vectors with the LacZi reporter vector. Selection with medium lacking both histidine and uracil selected for clones with both vectors integrated. The double-reporter clones were plated on medium lacking histidine and uracil and titrated with 0-50 mM 3-AT to

determine stringency levels of the leaky *HIS3* expression for the two clones Y187[pHISipLacZi(TRR)] and Y187[pHIS-1pLacZi(TRR)]. Thirty-five mM 3-AT was used to obtain the high-stringency clone Y187[pHIS-1pLacZi(TRR)] and the low-stringency clone Y187[pHISipLacZi(TRR)]. Additionally, transformed clones were assayed for auto-activity. The AH109 yeast strain was transformed with a human leukocyte cDNA library (Clontech) and selected on medium lacking leucine. The bait strain (Y187) and the prey strain (AH109) were mated, and double-positive diploid clones were selected on medium lacking histidine, uracil, and leucine, but supplemented with 35 mM 3-AT. Positive clones were restreaked on selective medium and tested for β-galactosidase activity with an agar overlay assay. Clones positive for β-galactosidase activity for 24 hr were then harvested. The prey plasmids from positive clones were extracted, amplified in *E. coli*, sequenced, and analyzed using the BLAST algorithm.

Table 2.1: Mating Pairs Assayed in Yeast One-Hybrid Screen

Y187 Strain	AH109 Strain
Y187[p53BLUEp53HIS]	AH109[pGAD53]
Y187[p53BLUEp53HIS]	AH109[pGad424]
Y187[pHISi(56-16)pLacZi(56-16)]	AH109[Library]
Y187[pHIS-1(56-16)pLacZi(56-16)]	AH109[Library]
Y187[pHISi(56-16)pLacZi(56-16)]	AH109[pACT2(PU.1)]

Cloning and Expression of PLAGL2

Reverse transcriptase-polymerase chain reaction (RT-PCR) was used to amplify PLAGL2 cDNA from human neutrophil RNA extracted using an RNeasy Mini Kit (Qiagen, Valencia, CA). Primer sequences of the *PLAGL2* sense and antisense primers were 5'-GAATTCAGCCTTGCCATGACCACATTT-3' and 5'-

GAATTCTTGAACCCAGCTCTGAAACG-3', respectively. Full-length *PLAGL2* cDNA was cloned into the pcDNA3.1 eukaryotic expression vector, and the pcDNA3.1(PLAGL2) plasmid was used to express full-length PLAGL2 in the rabbit reticulocyte lysate TNT system (Promega, Madison, WI). The TNT product was immunoblotted using anti-PLAGL2 antibody to confirm the presence and correct size of *in vitro* transcribed and translated PLAGL2. Specificity of the band was established using peptide antigen as a blocking agent.

cDNA and RT-PCR Panel Screening

PLAGL2 gene expression was analyzed in adult human, fetal human, and human immune system cDNA panels (Clontech) using standard PCR conditions (30 cycles of 94^{o}C, 15 sec, 55^{o}C, 30 sec, 68^{o}C, 30 sec). PLAGL2 specific primer sequences were - sense primer, 5'-CAGAGCCCGTGGACATGTT-3', and antisense primer, 5'-CATTACGTCCCGAGAGGCC-3'. Expression was normalized to two housekeeping genes, *18S* and *GAPDH* as previously published [167]. PCR product from neutrophil cDNA was extracted from the gel, re-cloned, amplified, and sequenced to establish that PLAGL2 was truly the PCR product.

Total RNA was isolated from cell lines and human neutrophils and monocytes, and cDNA was prepared, as previously described [131, 186]. PCR amplification was performed as above. *PLAGL2* expression was normalized to previously amplified housekeeping genes *18S* and *GAPDH* [131].

Anti-PLAGL2 Antibody Preparation and Characterization

A peptide corresponding to human PLAGL2 amino acid residues 50-68 (SNGEKLRPHSLPQPEQRPY) (Macromolecular Resources, Ft. Collins, CO) was conjugated to keyhole limpet hemocyanin (KLH, Sigma) using a 25% glutaraldehyde solution (Sigma). KLH-peptide was used to immunize rabbits for polyclonal antibodies and mice for monoclonal antibodies. Monoclonal antibodies were obtained through fusion of the hyperimmune splenocytes with the myeloma line Sp2/0, as previously described [187]. The fusion was screened against recombinant GST-PLAGL2 protein, and positive clones were subcloned by limiting dilutions and rescreened by immunoblotting. Polyclonal anti-PLAGL2 IgG was purified from rabbit antiserum using Protein G Sepharose 4 Fast Flow beads (GE Healthcare, Piscataway, NJ). Monoclonal and polyclonal anti-PLAGL2 antibodies were characterized using recombinant PLAGL2-GST, rabbit reticulocyte *in vitro* translated PLAGL2, and human cell line extracts (HL60 and MonoMac1). Specificity of immunoblot analysis was confirmed using 5 μg/ml peptide antigen as a blocking agent. Unless otherwise indicated, rabbit polyclonal anti-PLAGL2 antibodies were used for immunoblot analysis and mouse monoclonal anti-PLAGL2 antibodies were used for immunoprecipitation.

Immunoprecipitation and Immunoblot Analysis

Immunoprecipitation was performed by preclearing 2 μg MonoMac1 nuclear or cytoplasmic extract with TrueBlot anti-mouse IgG beads for 30 min at 4^{o}C and then incubating the samples with or without anti-PLAGL2 antibodies overnight at 4^{o}C. After addition of 50 μl of TrueBlot anti-mouse IgG beads, samples were incubated an

additional 4 hr at 25°C, and the beads were washed three times with wash buffer (50 μM Tris-HCl, pH 8.0, 150 μM NaCl, 1% NP-40). Bound proteins were eluted by heating the beads for 5 min at 95°C in SDS-PAGE sample buffer containing 50 μM dithiothreitol (DTT) and analyzed by immunoblotting with polyclonal anti-SUMO1 and anti-PLAGL2 antibodies.

For p67^{phox} immunoblot analysis, MonoMac1 cells were seeded at 3×10^5 cells/ml and treated with morpholino 36 hr prior to harvest. At 12 hr prior to harvest 20 ng/ml TNF-α was added. Protein was extracted using a CelLytic NuCLEAR extraction kit (Sigma), and cytosolic fractions were analyzed by immunoblotting with anti-p67^{phox} polyclonal antibodies [91]. Blots were quantified by densitometry.

Electrophoretic Mobility Shift Assay (EMSA)

Complementary oligonucleotides for the TRR and PLAG family consensus (PLAGcon) sequences (see Fig. 2.8) were annealed by heating to 95°C for 2 min and cooled to room temperature. Probes were end-labeled with [γ-^{32}P]ATP using T4 polynucleotide kinase (Ambion, Austin, TX), purified using NucAway Spin columns (Ambion), and specific activity was determined.

Binding reactions were performed by preincubating 3 μl of rabbit reticulocyte-generated PLAGL2 protein for 30 min on ice in buffer containing 10 mM Tris-HCl, pH 7.5, 100 mM NaCl, 50 μM $ZnCl_2$, 10% glycerol, 1 mM $MgCl_2$, 1 mM DTT, and 1 μg poly dA-dT. One ng of end-labeled probe was added to the reaction mixture and incubated for an additional 30 min. For competition assays, unlabeled double-stranded (ds) DNA was incubated with the reaction mixture prior to addition of labeled probe. For

supershift reactions, 10 μg of protein G purified, polyclonal anti-PLAGL2 antibody was added to the reaction mixture prior to addition of the labeled probe. Samples were run on NOVEX 6% DNA Retardation gels (Invitrogen) in TBE running buffer (89 mM Tris-Base, 89 mM boric acid, 2 mM EDTA, pH 8.3). Band shifts were visualized using autoradiography and quantified by densitometry.

Isolation of Nuclear Extracts

HL60 and MonoMac1 cells were seeded at 5×10^5 cells/ml, allowed to recover for 9 hr, and treated with 20 ng/ml TNF-α for the indicated times. Primary human monocytes were plated at 10^5 cells/ml in RPMI on Primaria plates (BD Biosciences) pre-coated with fetal bovine serum, allowed to recover overnight, and treated with fresh RPMI containing 20 ng/ml TNF-α for the indicated times. Primary human neutrophils were plated at 5.5×10^6 cells/ml RPMI on Primaria plates pre-coated for 1 hr with 20% autologous serum and treated immediately with 20 ng/ml TNF-α.

For all cells, nuclear extracts were prepared using a CelLytic NuCLEAR extraction kit (Sigma), according to the manufacturer's protocol. Lysis was performed in the presence of 20 mM N-ethylmaleimide (NEM) (Acros Organics, Geel, Belgium) for detection of PLAGL2. Nuclear extracts were snap-frozen in liquid nitrogen and stored at -80°C.

DNA-Binding Protein Affinity Purification

The bait sequence was prepared by ligation of the TRR sequence at 16°C to obtain a TRR multimer of ~11 to 23 repeats. Fifty pmole of TRR multimer was ligated to the biotinylated oligonucleotide linker sequence bound to streptavidin-coated magnetic

particles (Roche) at 25°C for 1 hr. The TRR-coated particles were washed repeatedly and incubated for 2 hr at 4°C with 50 μg HL60 cell nuclear extract in binding buffer (20 mM HEPES, pH 7.6, 1 mM EDTA, 10 mM ammonium sulfate, 1 mM DTT, 6.25 μg poly dI-dC, 0.63 μg poly-L-lysine). The beads were washed, TRR-binding proteins were eluted with binding buffer containing 2 M KCl for 30 min at 4°C, and the eluates were analyzed by SDS-PAGE. TRR-binding proteins were detected via silver staining and immunoblot analysis using anti-PLAGL2 antibodies. Magnetic beads lacking the ligated TRR sequence were analyzed in parallel to determine background protein binding.

Chromatin Immunoprecipitation (ChIP) Assay

ChIP assays were performed using a ChIP-IT kit (Active Motif), according to the manufacturer's protocol. Cells were seeded at 5×10^5 cells/ml and treated with 20 ng/ml TNF-α for 12 hr. The cells were harvested by centrifugation (4×10^7 total cells), resuspended in RPMI containing 1% formaldyhyde, and fixed for 10 min at room temperature. Nuclear extracts were prepared from the fixed cells, and enzymatic shearing of the chromatin was performed at 37°C for 10 min, followed by addition of ice-cold EDTA to stop the reaction. Sheared chromatin was precleared with protein G beads prior to incubation overnight at 4°C with 4 μg of anti-PLAGL2 antibody, negative IgG control antibody, or positive control antibody against TFIIB (Active Motif), which binds the *GAPDH* intragenic region. A sample of precleared chromatin was reserved for the input in PCR analysis. Antibody/DNA complexes were precipitated with protein G beads, washed, and eluted with a 1% SDS solution. RNA was digested with RNase A, and cross-links were reversed by overnight incubation at 65°C. Protein was digested with

Proteinase K for 2 hr at 42^{o}C, and DNA was purified using the on-column purification method (Active Motif).

Purified, immunoprecipitated chromatin fragments were subjected to quantitative real-time PCR using SYBR Green dye and an ABI 7500 Real Time PCR System, according to the manufacturer's protocol for absolute quantification (ABI). Twenty-five μl of immunoprecipitated DNA in a 50 μl reaction was subjected to 45 amplification cycles. The reserved input DNA was used to obtain the standard curve. PCR amplification of the *NCF2* TRR was performed with primers flanking the TRR (sense primer, 5'-ATCTGGCCCAGAAAGTGA-3', and antisense primer, 5'-CTTCATTCCAGAGGCTGATGG-3'). Primers were optimized on ChIP input template DNA, and specificity was established with dissociation curves. All real-time amplifications were performed in triplicate, and antibody enrichment for the TRR sequence was calculated as % of DNA input. For comparison of transcription factor binding efficiency between TNF-α-treated and untreated cells, anti-TFIIB immunoprecipitated DNA was amplified 40 cycles with primers to the GAPDH intragenic region (sense primer 5-'TACTAGCGGTTTTACGGGCG-3' and antisense primer 5'-TCGAACAGGAGGAGCAGAGAGCGA-3'). Anti-PLAGL2 immunoprecipitated DNA was amplified 40 cycles with primers to the TRR (see above). PCR products were subjected to agarose gel electrophoresis and stained with ethidium bromide.

Morpholino Oligomer Inhibition of PLAGL2 Expression

The morpholino antisense oligomer sequences used were MO1 (5'-CATGTTATTGAGAAAGCCTCCCCAT -3') and MO2 (5'-TACCCCTCCGAAAGAGTTATTGTAC –3'), and the inverted morpholino oligomer sequences used were MO1in (5'-CGCTGGTGAAAAATGTGGTCATGGC -3') and MO2in (5'- CGGTACTGGTGTAAAAGTGGTCGC –3'). Morpholinos were delivered into MonoMac1 cells using the EndoPorter delivery system (Gene-Tools, LLC, Philomath, OR). Briefly, MonoMac1 cells were resuspended in fresh medium with 10 μM morpholino oligomer and 6 μl/ml EndoPorter in complete medium. To verify morpholino delivery, cells were transfected with antisense FITC-labeled morpholino oligomer or mock-transfected and plated for 24 hr. Cells were harvested, washed, resuspended in fresh medium, and viewed with a fluorescent microscope at 100X. To assay for inhibition of PLAGL2 expression, cells were incubated 24 hr with the antisense morpholino oligomer, harvested, and lysed. Cell lysates were analyzed by immunoblotting with anti-PLAGL2 antibody. To evaluate changes in *NCF2* expression, MonoMac1 cells were incubated 24 hr with either the antisense or inverted morpholino oligomers, mock transfected, or not treated with morpholino. Half of each sample was then treated with TNF-α for 12 hr. Cells were harvested, and RNA was extracted using an RNeasy Mini Kit. *NCF2* mRNA was quantified using the ABI 7500 Real-Time PCR System with gene-specific *NCF2* and β-actin probes and primers (ABI). One-step amplification was achieved using the One-Step TaqMan RT-PCR kit (ABI), and amplification was carried out for 40 cycles. Samples were normalized to β-actin.

Analysis of O_2^- Production

MonoMac1 cells were seeded at 3×10^5 cells/ml and treated with morpholino 36 hr prior to harvest. Ten hr prior to harvest, the cells were treated with solvent (control) or 20 ng/ml TNF-α. After washing with Hank's balanced-salt solution containing 10 mM Hepes, pH 7.4 (HBSS), 2.5×10^5 cells were combined with 50 μl Diogenes Complete Enhancer Solution (National Diagnostics, Atlanta, GA), 50 nM PMA (Sigma), and HBSS containing $CaCl_2$ and $MgCl_2$ to a total volume of 100 μl per well in polystyrene flat bottom 96-well, half-area microtiter plates (Corning, Corning, NY). The reactions were monitored for 3 hr using a Fluoroskan Ascent FL microtiter plate reader (ThermoElectron Corp., Milford, MA) with a 1-min reading interval, and integrated chemiluminescence was determined over the full kinetic assay period using Ascent software. All assays were performed in triplicate.

Statistical Analysis

Paired t-tests and one-way ANOVA were performed on the indicated sets of data. Post-test analysis used Tukey's pair-wise comparisons (GraphPad Prism Software, San Diego, CA). Pair-wise comparisons with differences at $P<0.05$ were considered to be statistically significant.

Results

Identification of a TRR-Binding Protein by Yeast One-Hybrid

Previously, we found by DNase footprint analysis that nuclear proteins bind the *NCF2* TRR; however, no identifiable binding elements for known DNA-binding proteins

were apparent in the TRR sequence [131]. To identify TRR-binding proteins, we utilized a yeast one-hybrid assay. The integrated bait sequence used for this assay was a trimer of the TRR sequence located –56 to –16 bp upstream of the start site in the *NCF2* intragenic region (Figure 2.1, Panel A). The TRR-trimer sequence was cloned into the yeast integration and reporter plasmids pHISi, pHIS-1, and pLacZi (Figure 2.1, Panel B) and recombinant plasmids were integrated into the genome of the competent yeast strain Y187, combining pLacZi with either pHISi or pHIS-1 in the same yeast clone creating double-reporter yeast strains. Additionally, the control integration and reporter vectors p53BLUE and p53HIS were linearized and independently integrated into the Y187 yeast genome.

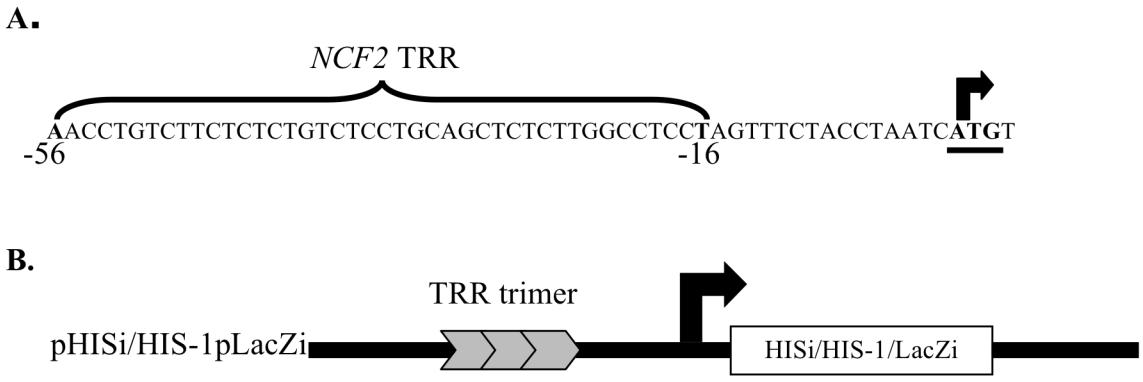

Figure 2.1: Cloning of the TNF-α responsive region (TRR) into the yeast one-hybrid integration and reporter vectors. Panel A: Nucleotide sequence of the *NCF2* TRR and its location relative to the translation start site. Location of the TRR relative to the ATG start site is indicated in basepairs below the sequence. Panel B: Schematic of the yeast one-hybrid TRR trimer bait construct as cloned into the yeast integration and reporter vectors pHISipLacZi or pHIS-1pLacZi.

The difference in the levels of leaky background of the pHISi and pHIS-1 integration and reporter vectors was used to design yeast one-hybrid assays of relative stringency. Using titrated levels of 3-AT with the two reporter strains,

pHISipLacZi(TRR) and pHIS-1pLacZi(TRR), bait strains of two different stringencies were obtained. The Y187 [pHIS-1pLacZi(TRR)] demonstrated high stringency with the leaky *HIS3* expression sensitive to only 10 mM 3-AT, while the Y187 [pHISipLacZi(TRR)] strain was of lower stringency and required 45 mM 3-AT to completely inhibit the leaky background (Figure 2.2). Additionally, all reporter strains were assayed for auto-activity (data not shown).The competent reporter strain AH109 was transformed with a human leukocyte cDNA library fused to the GAL4 activation domain and subsequently mated with the bait strains at a density of $4.5x10^6$ cells per cm^2. To confirm the mating strategy, the AH109 strain was transformed with the positive and negative control vectors pGAD53m and pGAD424, respectively, and diploids were screened for both nutritional and colorimetric gene activity (Figure 2.3, Panel A). The low-stringency assay screened $1.7x10^7$ library clones, while the high-stringency assay screened $4.6x10^7$ library clones. Double- positive, diploid clones were selected on synthetic complete medium lacking histidine, uracil, and leucine and supplemented with 35 mM 3-AT. Of 64 diploid, double-positive (HIS/URA) clones recovered, 21 were from the high-stringency screen and 43 were from the low-stringency screen. Twenty-seven of these clones tested positive for stable β-galactosidase activity in an agar overlay assay (Figure 2.3, Panel B). Of the 27 double-positives with β-galactosidase activity, eleven diploids contained the sequence of a zinc finger transcription factor, Pleomorphic Adenoma Gene-like 2 (PLAGL2) (GenBankTM/EBI accession number NM002657.2). These results implicated PLAGL2 as an *NCF2* TRR-binding protein.

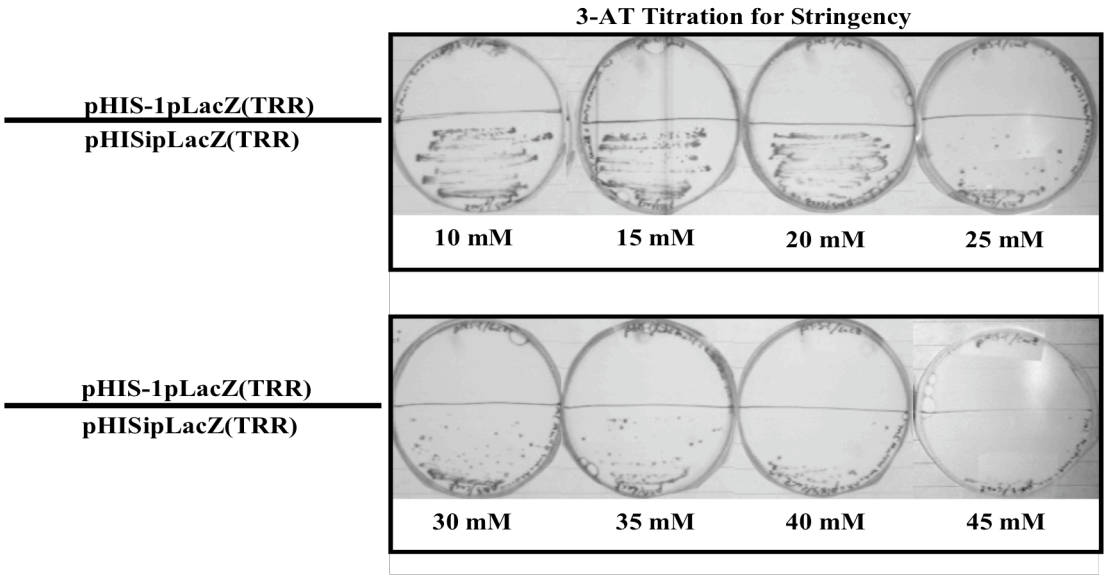

Figure 2.2: 3-AT stringency assay with the pHIS-1pLacZi(TRR) and the pHISipLacZi(TRR) Y187 reporter strains.

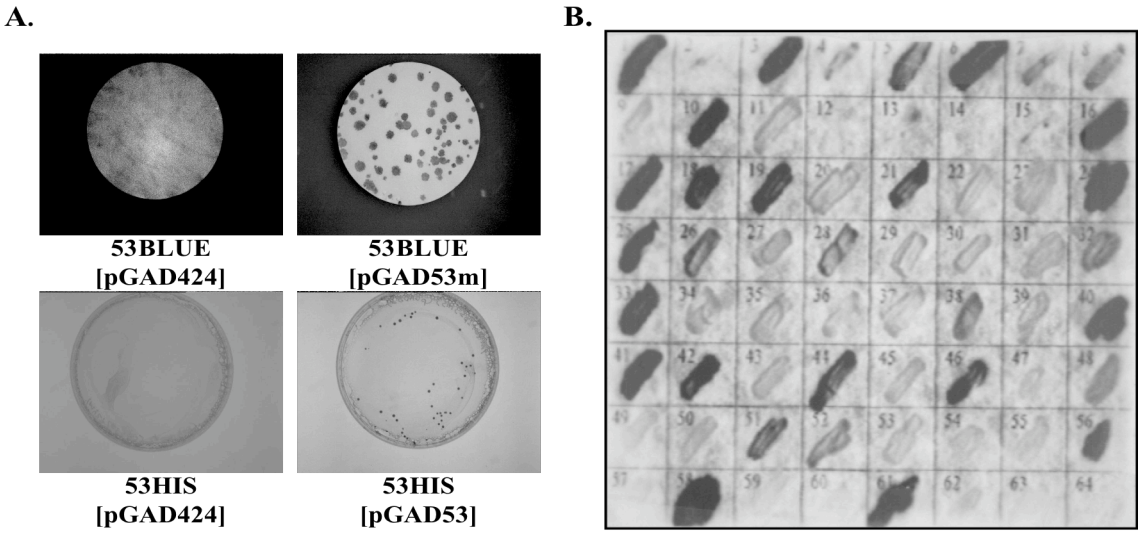

Figure 2.3: Identification of TRR-binding proteins by yeast one-hybrid screening. Panel A: Control assay for yeast mating strategy. The yeast strain Y187 clones were integrated with either the p53BLUE or p53HIS reporter strains. These clones were then mated with AH109 strains carrying the positive or negative control GAL4-AD vectors, pGAD53m or pGAD424, respectively. β–galactosidase activity was determined by filter lift assay. Panel B: Double-positive diploid clones were selected on complete medium lacking histidine, uracil, and leucine, and supplemented with 35mM 3-AT. β-galactosidase positive clones were determined with an agar overlay assay.

Analysis of PLAGL2 Expression in
Human Tissue, Leukocytes, and Cell Lines

The identification of PLAGL2 as a putative TRR-binding protein required that PLAGL2 be expressed in human phagocytes. We evaluated this issue here because initial studies suggested PLAGL2 was expressed in murine embryonic [188] and adult tissues [189], but only in human tissues during embryogenesis [188]. In contrast, a subsequent study by Yang et al. [190] using RT-PCR analysis indicated PLAGL2 was expressed in all human tissues, with higher expression observed in human lung tissues. Due to these inconsistencies, we used PCR to screen a series of human tissue cDNA panels for PLAGL2 expression and found PLAGL2 was ubiquitously expressed in all adult human tissues and almost all fetal human tissues, except for the relatively low level of expression observed in fetal brain (Figure 2.4, Panels A-C).

Although PLAGL2 expression has been reported in a mouse macrophage cell line [189], previous studies did not evaluate expression of PLAGL2 in the human immune system. Since the adult human cDNA panel indicated high levels of PLAGL2 expression in blood leukocytes (Figure 2.4, Panel B), a human immune system cDNA panel was screened for PLAGL2 expression. Consistent with results observed in Figure 2.4, Panel B, PLAGL2 was ubiquitously expressed, with relatively high expression in blood leukocytes (Figure 2.4 Panel D). Further analysis of human primary immune cells and human immortalized cell lines for PLAGL2 expression showed that PLAGL2 message was present in primary phagocytes and a wide range of cell lines including myeloid and lymphoid lineages (Figure 2.4, Panel E). Importantly, control samples containing no

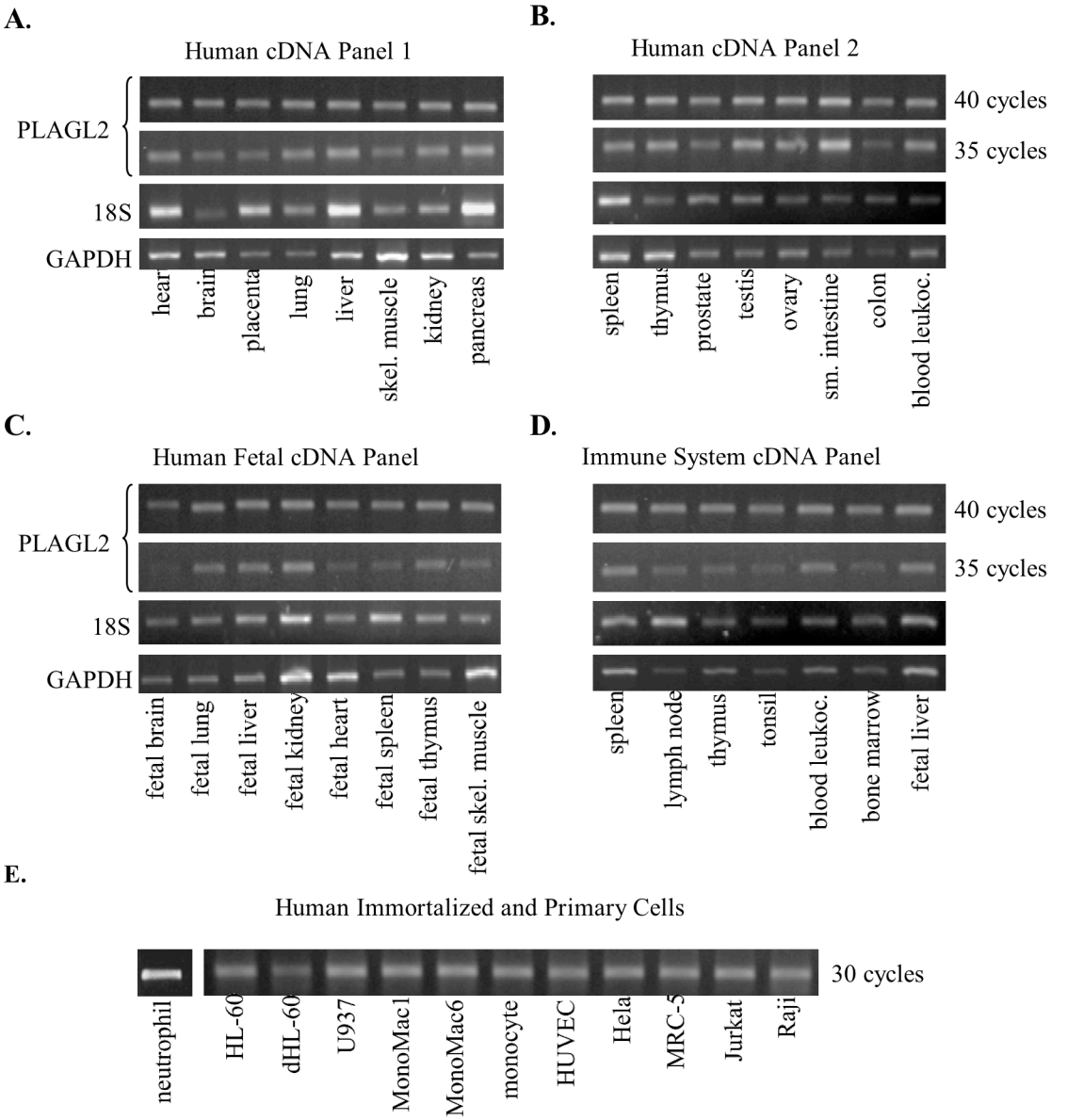

Figure 2.4: Expression of PLAGL2 in human tissue, primary leukocytes, and cell lines. Panel A-D: Semi-quantitative PCR screen of adult and fetal human cDNA panels. PCR amplification was performed with primers specific for PLAGL2, 18S, and GAPDH, as described under Materials and Methods. PCR products were subjected to gel elctrophoresis and stained with ethidium bromide. Panel E: PCR analysis of primary human leukocytes and cell lines. Total RNA was isolated from myeloid cell lines [HL-60, differenciated granulocytic HL-60 (dHL-60, U937, MonoMac1, MonoMac6], and isolated human blood moncytes and neutrophils, as indicated. Non-myeloid cell lines included human umbilical vein endothelial cells (HUVEC), Hela (epithelial cells), MRC-5 (fibroblasts), Jurkat (T cells), and Raji (B cells). RNA (500ng) was subjected to one-step RT-PCR analysis for *PLAGL2*, *18S,* and *GAPDH* and analyzed by agarose gel electrophoresis.

template demonstrated the absence of contamination (data not shown). In addition, the PCR product from neutrophil cDNA was extracted from the gel, re-cloned, amplified, and sequenced to establish that the PCR product was PLAGL2.

Preparation and Characterization of Anti-Human PLAGL2 Antibodies

A peptide corresponding to the published PLAGL2 amino acid sequence at residues 50-68 (CSNGEKLRPHSLPQPEQR) (Figure 2.5) was synthesized and conjugated to KLH. This peptide antigen was chosen because of its minimal sequence similarity to other PLAG family members [191]. Furthermore, this sequence is located between the first and second zinc finger regions of the amino terminus, and these zinc fingers do not appear to be required for DNA binding or transactivation [191, 192]. Thus, antibody binding would likely not interfere with these events. KLH-conjugated peptide was used to immunize rabbits and mice to obtain polyclonal and monoclonal antibodies to PLAGL2, respectively. Both monoclonal (data not shown) and polyclonal antibodies (Figure 2.6) stained endogenous PLAGL2 expressed in human MonoMac1 cells as well as *in vitro*-translated PLAGL2 produced in rabbit reticulocyte lysates. Furthermore, staining specificity was confirmed by addition of peptide antigen, which specifically blocked PLAGL2 staining (Figure 2.6).

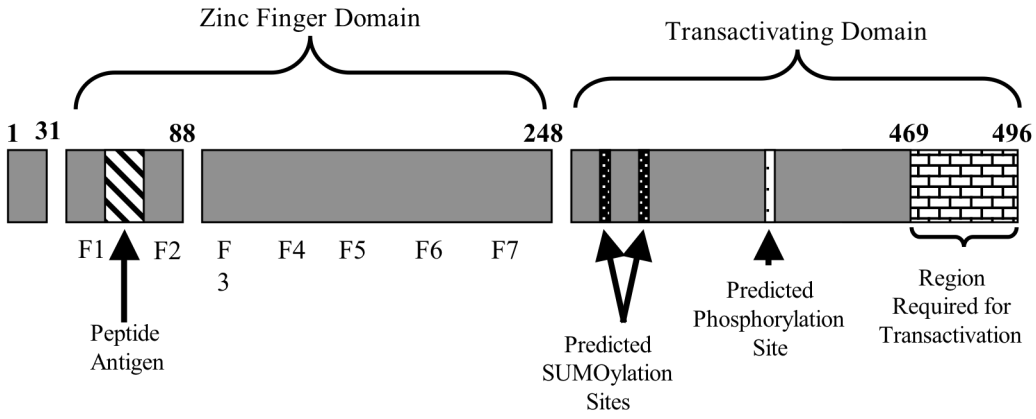

Figure 2.5: Schematic of PLAGL2 protein. See text for details.

Interestingly, immunoblots of MonoMac1 cell extract demonstrated the presence of two bands, and staining of both bands was blocked with peptide antigen (Figure 2.6). Since PLAGL2 has been shown to be modified by SUMO1 [193], we hypothesized that the two anti-PLAGL2 immunoreactive bands might correspond to the native and SUMO1-modifed forms of PLAGL2, which have predicted M_r of 55 and 68 kDa, respectively. To evaluate this issue, we immunoprecipitated PLAGL2 from MonoMac1 cell extracts with anti-PLAGL2 antibodies and blotted the immunoprecipitates with anti-PLAGL2 and anti-SUMO1 antibodies. Two immunoreactive bands, corresponding in size to the predicted M_r of native and SUMO1-modified PLAGL2, were observed in the anti-PLAGL2 immunoblot, and a band corresponding in size to a single SUMO1-modified PLAGL2 was observed in the anti-SUMO1 immunoblot (Figure 2.7). Thus, these data demonstrate our anti-PLAGL2 antibodies are specific for PLAGL2 and recognize both native and SUMO1-modified forms of the protein.

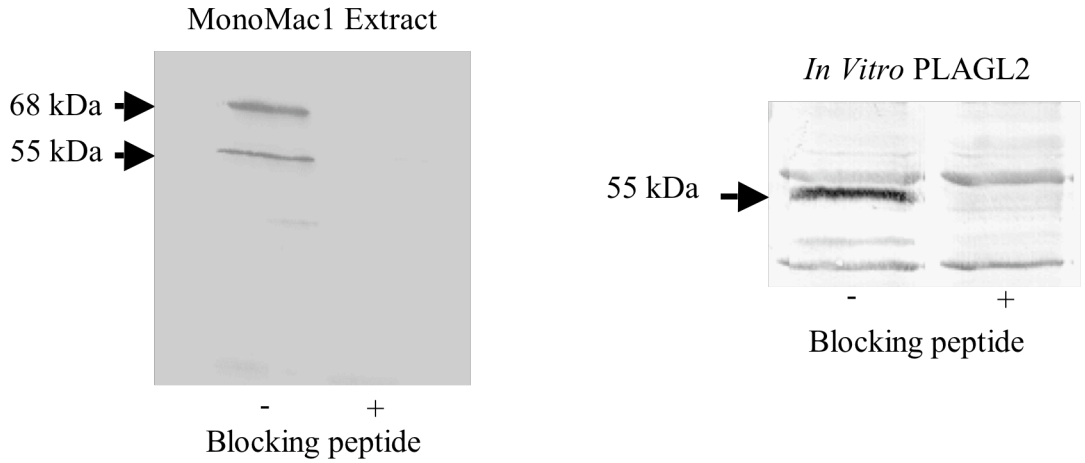

Figure 2.6: Characterization of anti-PLAGL2 antibodies. Immunoblot analysis of MonoMac1 cell extract and rabbit reticulocyte lysate-translated PLAGL2. Samples were probed with anti-PLAGL2 either in the presence (+) or absence (-) of blocking peptide. Arrows indicate locations of the specific anti-PLAGL2 immunoreactive bands.

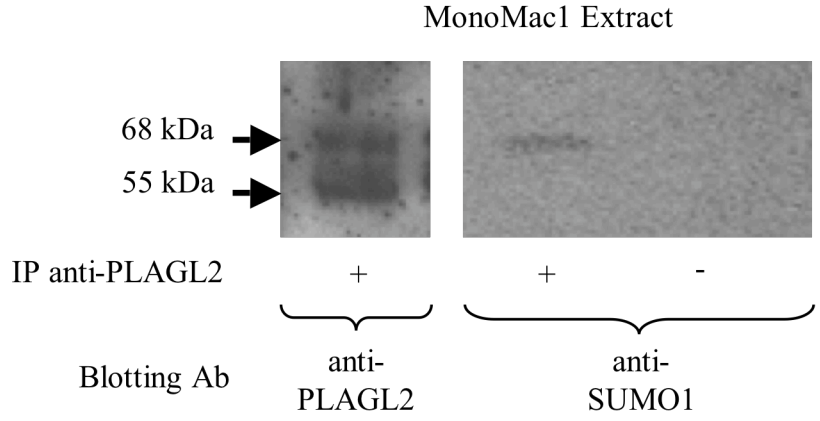

Figure 2.7: PLAGL2 extracts from MonoMac1 cells are SUMO1 modified. Immunoblot analysis of PLAGL2 immunoprecipitated from MonoMac1 cells. MonoMac1 extracts were immunoprecipitated with (+) or without (-) anti-PLAGL2 (IP anti-PLAGL2) antibodies, as indicated. Immunoprecipitates were subjected to SDS-PAGE, transferred to nitrocellulose membrane, and probed with either anti-PLAGL2 or anti-SUMO1 antibodies, as indicated. Arrows indicate locations of the two PLAGL2 immunoreactive bands.

In Vitro Translated PLAGL2 Binds the *NCF2* TRR

Electrophoretic mobility shift assay (EMSA) with *in vitro*-translated PLAGL2 was used to further investigate binding of PLAGL2 to the TRR. As seen in Figure 2.8, Panel B, (lane 1) PLAGL2 shifted the radiolabeled TRR probe, whereas pre-incubation with cold TRR double-stranded (ds) oligonucleotide completely eliminated this band shift (Figure 2.8, Panel B, lane 2). Because the mapped TRR sequence does not share sequence similarity to the published PLAG family consensus binding sequence (PLAGcon) [188] (Figure 2.8, Panel A), cold PLAGcon ds oligonucleotide was also used as a competitor for comparison. Pre-incubation of *in vitro*-translated PLAGL2 with cold PLAGcon also completely eliminated the EMSA band shift, establishing that *in vitro* translated PLAGL2 binds both the TRR and the PLAGcon (Figure 2.8, Panel B, lane 3). Furthermore, pre-incubation with an irrelevant, cold ds oligonucleotide did not compete away the EMSA band shift, indicating that *in vitro* PLAGL2 bound both the TRR and the PLAGcon in a sequence-specific manner (Figure 2.8, Panel B, lane 4).

To further establish specificity of PLAGL2 binding to the TRR sequence, *in vitro*-translated PLAGL2 was pre-incubated with anti-PLAGL2 antibodies prior to addition of TRR probe. As shown in Figure 2.8, Panel B the PLAGL2 band was supershifted by the anti-PLAGL2 antibody (lane 5) but not by a non-specific antibody (lane 6).

A.

- PLAGcon: AGCTACAACAGGGGGCCTTAGAAGGGGTACTAC
- *NCF2*(TRR): CCAACCTGTCTTCTCCCTGTCTCCTGCAGCTCTCTTGGCCTCCT

B.

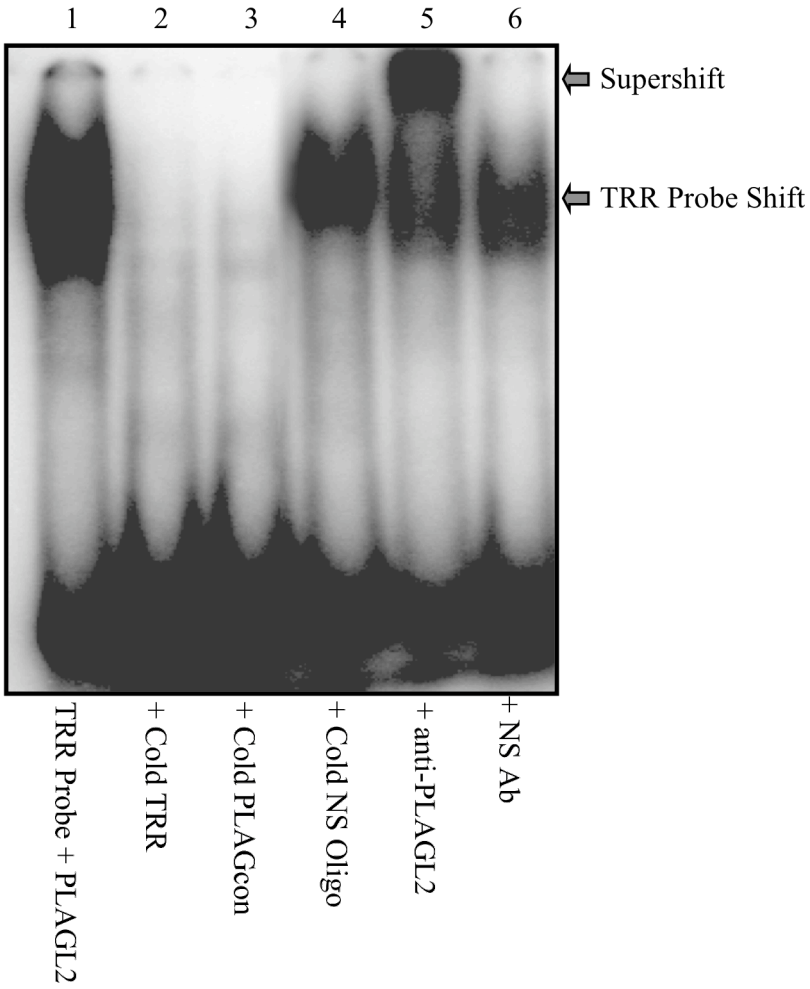

Figure 2.8: *In vitro* translated PLAGL2 binds the TRR. Panel A: Comparison of PLAG family consensus binding sequence (PLAGcon) and the NCF2 TRR sequence (NCF2 TRR). Panel B: EMSA analysis. Represents at least three experiments. See text for details.

The lack of similarity between the PLAGcon and TRR sequences prompted us to evaluate the relative affinity of PLAGL2 for these probes. Preincubation of PLAGL2 with increasing amounts of cold TRR prior to addition of labeled PLAGcon showed that

PLAGcon binding was reduced in a concentration-dependent manner and that 100-fold excess TRR completely blocked PLAGcon binding (Figure 2.9, Panel A, lane 9). Likewise, addition of cold PLAGcon reduced binding of labeled TRR; however, PLAGcon appears to bind with higher affinity, as only a 5-fold excess of cold PLAGcon was required to block binding of the labeled TRR probe (Figure 2.9, Panel B, lane 5). Densitometric analysis of the autoradiographs confirmed that PLAGL2 has a relatively higher affinity for the PLAGcon sequence relative to the TRR sequence (Figure 2.10).

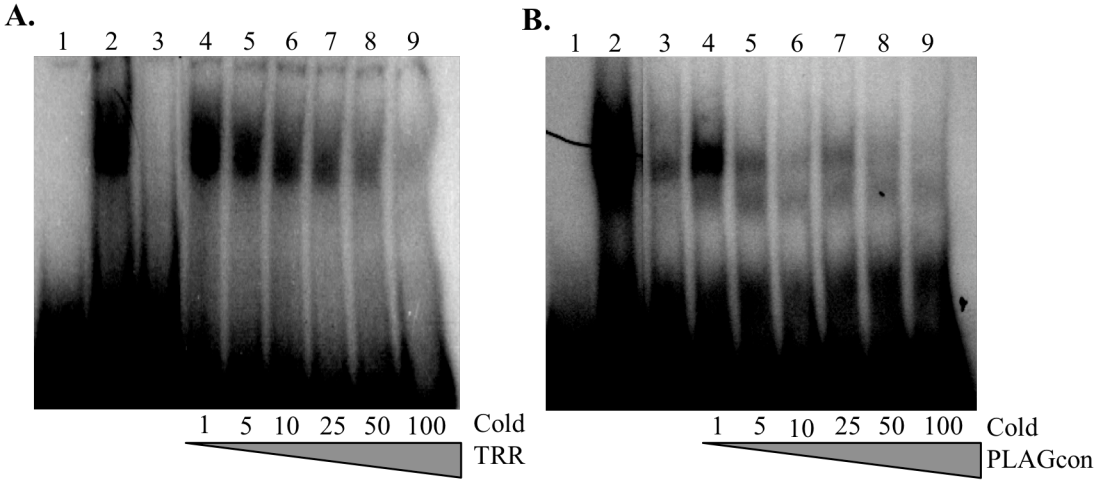

Figure 2.9: Analysis of PLAGL2 relative affinity for PLAGcon and *NCF2* TRR. Panels A and B: *In vitro* translated PLAGL2 protein-DNA complexes (lane 2) were competed with cold PLAGL2con or cold TRR (lane 3). Competitors were preincubated with protein in increasing concentrations of 1, 5, 10, 25, 50, and 100 fold excess of labeled probe (lanes 4-9 and lanes 4-9). Blot representative of at least three experiments.

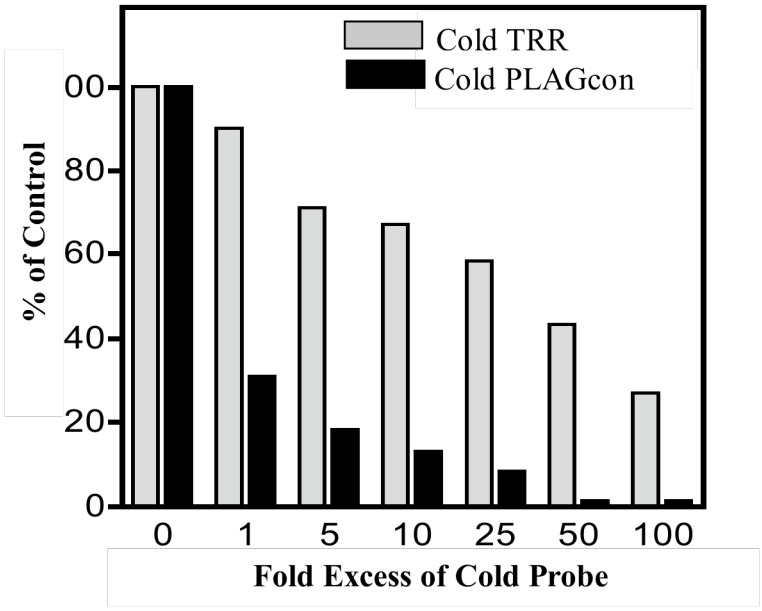

Figure 2.10: PLAGL2 protein has enhanced binding affinity for the PLAGcon sequence. Densitometric analysis of a representative EMSA blots plotted as % binding relative to the uncompleted probe.

Native and SUMO1-Modified
Endogenous PLAGL2 Bind the TRR *In Vitro*

In conjunction with the yeast-one hybrid screen, we performed DNA-binding protein affinity purification to isolate TRR-binding proteins. Magnetic particles coated with TRR concatamers were incubated with HL60 cell nuclear extract, and bound proteins were eluted and analyzed by SDS-PAGE and silver staining (Figure 2.11 Panel A). A band migrating at ~55 kDa, the predicted M_r of native PLAGL2, was observed in the sample containing the TRR but not in the TRR-negative sample.

With the development of the anti-PLAGL2 antibodies, we evaluated the affinity bead eluate to determine if the silver-stained band was PLAGL2 (Figure 2.11, Panel B).

Indeed, two bands were observed, corresponding in M_r to the native and SUMO1-modified PLAGL2 bands observed in previous immunoblots (Figure 2.11, Panel A-B). The SUMO1-modified PLAGL2 band observed in the PLAGL2 immunoblot (Figure 2.11, Panel B) was likely not observed in the silver stained gel (Figure 2.11, Panel A) due to the presence of non-specific background bands overlapping in the region where modified PLAGL2 migrated. Overall, these data clearly demonstrate that both the native and SUMO1-modified forms of endogenous PLAGL2 bind the TRR *in vitro*.

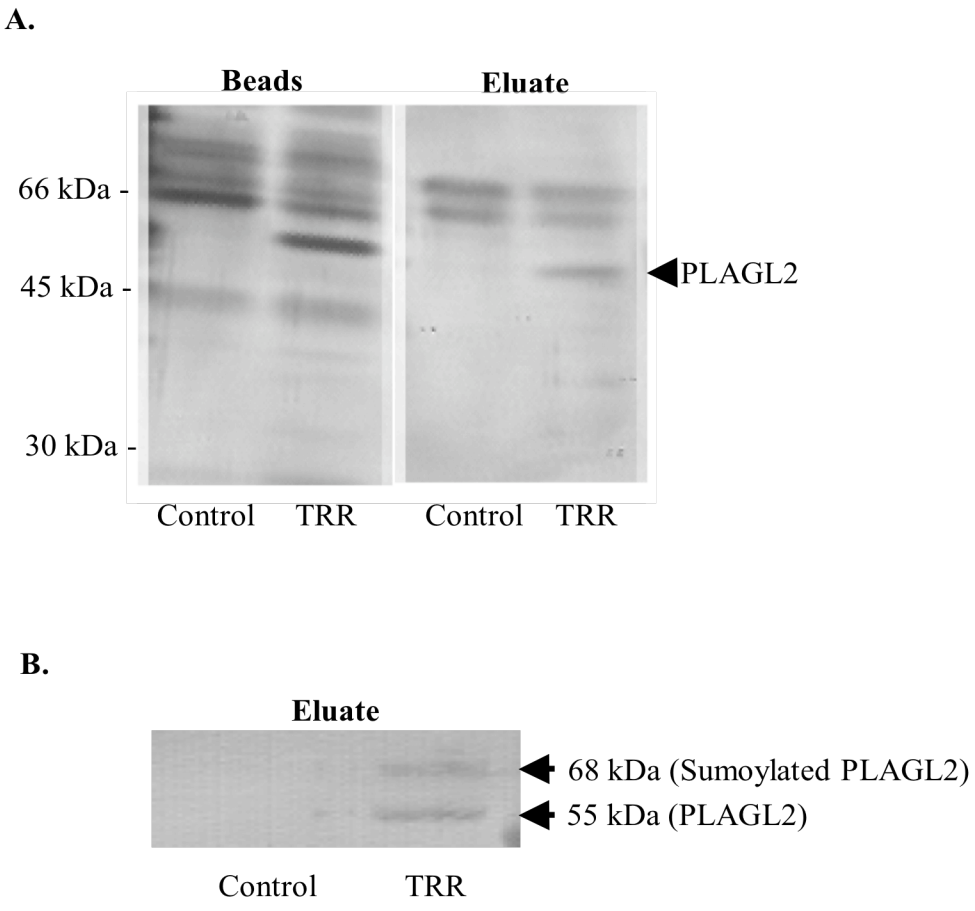

Figure 2.11: Native and SUMO1-modified PLAGL2 bind the TRR. Panel A: Analysis of proteins isolated by TRR DNA-binding protein affinity purification. Panel B: Immunoblot analysis of proteins isolated by TRR DNA-binding protein affinity purification. Two bands corresponding to the predicted Mr of native and SUMO1-modified PLAGL2 are indicated with arrows. Control indicates parallel experiment with OCT2A binding site ligated to beads.

In Vivo Binding of Endogenous PLAGL2 to the TRR is Enhanced with TNF-α Treatment

Quantitative chromatin immunoprecipitation assay (ChIP) analysis with PLAGL2-specific antibody was used to determine if PLAGL2 binds the TRR *in vivo*. As shown in Figure 2.12, Panel A, untreated MonoMac1 cells showed a significant enrichment of the TRR immunoprecipitated with PLAGL2 (anti-PLAGL2) as compared to mock immunoprecipitation (IgG). Furthermore, this enrichment was greatly enhanced by TNF-α treatment of the cells prior to cross-linking (Figure 2.12, Panel C). To insure that the enhanced enrichment with TNF-α was specific to the *NCF2* TRR, PCR samples of the anti-PLAGL2 immunoprecipitated TRR and an anti-TFIIB immunoprecipitated GAPDH intragenic region sequence were run in parallel for both untreated and TNF-α-treated cells. Whereas a similar PCR amplification was observed for the GAPDH intragenic region sequence immunoprecipitated with anti-TFIIB antibody (Figure 2.12, Panel C, lanes 1 and 2), the amplification of the TRR in TNF-α-treated cells was clearly enhanced when compared to that in untreated cells (Figure 2.12, Panel C, lanes 3 and 4). Thus, these data demonstrate that endogenous PLAGL2 binds to the TRR in the *NCF2* intragenic region *in vivo* and that this binding is enhanced by TNF-α treatment.

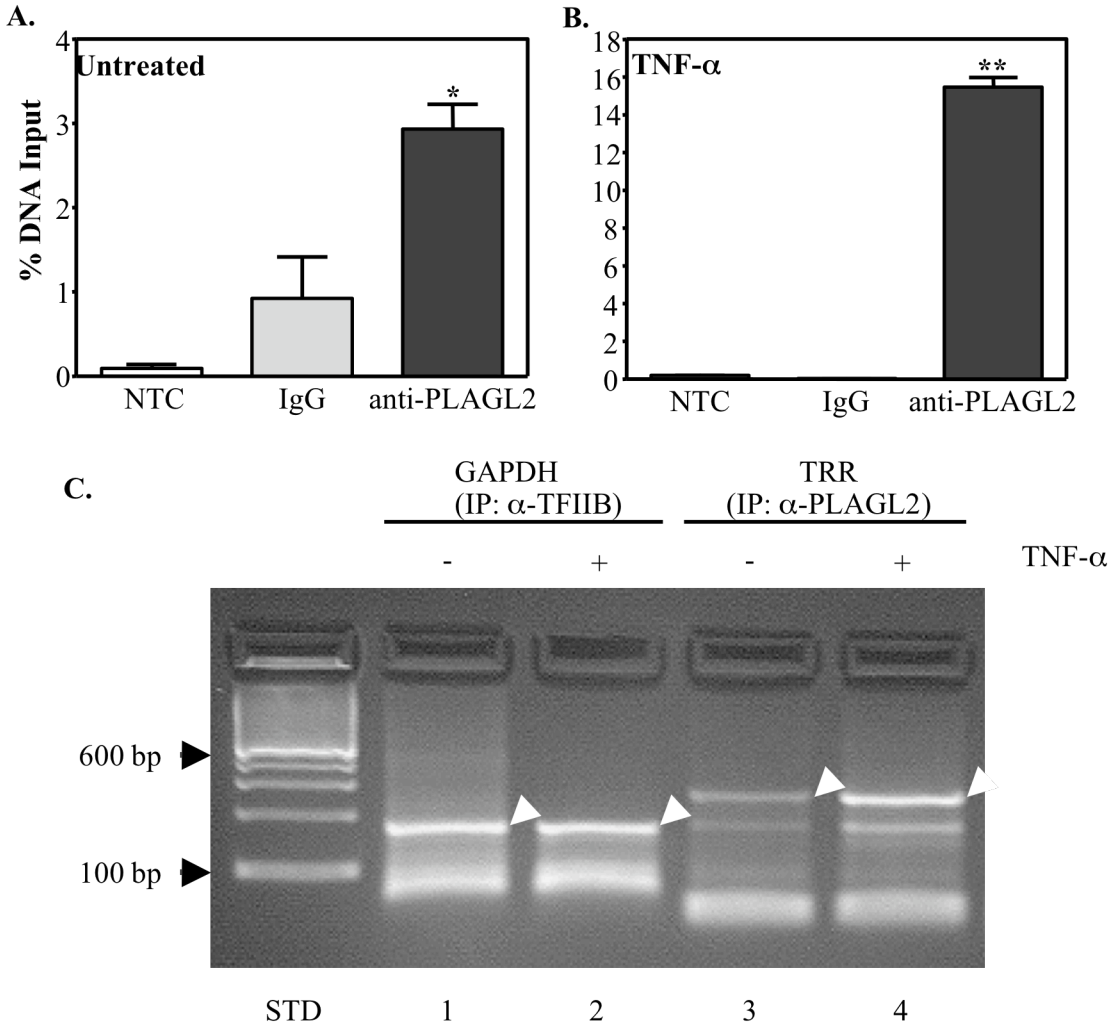

Figure 2.12: Endogenous PLAGL2 binds the *NCF2* TRR sequence *in vivo*. Panel A: Quantitative ChIP analysis of the *NCF2* TRR. Cross-linked chromatin was immunoprecipitated with either anti-PLAGL2 antibody or negative control IgG from MonoMac1 cells incubated without (untreated) and with TNF-α, as indicated. Crosslinks were reversed, and the DNA was purified and analyzed using quantitative PCR with *NCF2* TRR-specific primers. No template controls (NTC) were run in parallel and samples were analyzed in triplicate. Results are presented as % of input DNA (mean ± SD) from three experiments. Statistically significant differences between anti-PLAGL2 immunoprecipitated DNA and control IgG immunoprecipitated DNA (*, $P<0.05$; **, $P<0.001$) are indicated. Panel C: ChIP was performed as above using either anti-PLAGL2 or anti-TFIIB antibodies and chromatin isolated from cells without (-) or with TNF-α-treatment (+). Primers specific for amplification of either the *NCF2* TRR or the *GAPDH* intragenic region were used for PCR analysis of the immunoprecipitated DNA. PCR products were subjected to agarose gel electrophoresis and stained with ethidium bromide. Results are representative of three individual experiments.

Knock-Down of Endogenous PLAGL2 Inhibits the TNF-α Response in MonoMac1 Cells

Due to the toxicity of PLAGL2 over-expression in transfected MonoMac1 cells (data not shown), a knock-down strategy using morpholino oligonucleotides [194] was performed to determine if changes in PLAGL2 expression altered TNF-α-induced upregulation of *NCF2 in vivo*. We designed one morpholino oligonucleotide to bind to a region of *PLAGL2* mRNA just upstream of the start site (Figure 2.13, Panel A, PL2 AS MO1) and one morpholino oligonucleotide to bind a region of *PLAGL2* mRNA flanking the ATG start site (Figure 2.13, Panel A, PL2 AS MO2). A BLAST search with these morpholino sequences for non-specific targets demonstrated there were no known targets in the human genome besides PLAGL2. Morpholinos encoding the inverse of these sequences were used as controls.

To establish effective delivery of morpholinos, FITC-labeled morpholinos were combined with EndoPorter and incubated with MonoMac1 cells. In general, diffuse fluorescence across the cell was observed, indicating successful permeablization of the endosomal compartment and delivery to the cytosol (Figure 2.13, Panel B, upper right panel). Transfection efficiency was determined to be >90%. Mock treatment with the delivery agent alone showed only background fluorescence with no cell staining (Figure 2.13, Panel B, lower right panel).

To confirm PLAGL2 protein expression was successfully knocked-down, immunoblot analysis was performed using MonoMac1 cell lysates after mock treatment or treatment with PLAGL2 antisense morpholinos. After 24 hr of morpholino treatment,

both the native and SUMO1-modified PLAGL2 proteins were knocked-down to levels undetectable by immunoblot analysis (Figure 2.13, Panel C).

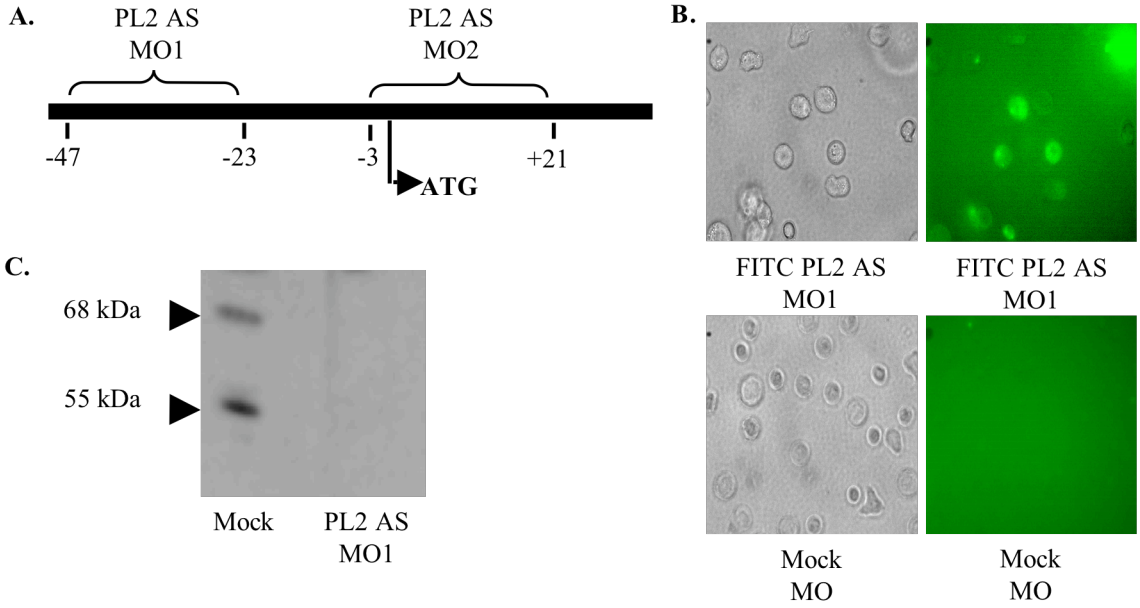

Figure 2.13: Morpholino knock-down of PLAGL2 protein expression. Panel A: Schematic showing location of antisense morpholino 1 (PL2 AS MO1) and 2 (PL2 AS MO2) relative to the ATG translation start site of the *PLAGL2* transcript. Control morpholinos were designed as inverted sequences of the corresponding antisense morpholino. Panel B: Delivery of morpholinos into MonoMac1 cells using EndoPorter. FITC-labeled antisense PLAGL2 morpholinos were delivered into MonoMac1 cells, and fluorescence was visualized. Successful morpholino delivery shows a diffuse fluorescence across the transfected cell. On the left are corresponding bright field images of the fluorescent images. Panel C: Inhibition of PLAGL2 protein expression by *PLAGL2* antisense morpholino treatment in MonoMac1 cells. Cells were treated for 24 hr with *PLAGL2* antisense morpholinos (PL2 AS MO1) or were mock transfected (mock), lysed, and analyzed by immunoblotting for PLAGL2. Native (55 kDa) and SUMO1-modified (68 kDa) PLAGL2 proteins are indicated with arrows.

Using these experimental conditions, we analyzed the effect of PLAGL2 protein expression on TNF-α-induced upregulation of *NCF2* mRNA. Quantitative RT-PCR analysis in MonoMac1 cells demonstrated an ~7-fold increase in *NCF2* mRNA levels in TNF-α-treated MonoMac1 cells compared to untreated cells (Figure 2.14, Panel A). As shown in Figure 2.14, Panel B, transfection with PLAGL2 antisense morpholino resulted

in a statistically significant decrease in the TNF-α-induced fold change in *NCF2* mRNA expression (Mock vs. PL2 AS MO1 or PL2 AS MO2). In comparison, the TNF-α-dependent fold increase in *NCF2* message in mock treated cells was not significantly inhibited by transfection with inverted PLAGL2 morpholinos (Figure 2.14, Panel B, Mock vs. PL2 MO1in or PL2 MO2in). Increasing the morpholino treatment to 48 hr did not significantly increase the knock-down effect on TNF-α-induced *NCF2* message (data not shown). Thus, these results directly confirm PLAGL2 is required for the TNF-α-induced increase in *NCF2* transcript.

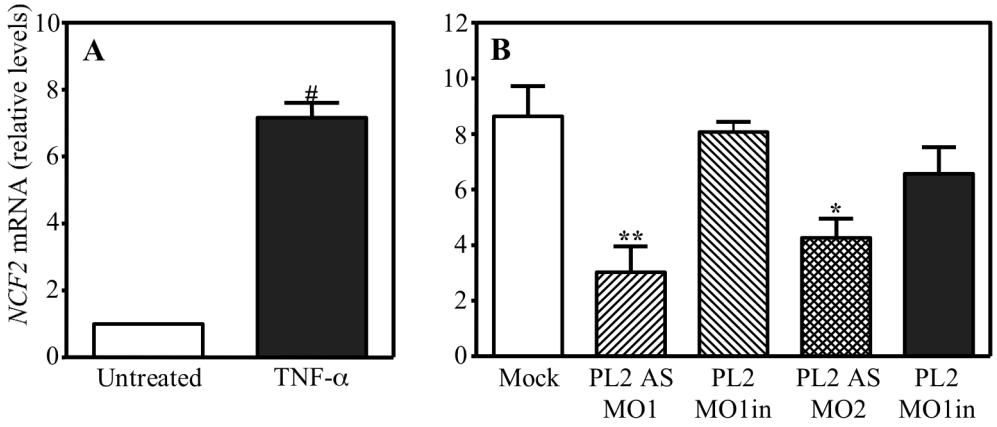

Figure 2.14: Morpholino knock-down of PLAGL2 protein expression inhibits TNF-α-induced up-regulation of *NCF2* transcript. Panel A: TNF-α-dependent upregulation of *NCF2* mRNA in MonoMac1 cells. Cells were untreated or treated with TNF-α for 12 hr prior to RNA extraction, and relative expression of *NCF2* was analyzed using quantitative RT-PCR with β-actin as the endogenous control. Data are presented as relative *NCF2* mRNA levels with the untreated sample set to 1. Statistically significant difference (#, $P<0.01$) between untreated and TNF-α-treated samples is indicated. Panel B: Knock-down of PLAGL2 expression inhibits the TNF-α-induced up-regulation of *NCF2*. MonoMac1 cells were either mock treated with EndoPorter, transfected with the antisense morpholinos (PL2 AS MO1, PL2 AS MO2), or transfected with the inverted morpholino controls (PL2 MO1in, PL2 MO2in), as indicated. After 24 hr, half of each sample was treated with TNF-α for 12 hr, and RNA was extracted. Expression of *NCF2* was analyzed using quantitative RT-PCR with β-actin as the endogenous control. Data are presented as fold change of *NCF2* mRNA levels in TNF-α cells relative to the corresponding untreated control for each sample and are representative of three separate experiments. Statistically significant differences (*, $P<0.01$; **, $P<0.05$) between the mock/TNF-α-treated and the morpholino/TNF-α-treated samples are indicated.

To determine whether expression of p67^{phox} protein correlated with the observed reduction in *NCF2* message in PLAGL2 antisense morpholino-treated cells, we also analyzed p67^{phox} expression by immunoblotting (Figure 2.15, Panel A) and densitometric analysis (Figure 2.15, Panel B) of the blots. As shown in Fig. 2.15, p67^{phox} protein expression increased ~80% after TNF-α treatment, relative to the non-TNF-α control (NT+ vs. NT-); whereas, knock-down of PLAGL2 almost completely blocked the TNF-α-induced upregulation of p67^{phox} protein (MO1+ vs. MO1-). In contrast, treatment with the inverted PLAGL2 morpholino had no significant effect on p67^{phox} expression (MO1in+ vs. MO1in-). Thus, these results confirm that PLAGL2 is required for TNF-α-induced upregulation of p67^{phox} protein.

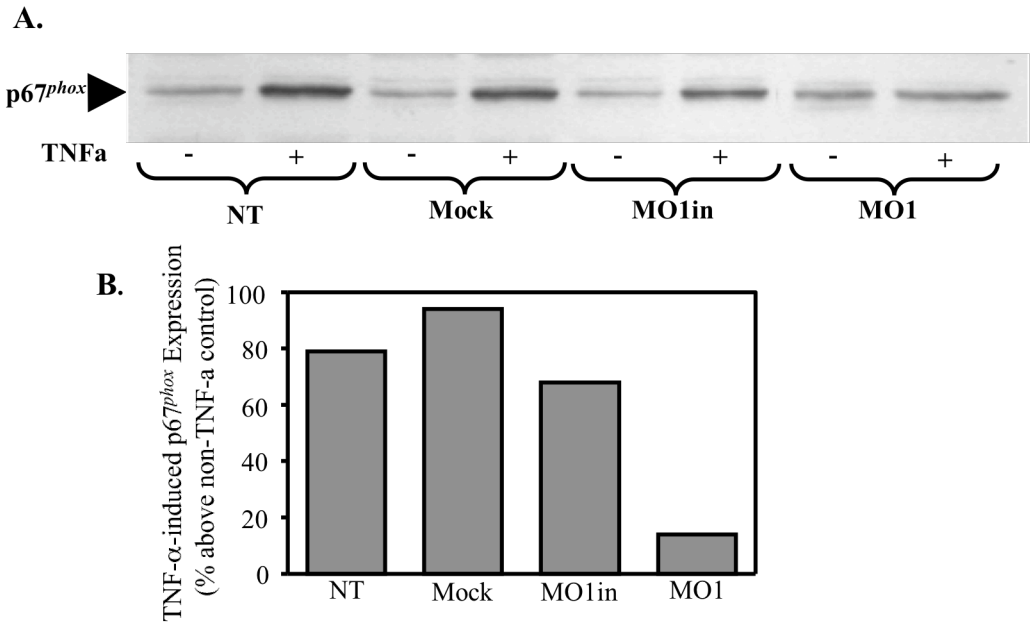

Figure 2.15: Knock-down of PLAGL2 protein inhibits TNF-α-upregulation of p67^{phox} protein. Panel A: MonoMac1 cells (NT), cells treated with EndoPorter (Mock), and cells treated with EndoPorter and the indicated antisense morpholino (MO1) or inverted morpholino (MO1in) were treated with control buffer or TNF-α. Cell extracts were immunoblotted with antibodies against p67^{phox}. Panel B: Immunoblots were analyzed by densitometry and data are presented as the relative % change in TNF-α-induced p67^{phox} protein expression vs. the corresponding non-TNF-α control sample.

Previous work in our lab showed a positive correlation between TNF-α-dependent upregulation of *NCF2* message and O_2^- production [131]. Having shown that knock-down of endogenous PLAGL2 protein inhibits the TNF-α-induced upregulation of *NCF2* message and $p67^{phox}$ protein, we used the morpholino knock-down strategy to evaluate the effect of PLAGL2 on O_2^- production in response to TNF-α. In MonoMac1 cells, TNF-α treatment for 10 hr increased PMA-induced O_2^- production ~3-fold (Figure 2.16, Panel A); whereas, morpholino antisense knock-down of PLAGL2 inhibited the TNF-α-dependent increase in O_2^- production, as compared to mock treated cells (Figure 2.16, Panel B). Importantly, the inverted morpholino control did not significantly affect O_2^- production, thus providing direct evidence that PLAGL2 is required for the TNF-α-dependent increase in O_2^- production observed in MonoMac1 cells.

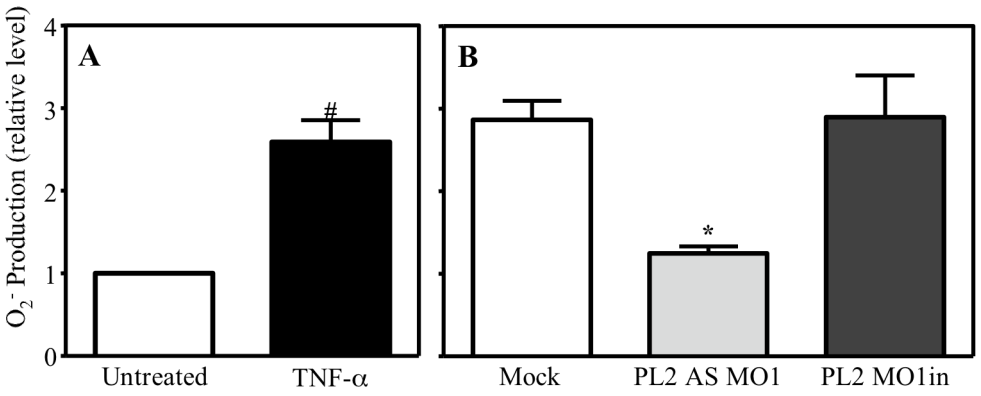

Figure 2.16: Knock-down of PLAGL2 protein inhibits TNF-α-upregulation of NADPH oxidase activity. Panel A: TNF-α treatment of MonoMac1 cells enhances O_2- production. Data are presented as relative levels of O_2-, the untreated sample set to 1. Statistically significant difference (#, $P<0.05$) between untreated and TNF-α-treated samples is indicated. Panel B: Knock down of PLAGL2 protein inhibits TNF-α induction of O_2- production. Cells were treated with EndoPorter alone (Mock) or EndoPorter and the indicated morpholinos, followed by TNF-α treatment. Data are presented as fold change in integrated chemiluminescence between TNF-α-treated samples and the untreated controls. Statistically significant differences between TNF-α-treated samples and morpholino + TNF-α-treated samples (*, $P<0.05$) are indicated.

TNF-α Modulates the Levels of Native and
SUMO1-Modified PLAGL2 Protein in MonoMac1
Cells and Human Primary Monocytes and Neutrophils

Based on the present data indicating PLAGL2 plays a role in regulating *NCF2*, we considered the possibility that this effect may be due to the effects of TNF-α on *PLAGL2* expression. Evaluation of *PLAGL2* in TNF-α. treated MonoMac1 cells showed no significant change in *PLAGL2* mRNA or protein levels relative to non-treated cells (Figure 2.17, Panel A-B).

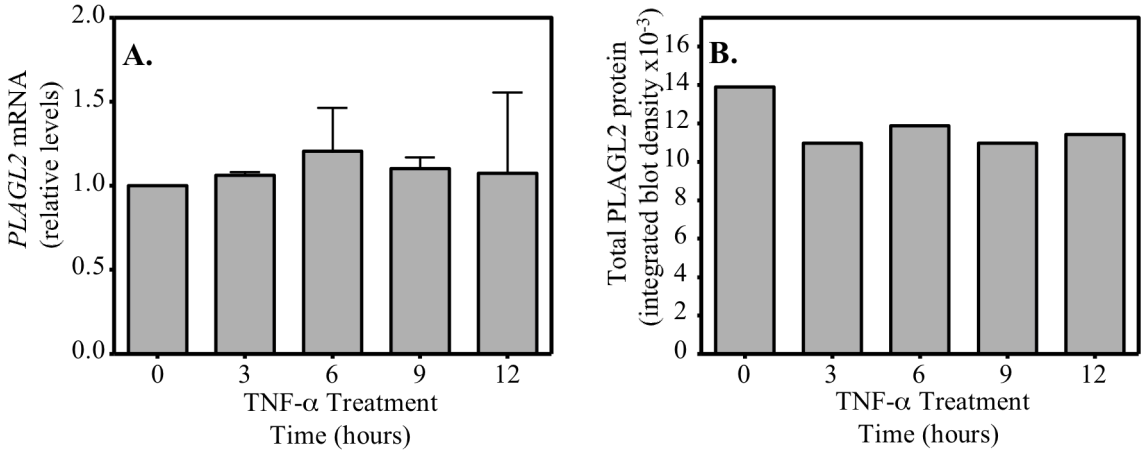

Figure 2.17: Neither PLAGL2 message or total protein changes with TNF-α treatment. Panel A: Relative expression levels of PLAGL2 mRNA do not significantly change over time with TNF-a treatment. Quantitative RT-PCR was used to determine the relative level of PLAGL2 mRNA in total RNA isolated at the indicated times from MonoMac1 cells treated with 20 ng/ml TNF-α. The data are presented as fold-change in PLAGL2 mRNA levels (mean ± SD) with the non-TNF-α treatment sample set to 1. Results are representative of three experiments run in triplicate. β-actin was used as the endogenous control. Panel B: Densitometry of total PLAGL2 protein in MonoMac1 cells treated with TNF-α. Nuclear and cytosolic fractions were prepared from MonoMac1 cells treated for the indicated times with 20 ng/ml TNF-α, and the samples were analyzed by immunoblotting for PLAGL2. Densitometric analysis of the PLAGL2 immunoreactive bands was preformed, and the combined densities of the nuclear and cytosolic fractions for each time point are plotted. The data are representative of three experiments.

Recent studies suggested that SUMO1 modification suppresses PLAGL2 transcription [193]; therefore, we hypothesized that TNF-α may affect PLAGL2 activity by modulating the relative levels of native versus SUMO1-modified PLAGL2. Nuclear and cytosolic extracts were isolated in the presence of NEM, a reagent shown to inhibit the loss of SUMO1 modification, and analyzed for PLAGL2. In untreated MonoMac1 cells, the majority of nuclear PLAGL2 was SUMO1-modified, while the majority of cytosolic PLAGL2 was not modified (Figure 2.18, Panel A). However, TNF-α treatment led to significant changes in the nuclear and cytosolic levels of both native and SUMO1-modified PLAGL2. In nuclear fractions, native PLAGL2 accumulated, while SUMO1-modified PLAGL2 decreased over the first 6 hr. At longer times (9-12 hr), this pattern was reversed, as native PLAGL2 decreased and SUMO1-modified PLAGL2 accumulated in the nucleus (Figure 2.18, Panel A). In cytosolic fractions, both native and SUMO1-modified PLAGL2 exhibited a biphasic expression pattern, decreasing for the first 3 hr and then increasing in a time-dependent manner from 6 to 12 hr after TNF-α treatment (Figure 2.18, Panel A). Thus, these data indicate that TNF-α treatment affects the relative levels of the active (native) and repressive (SUMO1-modified) forms of PLAGL2 protein in the nucleus and cytosol of MonoMac1 cells.

PLAGL2 was also analyzed in nuclear and cytosolic fractions isolated from TNF-α-treated human monocytes and neutrophils. In monocytes, TNF-α treatment induced a steady accumulation of native PLAGL2 in both the nuclear and cytosolic fractions, as well as a time-dependent accumulation of SUMO1-modified PLAGL2 in the cytosol (Figure 2.18, Panel B). In contrast to MonoMac1 cells, there was no detectable SUMO1-modified PLAGL2 in monocyte nuclear fractions, even after 12 hr of TNF-α treatment

(Figure 2.18, Panel B). It is possible, however, that SUMO1-modified PLAGL2 is present a very low levels below our detection limit. Neutrophils were also characterized by a unique pattern of PLAGL2 expression. As with MonoMac1 cells and monocytes, native PLAGL2 accumulated in a time-dependent manner in neutrophil nuclear fractions (Figure 2.18, Panel C). SUMO1-modified PLAGL2 was also detected in nuclear fractions from untreated neutrophils and slowly decreased over time with TNF-α treatment (Figure 2.18, Panel C). Additionally, SUMO1-modified PLAGL2 also accumulated in neutrophil cytosol, peaking at 3 hr and then decreasing to basal levels by 9 hr post-treatment (Figure 2.18, Panel C). Overall, these data clearly demonstrate that TNF-α treatment results in compartmentalized changes in the relative levels of native and SUMO1-modified PLAGL2, some consistent between cell types and others that are cell specific. Nevertheless, the one common feature in all of the cells analyzed was that TNF-α induced accumulation of active (native) PLAGL2 in the nucleus.

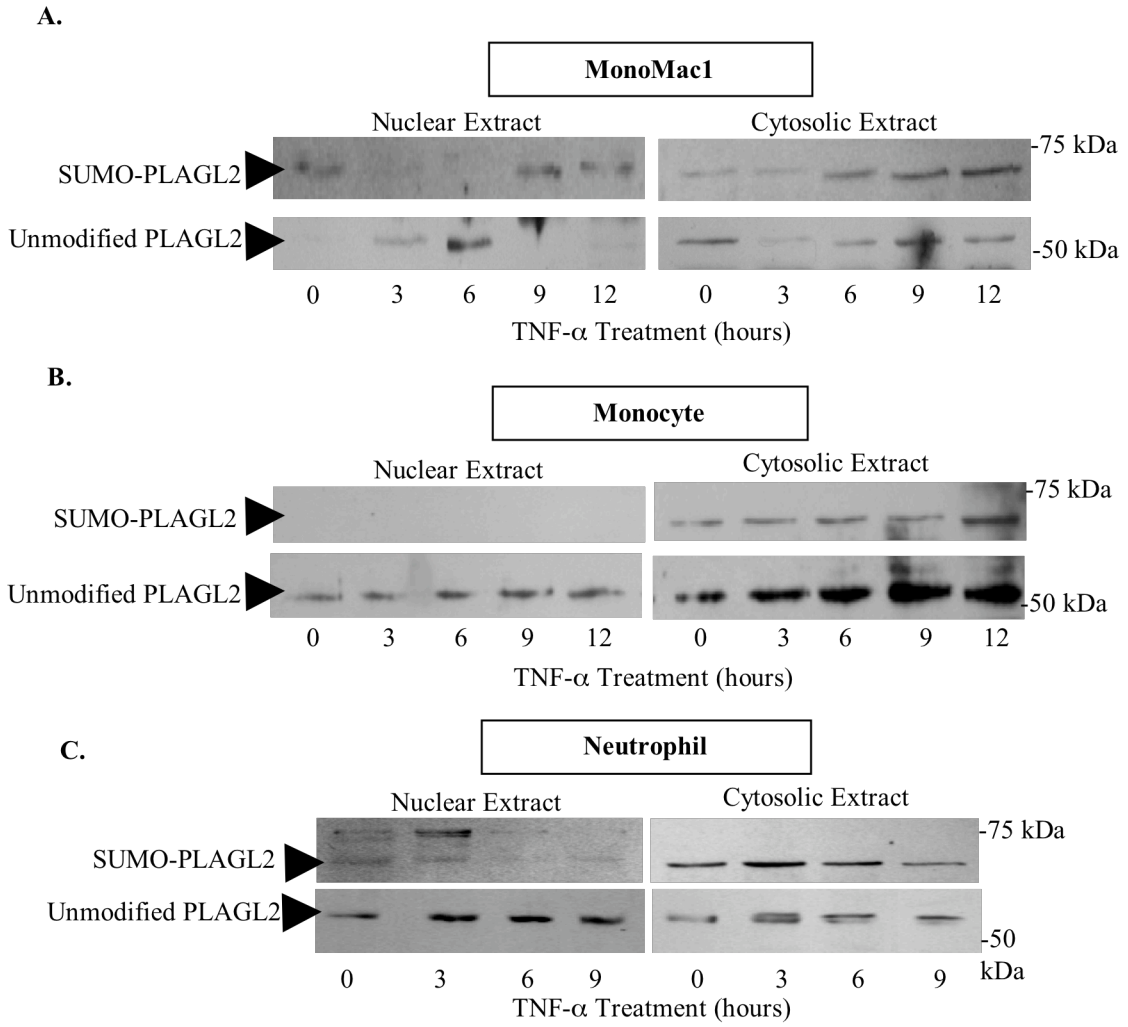

Figure 2.18: TNF-α modulates PLAGL2 protein in MonoMac1 cells and human primary monocytes and neutrophils. Panel A-C: Nuclear and cytosolic fractions were prepared in the presence of 20 mM NEM from MonoMac1 cells (Panel C), monocytes (Panel D), and neutrophils (Panel E) after treatment with 20 ng/ml TNF-α for the indicated times. Samples were analyzed by immunoblotting with anti-PLAGL2. The blots are representative of at least three experiments. Bands corresponding to native and SUMO1-modified PLAGL2 are indicated.

Discussion

Elevated TNF-α has been implicated in the pathology of numerous inflammatory syndromes, including septic shock, adult respiratory distress syndrome, rheumatoid arthritis, and Crohn's disease, and anti-TNF-α treatment has proven effective in reducing

the severity of these inflammatory diseases (reviewed in [195-197]). Additionally, the activity of the NADPH oxidase has also been implicated in these inflammatory syndromes (reviewed in [100, 198]), supporting a link between the effects of TNF-α and excessive oxidant production in disease pathogenesis. Despite intensive research into how TNF-α signaling regulates the oxidative burst, the mechanisms behind TNF-α-induced NADPH oxidase activation remain elusive.

Previous work in our lab indicated that TNF-α may regulate the oxidative burst at the transcriptional level through regulation of *NCF2* expression and, thus, expression of $p67^{phox}$, a rate limiting component of the NADPH oxidase [131]. We mapped the sequence of the TNF-α-responsive region (TRR) in the *NCF2* intragenic region [126] and, in the present study, identified the zinc finger transcription factor PLAGL2 as a TRR-binding factor. PLAGL2 is a recently discovered transcription factor that has been shown to play an important role in the pathogenesis of acute myeloid leukemia [199]. However, little is known about this transcription factor and its endogenous role. To date, only a few potential PLAGL2 target genes have been identified (reviewed in [200]); therefore, the demonstration of transcriptional regulation of *NCF2* by PLAGL2 is a significant and novel finding. Binding of PLAGL2 to the TRR was implicated by the yeast one-hybrid screen, which indicated that PLAGL2 bound with high-affinity to the TRR in yeast, as PLAGL2 was found in the majority of the double-positive interactions in the high-stringency screen. Furthermore, the yeast one-hybrid results were supported *in vitro* using EMSA and DNA-binding affinity purification assays and *in vivo* by ChIP analysis.

Binding of PLAGL2 to the TRR was surprising, as the PLAGcon sequence originally used to characterize the binding features of the PLAG family of transcription factors shares little sequence similarity to the TRR sequence [188]. In examining the relative affinity of *in vitro* expressed PLAGL2 for PLAGcon verses the TRR sequence, we found that PLAGL2 had relatively higher affinity for the PLAGcon sequence. Note, however, that the PLAGcon sequence was identified through random oligomer affinity purification and may not fully reflect the putative endogenous binding sequences for PLAGL2. Indeed, PLAGL2 was found to regulate the lactate dehydrogenase A promoter and, although the sequence of this element is also GC-rich, it does not contain the specific PLAGcon sequence [189]. Determining the specific PLAGL2-binding element within the TRR will require further analysis.

Our PLAGL2-specific antibodies recognized both native and SUMO1-modified forms of PLAGL2, and both forms of PLAGL2 bound specifically to the TRR sequence *in vitro*. SUMO modification has been reported to regulate the subcellular localization of substrates [201], however, the role of sumoylation in regulating PLAGL2 localization remains controversial. Zheng and Yang [193] reported that SUMO1-modified PLAGL2 localized to the nucleus in HEK293 cells. Although not directly demonstrated for PLAGL2, Van Dyck et al. [202] reported that mutation of SUMO sites in PLAG1, a close family member, did not alter its nuclear distribution. Indeed, we detected SUMO1-modified PLAGL2 in both cytosolic and nuclear fractions of MonoMac1 cells and neutrophils, but did not detect SUMO1-modified PLAGL2 in nuclear extracts from monocytes. It is therefore unlikely that SUMO1 modification alone mediates nuclear-cytoplasmic localization of PLAGL2.

SUMO1 modification has been shown to cause both activation and repression of transcription. For example, mutations at the site of sumoylation of the transcription factor Elk-1 or the coactivator p300 enhances transcription from responsive promoters, suggesting a repressive role for sumoylation [203, 204]. Conversely, sumoylation of the heat shock factors HSF1 and HSF2 enhances transcriptional activity of these factors [205]. GAL4 DNA-binding domain fusion protein assays were used to demonstrate that SUMO1 modification suppresses PLAGL2 transactivation activity [193] and others demonstrated that sumoylation-deficient PLAG1 led to increased transactivation [202]. Additional studies are required to determine if both forms of endogenous PLAGL2 bind the TRR *in vivo*, and, if so, the effect they have on the regulation of *NCF2* gene expression.

This is the first study to demonstrate the effects of TNF-α on the relative levels of native and SUMO1-modified endogenous PLAGL2 in the nucleus and cytoplasm. One possibility is that sumoylation may play a role in the regulation of TNF-α-dependent $p67^{phox}$ expression by modulating the activity of PLAGL2 at the intragenic region. Modulation by sumoylation is involved in non-classical regulation of the TNF-α-responsive transcription factor NFκB, and with similar kinetics to those observed in our TNF-α treated lysates. In the classical pathway of TNF-α activation of the NFκB pathway, IκBα is ubiquitinated and degraded, allowing NFκB to move to the nucleus within minutes. However, sumoylation of IκBα at the same lysine residue renders IκBα resistant to TNF-α-induced degradation and occurs slowly over several hours [206, 207]. Additionally, direct modification of transcription factors, such as the glucocorticoid receptor, by sumoylation suggests a model in which SUMO modification results in

modulation rather than a shut down of gene expression through synergy control motifs [208].

While our studies focused primarily on native and SUMO1-modified PLAGL2, we cannot rule out a possible role for other post-translational modifications, such as acetylation [193] and phosphorylation [188]. For example, Zheng and Yang [193] reported that sumoylation represses PLAGL2 transactivation, while acetylation enhances PLAGL2-mediated transactivation [193]. Thus, multiple modifications may be utilized in PLAGL2 regulation, and further studies are clearly needed to evaluate this issue.

In the present study, not only were both native and SUMO1-modifed forms of PLAGL2 shown to bind the TRR, but also the binding of PLAGL2 to the TRR was further enhanced with TNF-α treatment. Significantly, knock-down of PLAGL2 protein inhibited TNF-α-induced upregulation of *NCF2* transcript, $p67^{phox}$ protein, and O_2^- production. Furthermore, TNF-α treatment resulted in a time-dependent change in the relative levels of native versus SUMO1-modified PLAGL2 in MonoMac1 cells, monocytes, and neutrophils. On the other hand, we observed no changes in *PLAGL2* message or protein levels in TNF-α-treated MonoMac1 cells and no change in *PLAGL2* mRNA in TNF-α-treated HL60 cells (data not shown). Thus, PLAGL2 function appears to be determined by post-translational modification and the relative levels of active (native) versus repressive (SUMO1-modified) PLAGL2 in the nucleus. Accordingly, our data suggest that the modulation of PLAGL2 localization in phagocytes plays an important role in regulating TNF-α-dependent $p67^{phox}$ expression and subsequent NADPH oxidase activity. Overall, a better understanding of the mechanisms involved in

post-translational modification of PLAGL2 by TNF-α and subsequent effects on the NADPH oxidase activity may well prove to have significant therapeutic potential.

PLEOMORPHIC ADENOMA GENE-LIKE 2 BINDS THE TNF-α RESPONSIVE REGION AT A CONCERVED CORE SEQUENCE VIA ZINC FINGERS SIX AND SEVEN

Introduction

PLAGL2 is a member of the PLAG family of oncogenic transcription factors characterized by the prototype family member PLAG1 (reviewed in [209]). Originally identified from tumors of the salvilary glands [188], the PLAG family consists of three transcription factors characterized by a conserved region of classical C_2H_2 zinc fingers. The classical C_2H_2 zinc finger family is by far the most abundant type of transcription factor in the human genome. Of over 2000 predicted transcription factors in the human genome, 900 contain C_2H_2 zinc fingers [210]. This type of zinc finger is characterized by consensus sequences containing conserved cysteines, histidines, aromatic, and hydrophobic residues. In the presence of zinc, the conserved cysteines and histidines bind the zinc ion to form a ββα domain consisting of an anti-parallel β-sheet followed by an α-helix. The zinc finger tertiary structure is stabilized by zinc coordination between the β sheet and the α helix and by hydrophobic residues flanking the zinc-binding region. The zinc coordinating cysteines and histidine are absolutely required as substitution of these residues results in loss of function of the zinc finger [211]. The only exception to this rule is the LIM domain (named after LIN-11, Isl1, and MEC-3 in which the domain was first identified [212]). In the LIM domain the second histidine is replaced by aspartimate or glutamate [213].

C_2H_2 zinc fingers have been found to mediate protein-protein interactions and protein-RNA interactions [214, 215], but a vast body of research addresses the ability of

C_2H_2 zinc fingers to modulate protein-DNA interactions (reviewed in [216]). DNA recognition by the C_2H_2 zinc finger usually requires two to four tandom fingers, and one to two fingers usually requires some sort of secondary structural elements in order for the DNA recognition to occur [217]. Upon binding, the α-helix of the zinc finger fits into the major groove of the DNA thus inducing a conformational change in the DNA, enlarging the major groove so that the DNA assumes a B conformation [218]. As successive zinc fingers recognize the nucleotide sequence, the transcription factor wraps around the DNA.

Nucleotide base recognition is modulated by N-terminal residues of the α-helix. Thus, amino acid residues of the α-helix determine DNA binding sequence specificity [219]. Amino acid side chain recognition of a nucleic acid base can be approximated and predicted. Indeed, synthetic C_2H_2 zinc fingers have been designed using this recognition code and bind their target sequence, albeit with suboptimal specificity [220]. A final structural component of the DNA recognition and binding domain of the C_2H_2 zinc finger is the linker region between fingers. This conserved motif, TGEK, confers high affinity DNA binding as determined by mutational analysis [221]. NMR analysis [222] shows that the linker region is flexible until the flanking zinc fingers bind DNA, upon which the linker region becomes rigid forming a cap over the C-terminal of the proceeding α-helix, stabilizing nucleic acid binding [223].

Alignment of the zinc finger region of the three PLAG family members shows high conservation across all family members. PLAGL2 is 79% identical and 90% similar in sequence to PLAG1 at the zinc finger region [188]. PLAGL1 is less homologous, but still shares 73% identity and 83% similarity with PLAG1 at the zinc finger region [188].

The consensus binding sequences for this family have been identified using random sequence oligomer affinity purification [192, 224]. Despite strong sequence homology in the zinc finger regions of all the PLAG family members, PLAGL1 was identified to bind a different consensus sequence (GGGGGGCCCC) than PLAG1 and PLAGL2 ($GRGGCN_{6-8}RGGK$); however, note that the PLAGL1 sequence is contained within the PLAG1 and PLAGL2 consensus sequence [191].

The PLAG1 and PLAGL2 consensus sequence can be divided into two essential parts: the core (GRGGC) and the cluster (RGGK). The bipartite binding of PLAG1 and PLAGL2 is unusual among zinc finger transcription factors, however mutational analysis suggests that this unusual binding is the result of non-contiguous zinc finger binding. Indeed the sixth and seventh zinc fingers of PLAG1 and PLAGL2 were shown to bind the core sequence, while zinc finger three was shown to bind the cluster sequence [192]. Despite significant sequence homology at the residues in zinc finger three predicted to make contact with the nucleotide base, PLAGL1 does not recognize the cluster sequence. PLAGL1 does use zinc fingers six and seven to bind its consensus sequence reflecting both the high sequence homology of the predicted base contacts within the family and the similarity between the PLAGL1 consensus sequence and the cluster sequence of the PLAG1 and PLAGL2 consensus binding sequence [191].

PLAGL2 has been shown to bind and regulate only a few promoter sequences. Exogenously expressed PLAGL2 stimulates *IGFII* expression [191] and, although identification and characterization of the promoter binding in *IGFII* was performed with PLAG1 [192], it is likely that PLAGL2 binds the *IGFII* promoter in a similar fashion albeit with lower affinity. Using both chromatin immunoprecipitation (ChIP) and

quantitative real time PCR (qRT-PCR), endogenous PLAGL2 was shown to bind and regulate the surfactant protein C promoter [225]. Although exogenously expressed PLAGL2 was shown to increase transcription of the proapoptotic factor Nip3, direct PLAGL2 binding to the Nip3 promoter has yet to be confirmed [226]. Finally, our lab recently identified PLAGL2 as a novel regulator of the *NCF2* intragenic region [227].

NCF2 codes for a componant of the NADPH oxidase and can be transcriptionally regulated by TNF-α. Regulation of *NCF2* transcription by TNF-α occurs in the TNF-α Responsive Region (TRR) upstream of the ATG start site [131]. The functional oxidase requires the assembly of multiple subunits and at least two other subunits besides *NCF2* are transcriptionally responsive to TNF-α treatment. TNF-α transcriptional regulation of these subunits is mediated through the NF-κB pathway [134]. This suggests coordination of transcription regulation of these genes in response to TNF-α. Clearly, defining the site in the TRR to which PLAGL2 is binding could identify a regulatory element coordinating expression of the oxidase genes. In the current chapter, we identify the binding sequence within the TRR to which PLAGL2 binds. Additionally, we identify zinc fingers six and seven as essential for PLAGL2 binding to the *NCF2* TRR.

Materials and Methods

Electrophoretic Mobility Shift Assay (EMSA)

EMSA was carried out following the methods outlined in Chapter 2 with some exceptions as follows. Complementary oligonucleotides for the TRR and the PLAG family consensus sequences (PLAGcon) (see Chapter 2) were annealed by heating to 95^{o}C for 2 min and cooled to room temperature. PLAGL2 zinc finger mutants were

generated using the site directed mutagenesis kit QuickChange (Stratagene, Cedar Creek, TX) with the pcDNA3.1 (PLAGL2) wild-type vector as template. Zinc fingers were functionally disrupted by mutating the first histidine of each finger as described previously [228].

To determine the PLAGL2 binding element in the *NCF2* TRR and the PLAGL2 zinc fingers required for binding the TRR, PLAGL2 wild type and PLAGL2 zinc finger mutant proteins were generated in rabbit reticulocyte lysates in the presence of ^{35}S-methionine for 90 min at 30^{o}C. Proteins were analyzed by SDS-PAGE analysis prior to use to determine equivalent protein production. Binding reactions were performed as described in Chapter 2 using 3-5 ml of labeled protein and 50-100 ng of unlabeled double-strand wild type TRR DNA or mutant TRR DNA. Samples were run on NOVEX 6% DNA Retardation gels and band shifts analyzed as described previously in Chapter 2 above.

Luciferase Reporter Constructs

Wild type TRR intragenic region reporter constructs were prepared as previously described [131]. Luciferase reporter constructs were made by site-directed mutagenesis using the QuikChange mutagenesis kit (Stratagene, Cedar Creek, TX). PCR was used to generate nucleotide mutants using the wild type vector pGL-p67(500) or pGL-p67(75) to generate pGL-p67(mut500) or pGL-p67(mut75), respectively.

Transient Transfections

K562 cells were transiently transfected as previously described [131]. Briefly, cells were seeded one day prior to transfections at 5 X 10^5 cells/ml in fresh complete

medium. On the day of the transfection, 5 X 10^5 cells per transfection were resuspended in 500 μl DMEM with serum. Cells were transfected using LipoFectamine 2000 (Invitrogen). For each transfection 300 ng of luciferase contruct DNA and 50 ng of pRL-TK plus 2 μl of transfection reagent was added in 100 μl DMEM. TNF-α was added at 20 ng/ml to medium 4 hr post-transfection. At 24 hr post-transfection, cells were assayed for firefly and *Renilla* luciferase activity using the dual-luciferase reporter assay according to the manufacture's protocol (Promega, Madison, WI). Cells were washed in PBS and resuspended in 50 μl lysis buffer, and 10 μl cell lysate was assayed for luciferase activity in 50 μl Luciferase Assay Buffer II using a Lumat LB 9507 luminometer (EG&G Berthod, Germany). Subsequently, 50 μl Stop and Glo reagent was added to the sample, which was then analyzed for *Renilla* luciferase activity.

Results

In Vitro Translated PLAGL2 Binds the TRR -23 to -16 Basepairs Upstream of the Translation Start Site

The TNF-α Responsive Region (TRR) does not have any putative transcription factor binding sites. Further investigation lead to the isolation and characterization of PLAGL2 as a novel transcription factor which binds and regulates expression of *NCF2* via the TRR [227]. Although a PLAG family consensus sequence has been identified by CASTing [191], close inspection of the TRR sequence does not identify any clear regions of similarity between the known PLAG family consensus sequence and the TRR sequence (Figure 3.1). To address the question of where PLAGL2 binds within the TRR,

we utilized mutational analysis of the sequence in conjunction with electrophoretic mobility shift assays (EMSA).

To identify the nucleotides required for PLAGL2 binding to the TRR element in the intragenic region of *NCF2*, we performed EMSA with radiolabeled, *in vitro* translated PLAGL2 protein. We first verified that *in vitro* translated PLAGL2 can bind with sufficient efficiency to be detected by autoradiography. As can been seen in Figure 3.2, lane 2, radiolabled PLAGL2 clearly shifted with binding to the PLAGcon probe. This shift was significant when compared with background protein migration (Figure 3.2, lane 1). Furthermore, PLAGL2 binds specifically, as a band shift is not detected when *in vitro* translated PLAGL2 is incubated with a non-specific DNA probe (Figure 3.2, lane 3).

Previously, our lab had identified the region -58 to -36 basepairs upstream of the translation start site of *NCF2* as the regulatory element of the intragenic region responsive to TNF-α (unpublished results); however, further analysis identified that the TRR region extended downstream to -16 basepairs upstream of the translation start site [131]. To try to narrow down the region of PLAGL2 binding, we probed the radiolabel PLAGL2 protein with probes dividing the TRR into two domains. As shown in Figure 3.2, lanes 4 and 5, neither domain was sufficient to shift PLAGL2 protein.

While characterizing the AP-1 binding site in the intragenic region of the 5'UTR of *NCF2*, our lab found a region of polymorphism in this intragenic region -43 to -47 basepairs upstream from the translation start site [140]. Since the region -58 to -36 basepairs upstream from the start site might be of importance, we probed the radiolabeled PLAGL2 with full length TRR probes containing each of the known polymorphisms found at this region. Previously, in studies evaluating PLAGL2 binding the TRR the

sequence CTCCC at this region was used [227]. Although this polymorphism may play an endogenous role, it did not appear to affect the ability of PLAGL2 to bind the TRR (Figure 3.2, lanes 6, 7, and 8).

Finally, we sequentially mutated the TRR four basepairs at a time and probed radiolabeled PLAGL2 to identify the specific sequences required for PLAGL2 binding to the TRR. The double stranded DNA probe of the complete TRR, shown in Figure 3.1, was used with each of the sequential mutations as identified above the sequence (Figure 3.1). Although neither region -58 to -36 basepairs nor -35 to -16 basepairs upstream of the translation start site appeared to be sufficient for PLAGL2 binding (Figure 3.2, lanes 4 and 5), PLAGL2 binds the full length TRR (Figure 3.2, lanes 6-8). Base mutations within both the #10 and #11 probes completely eliminated binding by PLAGL2 (Figure 3.2, lanes 18 and 19). Thus, these data identify the region -23 to -16 basepairs upstream of the start site as the essential region to which PLAGL2 binds in the TRR.

Figure 3.1: Comparison of the *NCF2* TRR sequence and the PLAG family consensus sequence (PLAGcon). Additionally, mutations to the TRR probe are identified in red above the TRR sequence. Two domains of TRR are identified from -58 to -36 and -38 to -16.

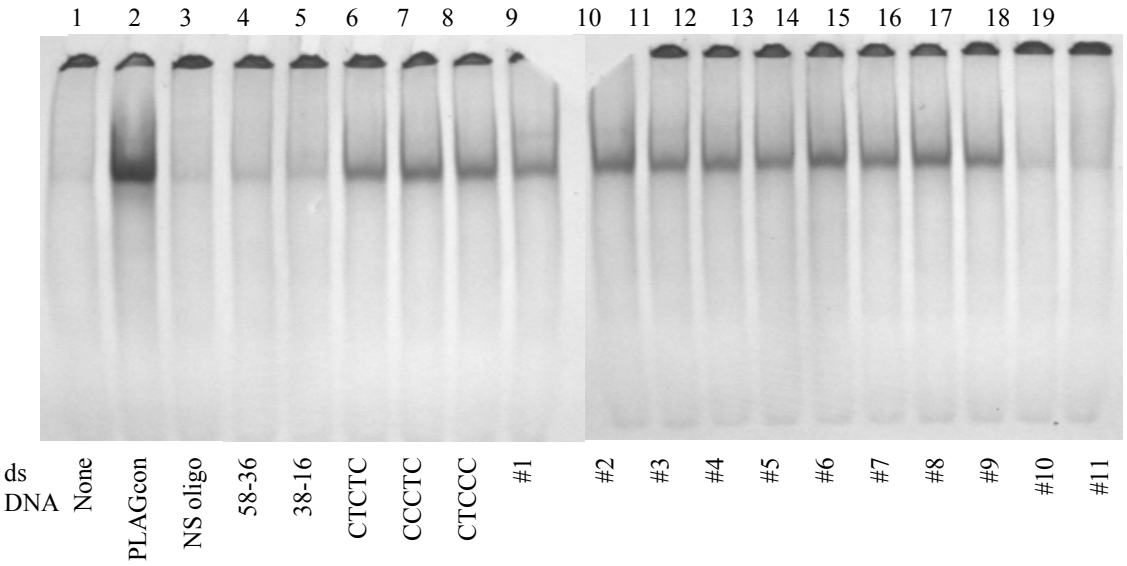

Figure 3.2: *In vitro* translated PLAGL2 binds the TRR -23 to -16 basepairs upstream of the translation start site of *NCF2*. EMSA analysis using ^{35}S-labeled *in vitro* translated PLAGL2 and dsDNA probe. PLAGcon was used to confirm binding (lane 2) and a non-specific ds oligomer (NS oligo) was used to confirm specificity (lane 3). TRR probe was divided into an upstream and downstream domain (lanes 4 and 5). Polymorphisms found in the TRR were analysed in full length TRR probes containing the polymorphism (lanes 6, 7, and 8). Sequential mutations of the TRR as identified in Figure 3.1 were used to probe PLAGL2 binding (lanes 9-19). Representative of repeated experiments.

Mutation of the Conserved GGCC in the TRR Inhibits Intragenic Region Activation in *NCF2* Reporter Constructs

Conserved in both the TRR and the PLAG consensus sequence is the sequence GGCC. When we mutated the TRR sequence in the above EMSA analysis, we found that this sequence was necessary for the binding of *in vitro* translated PLAGL2. To address whether this sequence is necessary for the *in vivo* activation of the *NCF2* intragenic region we used luciferase reporter assays as described previously [131]. 5' UTR sequence either -500 basepairs or -75 basepairs upstream of the *NCF2* translation start site was used as template in the pGL3 reporter vector to mutate the conserved GGCC sequence in

the *NCF2* intragenic region using site-directed mutagenesis. As previous work has shown that both c-Fos and c-Jun are required to transactivate these 5'UTR pieces in K562 cells [131], we used both these reporter constructs or the respective mutant reporter constructs in conjunction with exogenously expressed c-Fos and c-Jun.

As shown in Figure 3.3, mutation of the GGCC sequence in the TRR of the *NCF2* intragenic region inhibited transactivation of the reporter by about 75% when compared to the respective non-mutated sequence. This inhibition was observed for both the mutant reporter constructs including -500 basepairs and -75 basepairs upstream of the translation start site. Although overexpression of exogenous PLAGL2 was found to be toxic in our myeloid cell lines (data not shown), mutation of the binding site identified for *in vitro* translated PLAGL2 binding inhibited transactivation of the *NCF2* reporter construct *in vivo* in the myeloid K562 cell line.

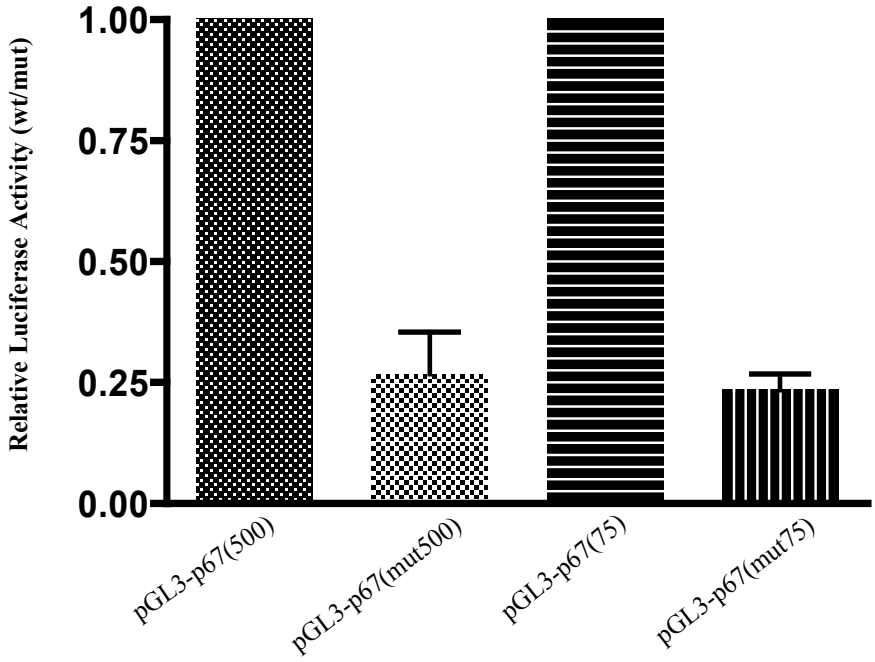

Figure 3.3: Mutation of GGCC in the TRR inhibits reporter transactivation in *NCF2* intragenic region reporter constructs. K562 cells were transiently transfected with pcDNA3.1(cFos), pcDNA3.1(cJun) and either wild-type *NCF2* intragenic region constructs [pGL3-p67(500) or pGL3-p67(75)] or GGCC mutant *NCF2* intragenic region constructs [pGL3-p67(mut500) or pGL3-p67(mut75)], as well as the pRL-TK transfection control construct. TNF-α (20 ng/ml) was added 4 hr post-transfection. At 24 hrs post transfection, cells were lysed, and luciferase activity was assayed. Luciferase activity was corrected for transfection efficiency. Luciferase activity is reported as the fold change between the mutated construct and its respective wild-type construct. The data are presented as mean ± SEM, N = 3.

PLAGL2 Zinc Fingers Six and Seven Recognize and Bind the TRR

Previous analysis of the prototypic PLAG family member PLAG1, showed that zinc fingers three, six, and seven were required for PLAG1 to bind to the PLAG family consensus sequence [192]. Futhermore, PLAGL2 shares strong homology to PLAG1 at these zinc fingers [188]. Because the sequence identified in the TRR to which PLAGL2

binds does not share complete identity with the canonical PLAG family concensus sequence, we attempted to identify which zinc fingers in PLAGL2 are required to bind the TRR. Using site directed mutagenesis, we mutated the first histidine of each zinc finger in PLAGL2. This mutation has been shown to prevent the formation of a functional zinc finger by disrupting interaction with zinc [228]. To check for radiolabled protein expression, rabbit reticulocyte lysate expressed and radiolabled wild-type PLAGL2 and zinc finger mutant PLAGL2 was subjected to electrophoresis and visualized by autoradiography. Importantly, all of the PLAGL2 zinc finger mutants expressed equally in the rabbit reticulocyte lysates (Figure 3.4).

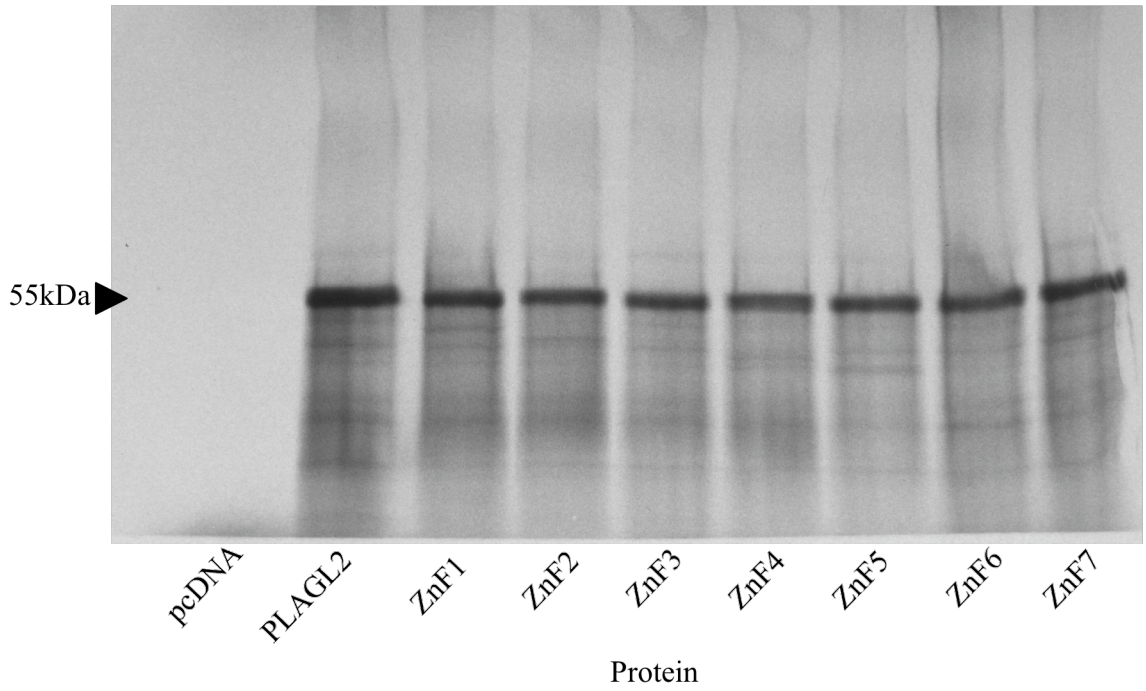

Figure 3.4: Zinc finger mutant and wild-type PLAGL2 protein is expressed equally in rabbit reticulocyte lysate. PLAGL2 zinc fingers were generated with site-directed mutagenesis of the first histidine of each finger. Radiolabled protein was generated in rabbit reticulocyte lysate, subjected to SDS-PAGE analysis, and visualized by autoradiography.

Using EMSA analysis with radiolabeled, *in vitro* translated PLAGL2 protein, we analysed the ability of the zinc finger mutant proteins to bind both the TRR and the PLAG family consensus sequence. Similar to what has been previously reported for PLAG1 [192], we found that zinc fingers six and seven were each involved in the ability for PLAGL2 to bind to the PLAG family consensus sequence. Futhermore, we found that mutation of zinc finger three also inhibited the binding of PLAGL2 to the PLAG family consensus sequence (Figure 3.5, Panel B, lanes 5, 8, and 9). Mutation of zinc finger three inhibited PLAGL2 binding to the PLAG family concensus sequence by about 50%, while mutations of zinc fingers six and seven inhibited PLAGL2 binding by about 75% (Figure 3.5, Panel D). As shown in Figure 3.5, Panel A, mutation of zinc fingers six and seven significantly inhibited the ability of PLAGL2 protein to bind the TRR. In contrast to PLAGL2 binding to the PLAG family consensus sequence, PLAGL2 binding to the TRR was not as significantly affected by mutation of zinc finger three (Figure 3.5, Panel A, lanes 5, 8, and 9). Mutation of zinc finger three inhibited PLAGL2 binding to the TRR by about 25%, while mutation of zinc fingers six and seven inhibited PLAGL2 binding to the TRR by about 75% (Figure 3.5, Panel C). These data indicate that zinc fingers six and seven and to a lesser extent zinc finger three are required for *in vitro* translated PLAGL2 to bind to the TRR of the *NCF2* intragenic region.

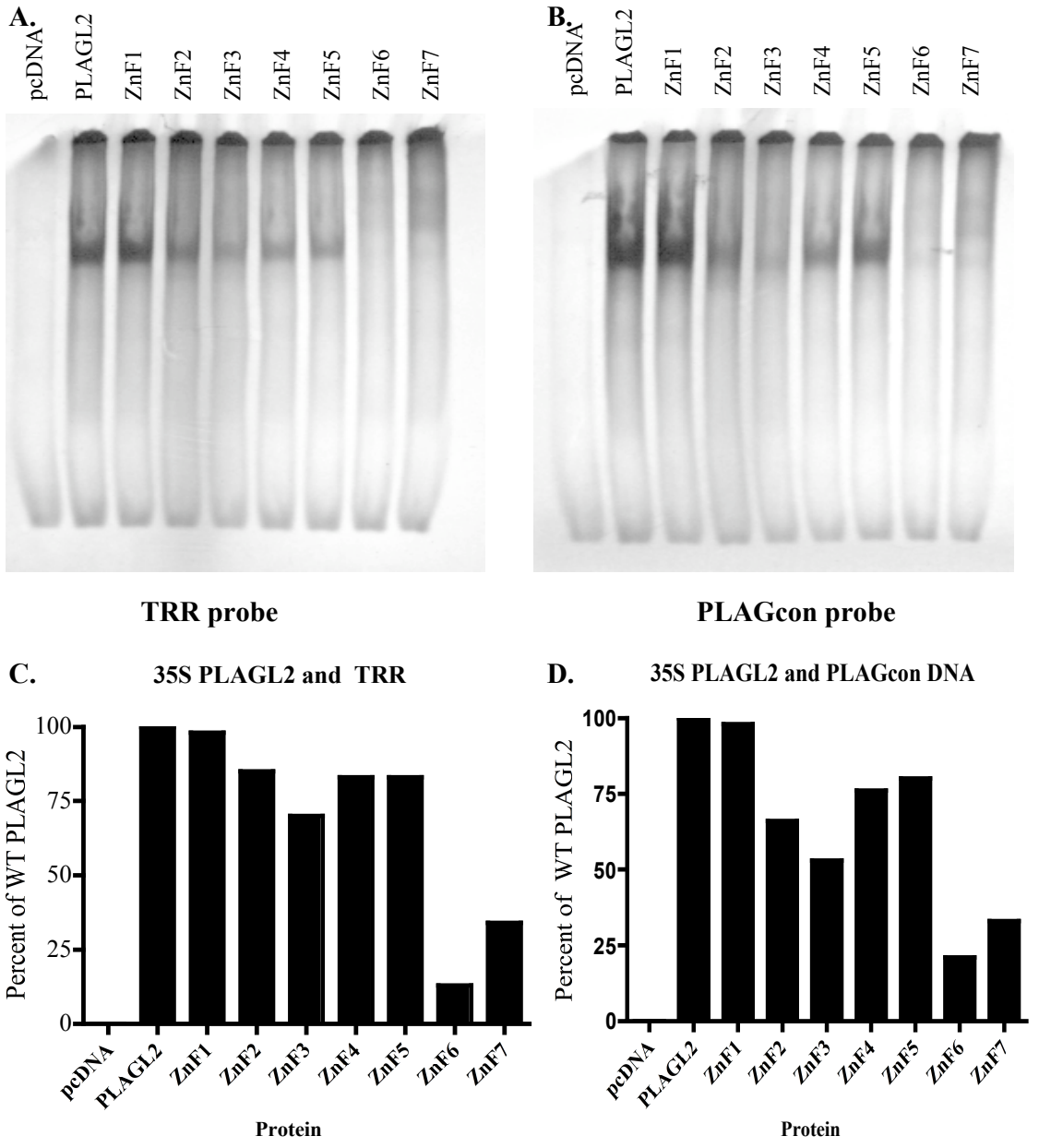

Figure 3.5: PLAGL2 zinc fingers six and seven bind the TRR sequence. Panel A and B: EMSA analysis performed with *in vitro* translated PLAGL2. Mutations to zinc fingers were performed using site-directed mutagenesis to disrupt the zinc finger by mutating the first histidine in the classical C_2H_2 fingers. The mutated PLAGL2 proteins were then incubated with either dsTRR oligomers or dsPLAGcon oligomers and shifts were visualized using autoradiography. Panels C and D: Densitometric analysis of above EMSA blots were performed to quantitate percent inhibition of PLAGL2 binding to either the TRR or the PLAGcon sequences due to zinc finger mutations. Data are plotted as a percent of wild-type PLAGL2 binding to either the TRR or PLAGcon sequences. Representative of repeated experiments.

Discussion

In the current chapter, we identified the sequence within the conserved TNF-α Responsive Region (TRR) of the *NCF2* intragenic region to which PLAGL2 binds. When sequentially mutated, the TRR probe identified the region -23 to -16 basepairs upstream of the translation start site as necessary for binding of PLAGL2. This sequence includes the conserved PLAG family core sequence. Originally identified using the CASTing method [192] of random sequence oligonucleotides, the PLAG family consensus sequence has been identified as RGGC(N_{6-7})RGGK containing both a core (RGGC) and cluster domain (RGGK). Within the sequence identified as the PLAGL2 binding sequence of the TRR is the core sequence at -18 to -22 (GAGGC) basepairs upstream of the translation start site (Figure 3.6, Panel A). The importance of this conserved region is also demonstrated by the loss of transactivation in reporter assays. Although we found overexpression of exogenous PLAGL2 to be toxic in our myeloid cell lines, making direct PLAGL2-intragenic region/reporter analysis difficult *in vivo*, the reduction of reporter transactivation resulting from the mutation of sequences bound by PLAGL2 *in vitro* suggests that endogenous PLAGL2 requires this sequence to bind and transactivate the TRR.

Although a cluster sequence does exist upstream in the TRR located at -43 to -47 basepairs upstream of the translation start site (Figure 3.6 Panel A), this site likely does not play a significant role in the binding of PLAGL2 to the TRR. Not only does the EMSA mutation analysis indicate that this core is not necessary for *in vitro* translated

PLAGL2 to bind to the TRR, but polymorphisms at this site also do not seem to affect the binding capacity of PLAGL2. The lack of ^{35}S-PLAGL2 binding to the TRR sequence -38 to -16 basepairs upstream of the translation start site may suggest some affinity for G rich region upstream of the core sequence similar to the G-cluster in the PLAG family consensus sequence, however, as the above data indicate, it is unlikely this region plays a strong role in PLAGL2 binding to the TRR.

As discussed in chapter one, *NCF2* appears to have multiple transcriptional start sites and location of initiation may be context dependent. Although there is some evidence to suggest that transcription initiation of *NCF2* occurs upstream of exon 1, one report [130] finds that the exon 1 site of intiation is dependent on treatment with IFN-γ and others find that the exon 1 transcript is in very low abundance [167]. Therefore, it is highly likely that transcription initiation more commonly occurs in the intragenic region of *NCF2* in intron 1. The TNF-α Responsive Region (TRR) flanks intron 1 and exon 2 upstream of the translation start site. If transcript intiated upstream of exon 1 in the presence of TNF-α, then the TRR would overlap with the acceptor site for splice recognition. Mutational analysis of the TNF-α-dependent regulation of transcription found that loss of reporter occurred upstream of the splice acceptor site [131], suggesting that splicing does not likely occur in the presence of TNF-α, and that transcription is intiated in the intragenic region of intron 1. PLAGL2 binding site analysis identified a region just downstream of the splice acceptor site to which PLAGL2 binds. If transcription initiation occurs upstream on exon 1, it is possible that PLAGL2 would interfer with RNA processing; however, in light of the current model, it is likely that in

the presence of TNF-α, PLAGL2 binds the intragenic region of *NCF2* and enhances transcription intitation in intron 1.

The bipartite nature of the PLAG family consensus is very unusual for a family of classical C_2H_2 zinc fingers. Typically, these types of transcription factors bind DNA via consecutive zinc fingers and usually with more than two fingers, with each finger wrapping around the DNA and contacting conserved sequence at predictable sites [216]. Although Voz *et al.* [192] have shown that for PLAG1, the prototype family member, binding requires zinc finger three to interact with the cluster, this interaction may not be as essential for PLAGL2. Indeed, despite high homology at zinc finger three, PLAGL1 does not recognize the cluster sequence and only binds the core sequence [191].

Recognition of the cluster sequence by PLAGL2 may be context dependant. While PLAGL2 has been shown to recognize the cluster sequence in EMSA analysis [192] and in the surfactant C promoter [190], this sequence accounts for only 25% of the transactivation capacity of PLAGL2 in the surfactant C promoter [190], suggesting that the cluster sequence is minimally important to PLAGL2 binding and transactivation. On the other hand, the core sequence does appear to be essential for PLAGL2 binding. Although similar in sequence to the surfactant C promoter (SPC), the surfactant B promoter (SPB) has a degenerate core sequence and is not responsive to exogenously expressed PLAGL2 [190]. Furthermore, PLAGL2 regulates the LDHA promoter, containing a core sequence, despite the lack of a cluster sequence [189]. Identification of the PLAG family consensus sequence required the use of an artificial system of oligomer affinity purification [192]. While analysis of the *SPC* promoter indicates that both the core and cluster sequence are important for *in vitro* binding, the binding of PLAGL2 *in*

vivo might not require the cluster sequence. Indeed, the core and cluster sequence are conserved in humans, however the cluster sequence is degenerate in mice, yet the promoter is still responsive to PLAGL2 [190]. This suggests that *in vivo* PLAGL2 may not utilize the cluster sequence for binding and regulation of the TRR in the intragenic region of *NCF2*.

Because PLAGL2 might bind the TRR in a unique manner independent of the cluster sequence of the PLAG family consensus sequence, we consecutively mutated the zinc fingers of PLAGL2 to identify the fingers required for binding to the TRR. Zinc fingers six and seven account for the majority of PLAGL2 binding to the TRR sequence. This agrees with previous work on PLAG family members. Zinc fingers six and seven were required for PLAG1 to bind to the core of the PLAG family consensus sequence [191]. While zinc finger three appears important for binding to the PLAG family consensus sequence *in vitro*, it does not appear to play a significant role in PLAGL2 binding to the TRR. Again, this agrees with previous analysis of PLAG1 that indicates that PLAG1 binds the cluster sequence with zinc finger three [191]. Since the TRR contains a cluster sequence unlikely to play a role in PLAGL2 binding, zinc finger three would not be expected to play a significant role in binding. Interestingly, only zinc fingers six and seven are required for PLAGL2 to bind the surfactant C promoter, despite the presence of a cluster sequence, suggesting that, for PLAGL2, zinc finger three may make a minimal contribution to binding *in vivo* [190], although direct analysis of zinc finger three binding was not analysed. Finally, only zinc fingers six and seven of the PLAG family members contain a linker region recognized to enhance DNA binding by capping the C-terminal of the α-helix of the preceeding zinc finger [221], suggesting that

these two fingers are the essential zinc fingers for PLAGL2 DNA recognition and binding.

Classical C_2H_2 zinc fingers have predictable DNA-protein contacts as determined from both structural studies and phage-display selections with site-directed mutagenesis (reviewed in [216]). These predictable DNA-protein contacts have led to the establishment of a recognition code determining zinc finger/DNA interactions. Using the zinc finger residues of PLAGL2 predicted to make protein/DNA contacts, alignment of the PLAG family consensus sequence with the TRR depicts strong agreement with the predicted binding site using the zinc finger recognition code (Figure 3.6, Panel B). These base contacts show strong agreement with the PLAG family consensus sequence, even in the cluster sequence, although it is unlikely this sequence plays a major role in PLAGL2 binding in the TRR, as discussed above. Alignment and analysis of the first zinc finger of PLAGL2 is not included as this zinc finger is likely non-functional due to degenerate sequence. The second cysteine of the first zinc finger is replaced by a serine and this mutation has been shown to ablate zinc binding and thus inhibit the formation of the zinc finger [229]. Additionally, the second histidine of the first zinc finger is replaced with glutamine. Although glutamine has been shown to recognize the phosphate backbone of DNA and induce DNA bending, it cannot coordinate zinc binding and therefore zinc finger formation [230]. Finally, analysis of the TRR with the zinc finger/DNA recognition code predicts the importance of zinc fingers six and seven as these fingers have predictable interactions, while other zinc fingers that have not been shown to interact with DNA have few residues with predictable DNA recognition. This further

supports our conclusion that PLAGL2 binds the TRR at a conserved core sequence through the DNA recognition of zinc fingers six and seven.

A.

TRR

5-AGGAGGCCAAGAGAGCTGCAGGAGACAGGGAGAAGACAGGTTGG-3

Core Cluster

PLAGcon

5-AGCTACAACAGGGGGCCTTAGAAGGGGTACTAC-3

B. Core Cluster

Zinc Finger	Base Contact	Amino Acid	Predicted	Consensus	TRR
F7	+6	R	G	G	G
	+3	H	G/A	G/A	A
	+2	D	G/C/A	G	G
	-1	R	G		
F6	+6	R	G	G	G
	+3	D	C	C	C
	+2	K			
	-1	T	T		
F5	+6	E			
	+3	A	T		
	+2	Q			
	-1	S			
F4	+6	R	G		
	+3	G			
	+2	L			
	-1	T	T		
F3	+6	N			
	+3	H	G/A	G/A	G
	+2	D	G/C/A	G	G
	-1	R	G	G	G
F2	+6	R	G	G/T/A	A
	+3	K	G		G
	+2	Y			
	-1	S			

Figure 3.6: Prediction and schematic representation of PLAGL2 binding site. Panel A: Comparison of core and cluster in PLAGcon verse the TRR. Panel B: Amino acids of PLAGL2 zinc finger at positions -1, 2, 3, and 6 (numbered according to position relative to the start of the α-helix) are indicated with the corresponding zinc finger. The bases predicted by the zinc finger/DNA recognition code are indicated [216, 221] along side the PLAG family consensus sequence [191] and the TRR binding sequence.

IDENTIFICATION AND CHARACTERIZATION OF NOVEL PLAGL2 PROTEIN-PROTEIN INTERACTIONS

Introduction

PLAGL2 is the least defined and least characterized member of the C_2H_2 zinc finger PLAG family of transcription factors. PLAGL2 was originally identified using a mouse embryonic cDNA library probed with the salivary gland oncogene PLAG open reading frame [188], and a growing body of evidence has now linked this ubiquitously expressed transcription factor to the regulation of a handful of promoters. Characterization of the regulation of transactivation of PLAGL2 remains minimal and little is know about how this transcription factor functions *in vivo*.

Although PLAGL2 was originally reported to be expressed only in the embryo [188], subsequent work has identified PLAGL2 as a ubiquitously expressed transcription factor [189, 227]. Suggesting a global function for PLAGL2, overexpression of this transcription factor can increase proliferation by inducing transition from G1 phase to S phase resulting in the expansion of hematopoietic progenitors *in vitro* [200]. Thus, dysregulation of PLAGL2 can be detrimental, as demonstrated by PLAGL2 co-operation with the CBFB-MYHII fusion gene in leukemogenesis [231]. Additionally, observation of a similar pattern of expression of *PCNA*, a proliferation marker, and *PLAGL2* in zones of active proliferation in the developing zebra fish suggests a global role for PLAGL2 in development [232]. Indeed, knock-out of PLAGL2 results in a severe post-natal growth retardation and high lethality in mice. Less than five percent of homozygous knock-out mice survive to weaning. Lethality appears to result from defects in lipid absorption and

metabolism. The knock-out mice appear to succumb to wasting due to starvation [209, 233].

The PLAG family members are expressed in both unique and overlapping patterns in the nervous system [234], suggesting that despite strong homology, each family member can transactivate uniquely and that regulation of each family member is likely dependent on differential protein modification and protein-protein interactions. Indeed, closer analysis of PLAGL2 regulation supports the notion that transactivation by this transcription factor is context dependent. Whereas zinc finger six and seven are required for DNA binding and share high sequence homology among the PLAG family members, zinc fingers two through five demonstrate much less homology across the family [192]. Furthermore, zinc fingers two, four, and five have no predicted DNA binding sequence recognition (see Chapter 3). This suggests that zinc fingers two though five may mediate protein-protein interactions. Indeed, a recent report, presents a role for PLAGL2 independent of DNA binding. PLAGL2 was determined to bind the E3 ubiquitin ligase Pirh2 dimer and stabilize the complex by inhibiting proteosome-mediated Pirh2 degredation [235].

Luciferase reporter activation by PLAGL2 also indicates that this member of the PLAG family has distinct transactivation capacity. For example, luciferase reporter assays with exogenously expressed PLAGL2 resulted in transactivation capacity half that of the prototypic family member PLAG1 [191]. Additionally, this transactivation capacity is context dependent, as PLAG1 has six-fold and a 113-fold activation in COS cells verses HEK293 cells, respectively, while PLAGL2 has only two-fold and three- fold activation in COS cells verses HEK293 cells, respectively [188]. This also appears to be

the case with endogenous PLAGL2 transactivation. For example, Tip60 is an acetyltransferase that can act either as a transcriptional activator [236] or as a transcriptional respressor [237]. Recently, Tip60 has been shown to enhance PLAGL2 transactivation when cotransfected by acetylating PLAGL2 and thus inhibiting PLAGL2 sumoylation [238]. Furthermore, Tip60 enhances PLAGL2 regulation of the *IGFII* promoter but does not seem to affect PLAGL2 regulation of the surfactant-C promoter [238] despite the fact that the promoters both include the high affinity PLAG family consensus binding site. Although PLAGL2 has been shown to endogenously bind the surfactant-C promoter in the lung adenocarcinoma epithelial cell line NCI-H441, the promoter had no activity *in vivo* [225]. Again, this suggests that PLAGL2 transactivation requires distinct interactions in order to enhance PLAGL2 activity and/or DNA affinity and that differential regulation of PLAGL2 is context dependent.

Post-translational modifications also appear to play an important role in PLAGL2 transactivation. Using PLAGL2 in a yeast bait construct Van Dyck, *et al.* [204] identified several members of the PIAS protein family in addition to the ubiquitin-conjugating enzyme 9 (UBC9) as putative PLAGL2 interactors in a yeast two-hybrid assay. Further analysis determined that PLAGL2 transactivation capacity was enhanced via acetylation by the co-factor p300 and repressed via both deacetylation by HDAC7 and sumoylation [193]. Sumoylation represses transactivation by a number of different mechanisms. For example, sumoylation can inhibit subcellular localization required for activation; however, sumoylation did not effect subcellular localization of PLAG1 [204] and, despite lacking a nuclear localization signal, PLAGL2 localized to the nucleus, likely through interactions mediated by the N-terminal zinc finger domain [239]. Additionally,

sumoylated PLAGL2 can be found in both the cytosolic and nuclear fractions of monocytic cell lines [227]. Therefore, regulation of PLAGL2 transactivation by post-translational modifications likely depends on protein-protein interactions. For example, sumoylation can repress transactivation either through inhibiting transcription enhancing protein-protein interactions [240] or through recruitment of transcription repressors [241]. Post-translational modifications such as sumoylation and acetylation likely determine PLAGL2 interactions and thus transactivation. Despite suggestive evidence for the importance of protein-protein interactions to the activity of PLAGL2, there are few known PLAGL2-protein interactions.

PLAGL2 binds the TNF-α responsive region (TRR) in the intragenic region of *NCF2* both *in vitro* and *in vivo* [227]. While TNF-α treatment enhances *in vivo* binding of PLAGL2, neither PLAGL2 message nor total protein changes in response to TNF-α treatment, suggesting that TNF-α mediates PLAGL2 transactivation via alternate means. Although PLAGL2 can bind the TRR independently in EMSA [227], gel shift analysis with nuclear extracts results in a complex pattern suggesting that *in vivo* binding and activation at the TRR utilizes a nucleoprotein complex including PLAGL2. Relative affinity analysis of PLAGL2 indicates that PLAGL2 has a significantly higher relative affinity for the PLAG family consensus sequence than for the *NCF2* TRR [227], and PLAGL2 binds the TRR at a core sequence through zinc fingers six and seven, but does not appear to require the G-cluster sequence (see Chapter 3). This DNA binding pattern has also been shown for the LDHA promoter and the erythropoietin promoter, which utilize only the core sequence [189], and the surfactant-C promoter in which the cluster accounts for only twenty-five percent of promoter activation by PLAGL2 [190]. These

data indicate that PLAGL2 TRR-binding and transactivation is context-dependent and relies on protein-protein interactions for enhanced affinity and specificity.

To identify such protein-protein interactions we utilized the yeast two-hybrid assay with full length PLAGL2 as bait. We identified the following putative PLAGL2 interactors: E2I, $PC2_{434-784}$, FHL3, and $CHD3_{1585-1966}$. Interaction for $PC2_{434-784}$, FHL3, and $CHD3_{1585-1966}$ was further confirmed both *in vitro* and *in vivo*. In general, SUMO1-modification did not appear to affect protein-protein interaction with the exception of $CHD3_{1585-1966}$. Finally, we used mutational analysis to map the PLAGL2 domains to which the interactors bound.

Methods

Yeast Two Hybrid Assay

The Matchmaker yeast two-hybrid system 2 (Clontech, Mountain View, CA) was used according to the manufacturer's protocol with some modifications. Full length PLAGL2 was excised with *EcoR1* from the pCR-TOPO(PLAGL2) vector and ligated into the yeast reporter vector pAS2-1 (Clontech). Recombinant plasmid was used to transform Y187 using a standard lithium acetate small-scale transformation, and clones were selected on medium lacking trypotophan. Transformation-positive clones were restreaked and assayed for autoactivity. The bait strain Y187 [pAS2-1(PLAGL2)] was mated with the prey strain AH109 [pACT2(human leukocyte cDNA library)] and positive clones were selected on medium lacking histidine, tryptophan, and leucine. Leaky *HIS3* background was utilized to give the diploid a histidine jump-start on medium lacking 3AT. The diploids were then replated on medium lacking histidine, tryptophan, adenine,

leucine and supplemented with 45 mM 3-AT to select for reporter activation. Positive diploids were restreaked and assayed for β-galactosidase activity using a filter lift assay. Positive diploids were further assayed for α-galactosidase activity by restreaking the reporter positive diploids on plates containing X-α-Gal. Prey plasmids were then recovered from reporter positive clones, amplified in *E. coli*, sequenced, and analyzed using the BLAST algorithm.

In vitro Co-immunoprecipitaion (Co-IP)

Yeast vectors pAS2-1(PLAGL2), pACT2($PC2_{434-784}$), pACT2(FHL3), and pACT2($CHD3_{1585-1966}$) were used as DNA template to generated PCR product with a T7 promoter and either a Myc or HA tag. PLAGL2 was tagged with Myc, and interactors were tagged with HA. The primers used to generate Myc-tagged PLAGL2 were as follows: sense primer, 5'-AAAATTGTAATACGACTCACTATAGGGCGA GCCGCCACCATGGAGGAGCAGAAGCTGATCTCAGAGGAGGACCTGGGTCAA AGACAGTGGACTGTATCG-3' and antisense primer, 5'-TACCTGAGAAAGCAACCTGACCTA-3'. The primers used to generate HA-tagged putative PLAGL2 interactors were as follows: sense primer, 5'-AAAATTGTAATACGACTCACTATAGGGCGAGCCGCCACCATGTAC CCATACGATGTTCCAGATTACGCTAGCTTGGGTGGTCATATG-3' and antisense primer, 5'-ACTTGCGGGGTTTTTCAGTATCTACGAT-3'. For domain analysis, primers were used to PCR either the C-terminal or N-terminal domain of PLAGL2. The primers used to generate Myc-tagged N-terminal PLAGL2 were as follows: the sense primer was the same as the sense primer for full length PLAGL2 above and the antisense

primer was 5'-GCGCCGGGAATTCTTACTTGAGCAGCTCCTGCGAGT-3'. The primers used to generate Myc-tagged C-terminal PLAGL2 were as follows: the sense primer was 5'-AAAATTGTAATACGACTCACTATAGGGCGAGCCGCCACCA TGGAGGAGCAGAAGCTAATCTCAGAGGAGGACCTGATCAAGACAGAGCCCG TGGA-3' and the antisense primer was the same as the antisense used above to generate full length PLAGL2.

A total of 1 μg of PCR product was used to produce *in vitro* translated protein generated in rabbit reticulocyte lysates in the presence of ^{35}S-methionine for 90 minutes at 30^{o}C. Ten μl of *in vitro* generated PLAGL2 and 10 μl of *in vitro* generated putative interactor were incubated with 1 μg Myc antibody or an isotype-matched irrelevant antibody in 500 μl $NENT_{500}$ buffer (500 mM NaCl, 20 mM Tris-HCl, pH 8.0, 1 mmM EDTA, 0.5% NP-40, and mammalian protease inhibitor cocktail) at 4^{o}C rotating overnight. Protein A Sepharose 4Fast Flow beads (Pharmacia Biotech, Piscataway, NJ) were washed three times and resuspended in $NENT_{500}$ buffer with 1 mg/ml BSA. Fifty μl of beads were added to each co-immunoprecipitation incubation and rotated for one hour at 4^{o}C. Reactions were then washed five times with 500 μl of $NENT_{500}$ buffer. After the final wash, 25 μl of SDS-PAGE sample buffer was added to the beads and boiled for 10 minutes. Twenty μl of each co-immunoprecipitation was subjected to SDS-PAGE and visualized using autoradiography.

In vitro SUMO1-modified proteins were generated using the SUMOlink kit for SUMO1 (Active Motif, Carlsbad CA). Briefly, 4 μl of rabbit reticulocyte lysate generated protein was combined with SUMO-1 kit components in a total of 20 μl. Sumoylation

reactions were incubated for three hours at 30^{o}C. For co-immunoprecipitations equal amounts of interacting non-sumoylated and sumoylated protein were added to each reaction.

Cloning of PLAGL2 and Putative Interactors for
In Vivo Co-Immunoprecipitation (Co-IP)

PLAGL2 was cloned into the mammalian expression vector pAcGFP (Clontech) using PCR product generated with pcDNA3.1(PLAGL2) as template and *EcoRI* and *BamHI* as ligation sites. The primers used to generate full length PLAGL2 were as follows: sense primer, 5'-GCGCGAATTCCATTAGCCTGGCCATGACCAC-3' and antisense primer, 5'-CCACGGATCCGGTACTAAGGCTCCATAACAGAG-3'. PLAGL2 zinc finger mutants were generated using site directed mutagenesis, as described previously in Chapter 3 using pAcGFP(PLAGL2) as template. The putative interactor $PC2_{434-784}$ was cut from the yeast vector pACT2($PC2_{434-784}$) and ligated into the pProLabel-C mammalian expression vector using *EcoRI* and *XhoI*. The putative interactor FHL3 was PCR cloned from pACT2(FHL3) using the following primers: sense primer, 5'-GGCCGGATCCTGGTTCTCTCCCCTTGCCACCAT-3' and antisense primer, 5'-CTGAGGATCCCACCGCTTATTGCAGAATC-3'. The FHL3 PCR product was cloned into the *BamHI* sites of pProLabel-C. The putative interactor $CHD3_{1585-1966}$ was also PCR cloned from pACT2($CHD3_{1585-1966}$) using the following primers: sense primer, 5'-CTGACCCGGGCAAGAACAGCAGAATTGGGGA-3' and antisense primer, 5'-CTGACCCGGGTCTGAGGCTGAACAGCAGTTG-3'. The $CHD3_{1585-1966}$ PCR product was cloned into the *SmaI* site of pProLabel-C.

Transient Transfections

HEK293 cells were grown in DMEM supplemented with 10% fetal bovine serum (FBS), penicillin/streptomycin, non-essential amino acids, sodium pyruvate, and L-glutamate. Transient transfections were carried out according to the manufacturer's protocol for Lipofectamine 2000 (Invitrogen), with some modifications. For ProLabel verification, cells were seeded the day before transfection at 10^5 cells in 500 μL in growth medium in 24 well tissue culture plates. On the day of transfection, 800 ng of total DNA was combined with 2 μL Lipofectamine 2000 reagent and incubated for 20 minutes at room temperature before being added to the cell culture. After six hours, medium was replaced with fresh complete medium. Cells were allowed to grow 24 hours before harvesting for ProLabel verification. For *in vivo* co-immunoprecipitations, two days prior to transfection, cells were seeded at $5X10^5$ cells in 5 ml complete medium in tissue culture plates. On the day of transfection, medium was replaced with 5 ml fresh medium lacking antibiotics. Eight μg total DNA per transfection was combined with 20 μL Lipofectamine reagent in 1mL DMEM for 20 minutes at room temperature. DNA-reagent complexes were then added to each seeded tissue culture plate. Cells were allowed to grow 48 hours before harvest for co-immnoprecipitations.

In Vivo Co-immunoprecipitaion (Co-IP)

In vivo co-immuoprecipitation was performed using the Matchmaker Chemiluminescent Co-IP System (Clontech), according to the manufacturer's protocol. Briefly, cells were seeded as above for ProLabel verification and for co-immunoprecipitation. Forty-eight hours after transfection, cells were harvested for

ProLabel verification and co-immunoprecipitation. For ProLabel verification, medium was removed and washed with 500 μL of PBS. To each well was added 200 μL of ProLabel Chemiluminescent lysis/complementation assay buffer. To 80 μL of each lysate, 30 μL of ProLabel substrate mix was added and transferred to a 96-well plate with clear bottom and black sides. Substrate activation was assayed at 5 minute intervals using a 96 well luminometer. For co-immunoprecipitations, fluorescence of AcGFP was detected 48 hours after transfection to measure transfection efficiency. Medium was removed, and cells were washed twice with 5 mL PBS. Cells were trypsinized and lysed. 250 μg of cell lysate was added to each co-immunoprecipitation reaction and rotated with 1 μg of antibody to AcGFP in 500 μl cell lysis buffer for one hour at 4^{o}C. 25 μL of protein G Plus/A agarose beads (Clontech) were added to each co-immunoprecipitation and incubated rotating overnight at 4^{o}C. After incubation, beads were washed, and bead-bound interactors were detected as above for ProLabel verification.

Statistical Analysis

One-way ANOVA was performed on the indicated sets of data. Post-test analysis used Tukey's pair-wise comparisons (GraphPad Prism Software). Pair-wise comparisons with differences at $P<0.05$ were considered to be statistically significant.

Results

Identification of Putative PLAGL2 Binding Factors by Yeast Two-Hybrid

To identify potential protein-protein interactions, we utilized a yeast two-hybrid assay with PLAGL2 as the bait. Full length PLAGL2 was cloned into the yeast reporter vector pAS2-1, and the recombinant vector was used to transform the competent yeast strain Y187. The bait strain Y187[pAS2-1(PLAGL2)] was assayed for autoactivity of the reporter and leaky *HIS3* background. We determined that 45 mM 3-AT was sufficient to inhibit leaky *HIS3* expression.

To perform the yeast two-hybrid screen, we utilized a yeast mating strategy with the previously transformed reporter strain AH109 carrying a human leukocyte cDNA library fused to the GAL4 activation domain (Chapter 2). Mating was performed as described previously for the yeast one-hybrid screen (Chapter 2). Briefly, the AH109[pACT2(human leukocyte cDNA)] strain was mated with the bait strain Y187[pAS2-1(PLAGL2)] at a density of 4.5×10^6 cells per cm^2. Diploid cells were selected on medium lacking tryptophan and leucine. The mating strategy assay screened 1.3×10^8 library clones, sufficiently covering the library. Diploid clones were then replica plated onto plates lacking histidine, tryptophan, and leucine to allow leaky *HIS3* background for a histidine jump-start assay. These plates were allowed to grow six days at 30^oC before colonies were harvested and replated on medium plates lacking histidine, adenine, tryptophan, and leucine and supplemented with 45 mM 3AT. From selection plates, 192 diploid reporter-positive clones were restreaked onto fresh selection plates (Figure 4.1, Panel A). These clones were then assayed for β−glactosidase activity using a

filter lift assay (Figure 4.2, Panel A) and for α-galactosidase activity using X-α-Gal medium plates (Figure 4.2, Panel B). All 192 diploid clones were positive for nutritional and colormetric reporter gene activity. From each diploid clone, the prey plasmids were recovered, amplified, sequenced, and analyzed using the BLAST algorithm.

Of the reporter positive diploid clones, the vast majority of prey plasmids recovered sequenced as the ubiquitin conjugating enzyme E2I (GenBankTM/EBI accession number NM194261), the human homolog to the well-characterized yeast enzyme UBC9. Interaction with UBC9 has previously been observed in a yeast two-hybrid assay using murine PLAGL2 as bait [204]. Other putative PLAGL2 interactors of interest included positive cofactor 2 (PC2) (GeneBankTM/EBI accession number NM001003891), four and a half LIM domains 3 (FHL3) (GeneBankTM/EBI accession number NM004468), and chromodomain helicase DNA binding protein (CHD3) (GeneBankTM/EBI accession number NM001005271). While both clones for E2I and FHL3 isolated from the human cDNA leukocyte library were full length, both PC2 and CHD3 were partial clones. The PC2 clone consisted of the amino acid residues 434-784, a region which includes a number of phosphorylation sites, a nuclear localization signal, an putative SUMO recognition sites. The $CHD3_{1585\text{-}1966}$ clone consisted of the amino acid residues 1585-1966, a region which contains the PHD/RING domain and the chromodomain associated CHD-like helicase. Therefore these clones will be refered to as $PC2_{434\text{-}784}$ and $CHD3_{1585\text{-}1966}$.

To confirm *in vivo* interaction in yeast, the bait vector pAS2-1(PLAGL2) was recovered from Y187 and used to transform AH109. The plasmids recovered from AH109, the putative PLAGL2 interactors [pACT2(E2I), pACT2($PC2_{434\text{-}784}$),

pACT2(FHL3), and pACT2($CHD3_{1585-1966}$)], were used to transform Y187. The bait and prey strains were then mated and selected for both nutritional and coloremetric gene reporter activity (Figure 4.1, Panel B). Interaction in yeast was confirmed for E2I, $PC2_{434-784}$, FHL3, and $CHD3_{1585-1966}$. These results implicate E2I, PC2, FHL3, and CHD3 as PLAGL2-binding proteins.

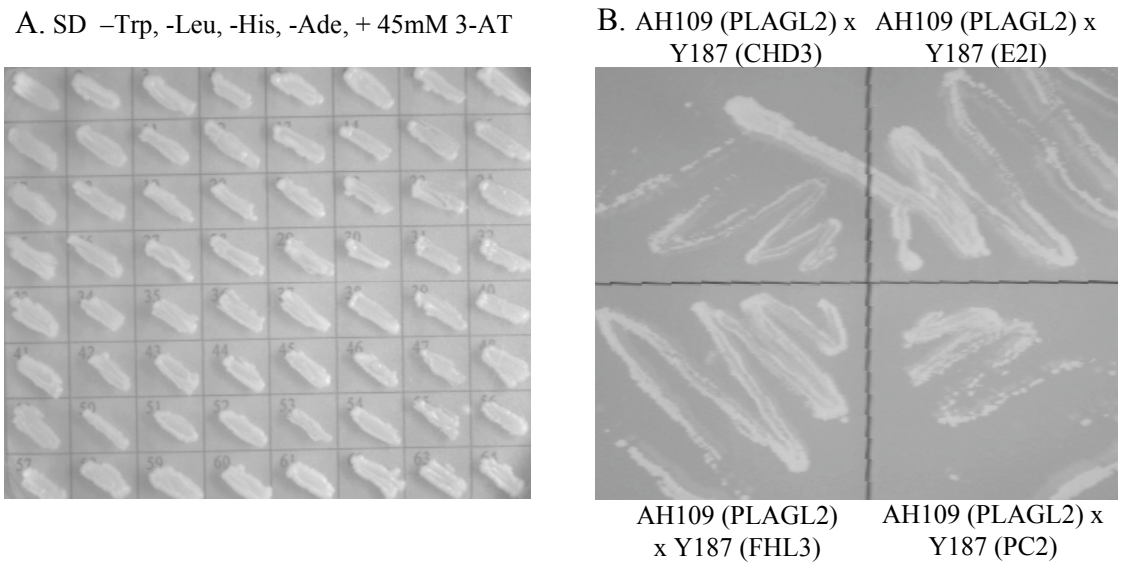

Figure 4.1: Identification of PLAGL2-binding proteins by yeast two-hybrid analysis. Panel A: Reporter positive diploid clones were nutritionally selected on medium lacking histidine, adenine, trypotophan, and leucine and supplemented with 45 mM 3AT. Panel B: Putative interactions were confirmed in yeast by recovering plasmids and repeating yeast two-hybrid with opposite transformants from the original yeast screen, i.e. with the bait (PLAGL2) transformed into the competent strain AH109 and the prey (E2I, $PC2_{434-784}$, FHL3, or $CHD3_{1585-1966}$) transformed into the competent strain Y187.

A. β-Galactosidase Filter Lift Assay

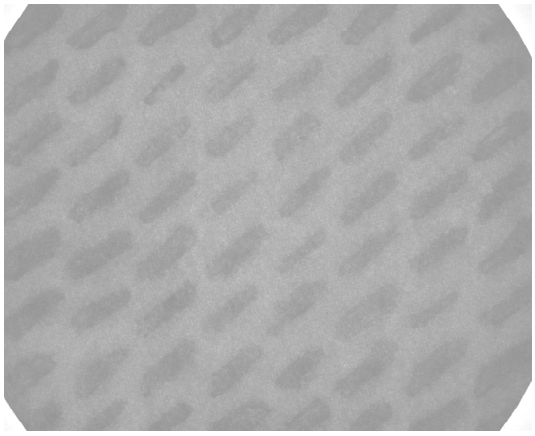

B. X--α-Galactosidase Agarose Plate Assay

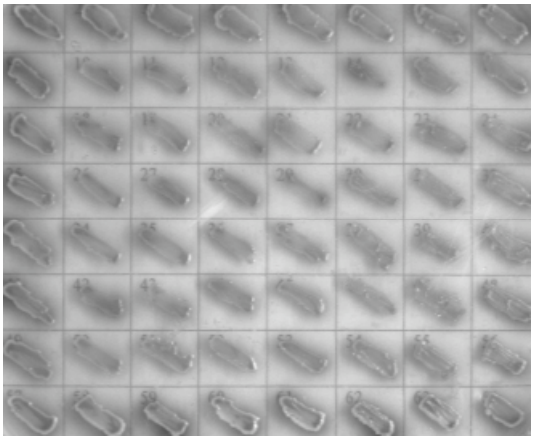

Figure 4.2: Verification of putative PLAGL2-binding proteins by colormetric assay. Panel A-B: Reporter positive diploid clones were assayed for colormetric reporter activity using filter lift for β-galactosidase (Panel A) and X-α-Gal medium plates for α-galactosidase (Panel B).

In Vitro Co-immunoprecipitaion Confirms
Direct Interaction Between PLAGL2 and $PC2_{434-784}$, FHL3, or $CHD3_{1585-1966}$

The yeast two-hybrid allowed us to identify putative PLAGL2 interacting proteins. We isolated three DNA transcription-modifying proteins PC2, FHL3, and CHD3. Although the yeast two-hybrid identified these as putative PLAGL2-binding proteins *in vivo*, the yeast two-hybrid did not determine whether PLAGL2 interaction was direct or whether interaction was via a nucleocomplex. Since each of the putative PLAGL2 interactors is known to participate in nucleocomplexes, we utilized *in vitro* translation in rabbit reticulocyte lysates to accertain whether our putative PLAGL2 interactors bound PLAGL2 directly.

Myc-tagged PLAGL2 was translated *in vitro* and HA-tagged $PC2_{434-784}$ and $CHD3_{1585-1966}$ were translated *in vitro* using rabbit reticulocyte lysates (Promega). Proteins were translated *in vitro* in the presence of ^{35}S-labeled methionine for

visualization by autoradiographgy. *In vitro* translated proteins were then incubated together with either Myc antibody or an isotype matched irrelevant antibody. Interacting complexes were then isolated using protein A/G beads, washed, removed with sample buffer, subjected to SDS-PAGE separation, and visualized by autoradiography. Immunoprecipitation of $PC2_{434\text{-}784}$, FHL3, and $CHD3_{1585\text{-}1966}$ occurred in the presence but not in the absence of PLAGL2 (Figure 4.3, lanes 3, 5, and 7 verses lanes 2, 4, and 6, respectively).

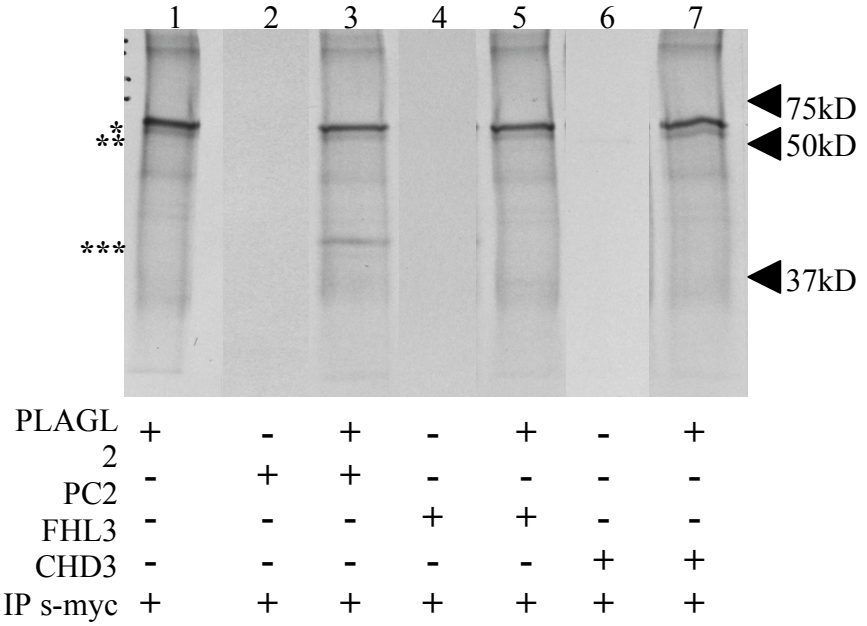

Figure 4.3: *In vitro* $PC2_{434\text{-}784}$, FHL3, and $CHD3_{1585\text{-}1966}$ co-immunoprecipitaion with PLAGL2. Panel A: PLAGL2 (lanes 1, 3, 5, and 7), $PC2_{434\text{-}784}$ (lanes 2 and 3), FHL3 (lanes 4 and 5), and $CHD3_{1585\text{-}1966}$ (lanes 6 and 7) were *in vitro* translated in rabbit reticulocyte lysates in the presence of ^{35}S-methionine. Putative PLAGL2 interactors (10 μL) were incubated with (lanes 3, 5, and 7) or without (lanes 2, 4, 6) PLAGL2 (10 μL). Interacting complexes were immunoprecipitated with 1 μg myc antibody (lanes 1-7). Interacting complexes were subjected to SDS-PAGE and visualized using autoradiography. Immnoprecipitated bands are identified as (*) for PLAGL2, (**) for $CHD3_{1585\text{-}1966}$, and (***) for $PC2_{434\text{-}784}$.

In Vitro Co-translation Enhances PLAGL2 Complex Formation with FHL3 and $CHD3_{1585-1966}$

Lack of interaction for FHL3 could have been the result of few ^{35}S-labeled methionines, as FHL3 has only two methionies, or it might be the result of poor protein tertiary structure. *In vivo*, zinc finger proteins often are co-translated so that tertiary structure evolves as interactions occur [242]. To determine whether this was the case for the zinc finger containing FHL3 and $CHD3_{1585-1966}$, we co-translated PLAGL2 with $PC2_{434-784}$, FHL3, or $CHD3_{1585-1966}$ and repeated the co-immunoprecipitations. As shown in Figure 4.4, co-translation of FHL3 and $CHD3_{1585-1966}$, both zinc finger proteins, with PLAGL2, also containing a zinc finger domain, enhanced interaction and immunoprecipitation (Figure 4.4, lanes 7 and 10) when compared to immunoprecipitations with proteins translated separately (Figure 4.4, Panel A, lanes 6 and 9). $PC2_{434-784}$ does not contain a zinc finger domain and co-translation did not enhance immunoprecipitate with PLAGL2. These data indicate that zinc finger interaction between PLAGL2 and FHL3 or $CHD3_{1585-1966}$ was strengthened by co-translation of the proteins.

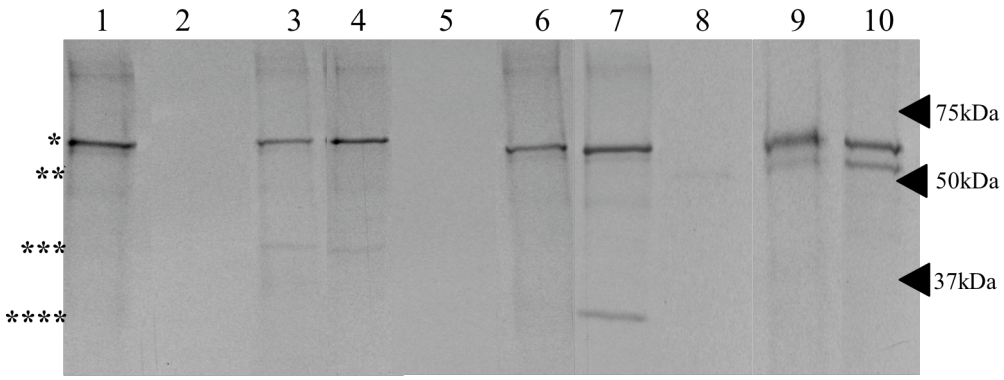

PLAGL2	+	-	+	-	-	+	-	-	+	-
PC2	-	+	+	-	-	-	-	-	-	-
PLAGL2 x PC2	-	-	-	+	-	-	-	-	-	-
FHL3	-	-	-	-	+	+	-	-	-	-
PLAGL2 x FHL3	-	-	-	-	-	-	+	-	-	-
CHD3	-	-	-	-	-	-	-	+	+	-
PLAGL2 x CHD3	-	-	-	-	-	-	-	-	-	+
IP s-myc	+	+	+	+	+	+	+	+	+	+

Figure 4.4: Co-translation of PLAGL2 zinc finger interactors with PLAGL2 enhances binding to PLAGL2. Panel A: Putative interactors $PC2_{434-784}$, FHL3, and $CHD3_{1585-1966}$ were either co-translated in rabbit reticulocyte lysates with PLAGL2 or translated independent of PLAGL2 and allowed to interact. Interacting complexes were immunoprecipitated with myc antibody and visualized using autoradiography. PLAGL2 immnoprecipitated by itself (lane 1), while none of the interactors immunoprecipitated without PLAGL2 (lanes 2, 5, and 8). For FHL3 and $CHD3_{1585-1966}$, co-translation with PLAGL2 enhanced complex immoprecipitation (lanes 6 and 7 and lanes 9 and 10, respectively). Co-translation did not enhance $PC2_{434-784}$ complex formation and immunoprecipitation with PLAGL2 (lanes 3 and 4). Immunoprecipitated proteins are identified as (*) for PLAGL2, (**) for $CHD3_{1585-1966}$, (***) for $PC2_{434-784}$, and (****) for FHL3.

PLAGL2 and $CHD3_{1585-1966}$ Interaction is Weakened by SUMO1-Modification

Recent research on PLAGL2 suggests that sumoylation may modulate protein-protein interactions [238]. To address whether SUMO1-modification mediates protein-protein interactions between PLAGL2 and the putative PLAGL2 interactors $PC2_{434-784}$, FHL3, and $CHD3_{1585-1966}$, we translated the proteins *in vitro* in rabbit reticulocyte lysates. We also modified *in vitro* translated PLAGL2 with SUMO-1 and repeated the co-

immunoprecipitaions. Although PLAGL2 was successfully sumoylated, interaction with either $PC2_{434-784}$ or FHL3 was not affected by SUMO-1 modification of PLAGL2, however because of the presence of unmodifed PLAGL2 in the immunoprecipitations, it can not be concluded that SUMO1-modified PLAGL2 does not interact with $PC2_{434-784}$ or FHL3 (data not shown).

While neither $PC2_{434-784}$ nor FHL3 contain the conserved SUMO-modification motif ΨKXE (where Ψ indicates a hydrophobic residue and X indicates a random amino acid), $CHD3_{1585-1966}$ does contain a SUMO-modification site within a region identified as the SUMO-1-interacting region [243]. *In vitro* sumoylating PLAGL2 did not seem to enhance or inhibit $CHD3_{1585-1966}$ complex formation (Figure 4.5, lane 6); however, the immunoprecipitated $CHD3_{1585-1966}$ could be forming a complex with only the unmodified PLAGL2 and not the SUMO1-modified PLAGL2. To address whether sumoylation of $CHD3_{1585-1966}$ might affect PLAGL2-$CHD3_{1585-1966}$ protein-protein interactions, we also sumoylated $CHD3_{1585-1966}$ *in vitro* and evaluated binding to PLAGL2. While *in vitro* sumoylated $CHD3_{1585-1966}$ poorly immunoprecipitated with unmodified PLAGL2 (Figure 4.5, lane 7), the unmodified $CHD3_{1585-1966}$ formed a complex with unmodified PLAGL2 (Figure 4.5, lane 7). Finally, sumoylation of $CHD3_{1585-1966}$ and PLAGL2 eliminated interaction with SUMO1-modified $CHD3_{1585-1966}$ (Figure 4.5, lanes 7 and 8). To more clearly establish the affects of SUMO-1 modification, these *in vitro* translated and sumoylated proteins would have to be immunoprecipitated with an antibody to SUMO1 to eliminate the remaining unmodified protein. Therefore, these preliminary data indicate that SUMO1-modification of CHD3 may interfere with or weaken the interaction between PLAGL2 and CHD3 *in vitro*.

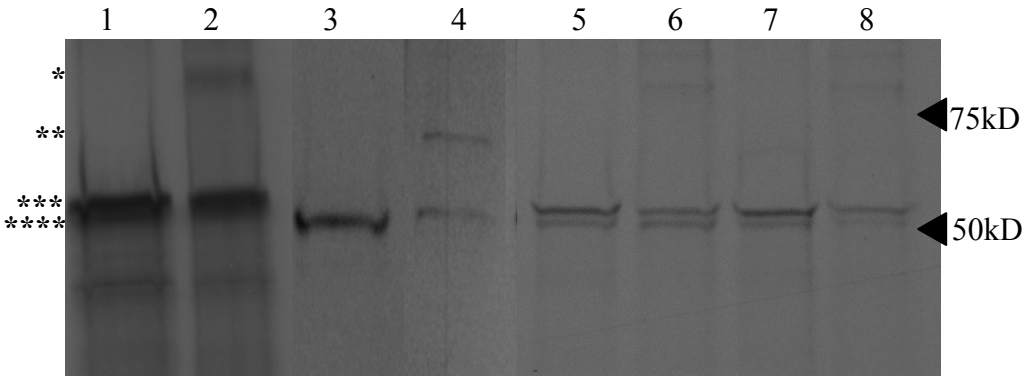

PLAGL2	+	-	-	-	+	-	+	-
SUMO1-PLAGL2	-	+	-	-	-	+	-	+
CHD3	-	-	+	-	+	+	-	-
SUMO1-CHD3	-	-	-	+	-	-	+	+
IP-Myc	+	+	-	-	+	+	+	+
IP-HA	-	-	+	+	-	-	-	-

Figure 4.5: PLAGL2 and $CHD3_{1585-1966}$ complex formation is weakened by SUMO1-modification. $CHD3_{1585-1966}$ and PLAGL2 ^{35}S-methionine labeled protein was generated in rabbit reticulocyte lysates. Half of the protein generating rabbit reticulocyte lysates were then *in vitro* sumoylated with SUMO-1 protein. Immunoprecipitations were carried out with anitibody to either HA or myc tags. Control immunoprecipitations were performed with either unmodified or SUMO1-modified protein with anti-myc antibody for PLAGL2 (lane 1 and 2) and anti-HA to $CHD3_{1585-1966}$ (lane 3 and 4). Non-SUMO1-modifed PLAGL2 was immunoprecipitated non-SUMO1-modified $CHD3_{1585-1966}$ (lane 5). SUMO1-modified PLAGL2 was immunoprecipitated with unmodified $CHD3_{1585-1966}$ (lane 6). SUMO1-modification of $CHD3_{1585-1966}$ appeared to interfere with complex formation (lanes 7 and 8). Complexes were allowed to form during incubation before immunoprecipitation with respective antibodies. Protein was then subjected to SDS-PAGE and visualized using autoradiography. Immunoprecipitated proteins are identified as (*) sumoylated PLAGL2, (**) sumoylated $CHD3_{1585-1966}$, (***) non-modified PLAGL2, and (****) non-modifed $CHD3_{1585-1966}$.

In Vitro $CHD3_{1585-1966}$ Interacts with the Zinc Finger Domain of PLAGL2

Co-translation of $CHD3_{1585-1966}$ and FHL3 with PLAGL2 *in vitro* enhanced complex formation and immunoprecipitation. It is likely that this enhanced immunoprecipitation was the result of a properly forming tertiary structure, which enhanced the protein-protein interaction. Co-translation often occurs when the interaction is between two zinc finger proteins. PLAGL2 contains two main domains, the C-terminal domain, consisting of the conserved sumoylation sites and the transactivation domain, and the N-terminal domain, consisting of the C_2H_2 zinc fingers (see Chapter 2, Figure 2.4). Since protein-protein interactions are often mediated through the zinc finger domain, we investigated which domain $PC2_{434-784}$, FHL3, and $CHD3_{1585-1966}$ bound in PLAGL2.

Rabbit reticulocyte lysates were used to generate full length PLAGL2 (FL-PLAGL2), N-terminal PLAGL2 (NT-PLAGL2), C-terminal PLAGL2 (CT-PLAGL2), $PC2_{434-784}$, FHL3, and $CHD3_{1585-1966}$ in the presence of ^{35}S-methionine. Co-immunoprecipitations were carried out as previously described using an antibody to Myc-tagged PLAGL2. All three PLAGL2 constructs were immunoprecipitated with the Myc antibody (Figure 4.6, lanes 1-3), although most of the methionines contained within PLAGL2 are in the C-terminal, so this domain (Figure 4.6, lane 2) was easier to visualize than the N-terminal domain (Figure 4.6, lane 3). Because FHL3 has only two methionines, immunoprecipitation with the PLAGL2 domains was difficult to visualize; however, the co-translational data suggest that interaction between PLAGL2 and FHL3 is mediated through the zinc finger domain.

Co-translation of PLAGL2 and $PC2_{434-784}$ *in vitro* did not enhance complex formation between these two proteins. As $PC2_{434-784}$ does not contain a zinc finger domain, the same logic as applied to FHL3 and $CHD3_{1585-1966}$ with regard to co-translation does not apply to $PC2_{434-784}$. Therefore, it is not surprising that $PC2_{434-784}$ appears to weakly interact with both the zinc finger domain (Figure 4.6, lane 5) and C-terminal transactivation domain (Figure 4.6, lane 6) of PLAGL2.

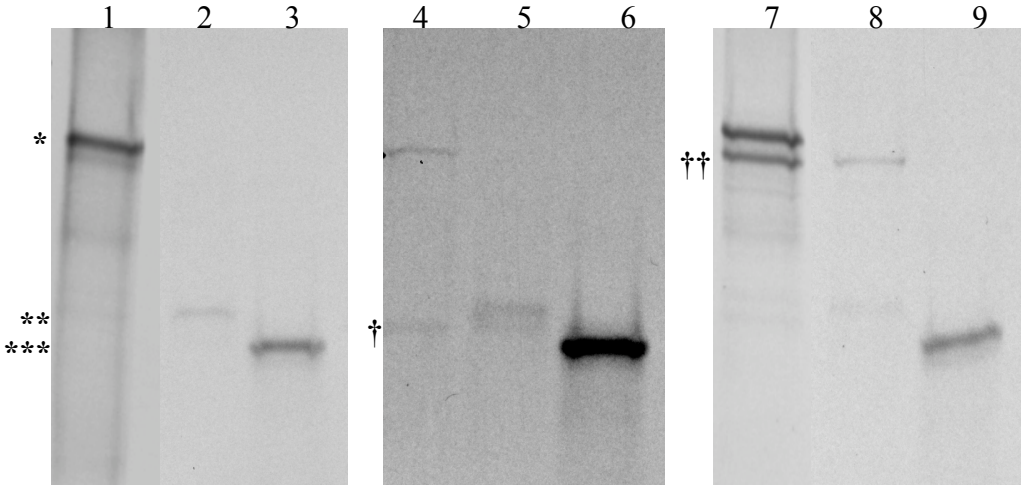

FL-PLAGL2	+	-	-	+	-	-	+	-	-
NT-PLAGL2	-	+	-	-	+	-	-	+	-
CT-PLAGL2	-	-	+	-	-	+	-	-	+
PC2	-	-	-	+	+	+	-	-	-
CHD3	-	-	-	-	-	-	+	+	+
IP-Myc	+	+	+	+	+	+	+	+	+

Figure 4.6: Domain mapping of PLAGL2 interaction. Full length PLAGL2 (FL-PLAGL2), N-terminal domain PLAGL2 (NT-PLAGL2), and C-terminal domain PLAGL2 (CT-PLAGL2) were *in vitro* generated in the presence of ^{35}S-methionine. FL-PLAGL2, NT-PLAGL2, and CT-PLAGL2 immunoprecipitated with an antibody to myc (lanes 1-3). $PC2_{434-784}$ immunoprecipitated with FL-PLAGL2 (lane 4), and weakly with both NT-PLAGL2 (lane 5) and CT-PLAGL2 (lane 6). $CHD3_{1585-1966}$ immunoprecipitated with FL-PLAGL2 (lane 7) and NT-PLAGL2 (lane 8), but did not immunoprecipitate with CT-PLAGL2 (lane 9). Immunoprecipitated proteins are identified as (*) FL-PLAGL2, (**) NT-PLAGL2, (***) CT-PLAGL2, (†) $PC2_{434-784}$, and (††) $CHD3_{1585-1966}$.

$CHD3_{1585\text{-}1966}$ contains a PHD/Ring finger zinc finger domain and co-translation of $CHD3_{1585\text{-}1966}$ with PLAGL2 *in vitro* greatly enhanced complex formation and immunoprecipitation (Figure 4.5, lanes 9 and 10), suggesting that protein-protein interaction may be mediated through zinc finger interaction. To determine whether $CHD3_{1585\text{-}1966}$ binds the zinc finger domain of PLAGL2, we performed $CHD3_{1585\text{-}1966}$ co-immunoprecipitations with full length, N-terminal, and C-terminal PLAGL2. As shown in Figure 4.6, lanes 7-9, only full length and N-terminal PLAGL2 formed a complex with $CHD3_{1585\text{-}1966}$, indicating that $CHD3_{1585\text{-}1966}$ binds PLAGL2 at the N-terminal zinc finger domain. Together with the co-translational data, these data indicate that CHD3 and PLAGL2 mediate complex formation through zinc finger contact.

PLAGL2 Localizes to the Nucleus in HEK293 Cells

The yeast two-hybrid studies indicated that PLAGL2 interacts *in vivo* either directly or in a complex with $PC2_{434\text{-}784}$, FHL3, and $CHD3_{1585\text{-}1966}$. Furthermore, *in vitro* co-immunoprecipitation suggested that $PC2_{434\text{-}784}$, FHL3, and $CHD3_{1585\text{-}1966}$ interact directly with PLAGL2; however, putative protein-protein interactions needed to be verified *in vivo*. In order to determine whether PLAGL2 binds $PC2_{434\text{-}784}$, FHL2, and $CHD3_{1585\text{-}1966}$, we utilized an *in vivo* co-immunoprecipitation assay (Matchmaker Mammalian Chemiluminescent Co-immunoprecipitation; Clontech). To generate reagents for the assay, we cloned full length PLAGL2 into the fluorescent-tagged vector pAcGFP (Clontech) and cloned the putative PLAGL2 interactors $PC2_{434\text{-}784}$, FHL3, and $CHD3_{1585\text{-}1966}$ into the ProLabel tagged vector pProLabel-C (Clontech).

Previous work in our lab found high toxicity in myeloid cells that were transfected with high-expression PLAGL2 plasmids; however, Zheng *et al.* [193] have had success with exogenously expressed PLAGL2 in the human embryonic kidney cell line HEK293. Therefore we initially determined whether this cell line would tolerate exogenously expressed PLAGL2. When HEK293 cells were transiently transfected with AcGFP-tagged PLAGL2, fluorescence microscopy revealed high efficiency of transfection (Figure 4.7, Panel B), although the cells were sickly and beginning to lift from the plate (Figure 4.7, Panel A). In addition to PLAGL2 expression, we also confirmed expression of the putative interactors $PC2_{434\text{-}784}$, FHL3, and $CHD3_{1585\text{-}1966}$ through verification of the ProLabel tag expression (Figure 4.8).

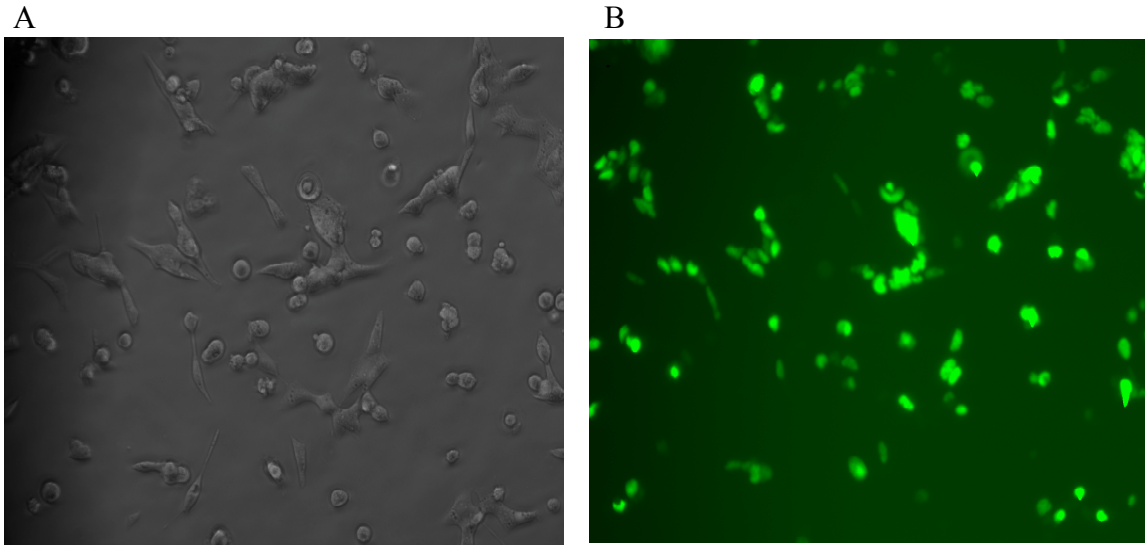

Figure 4.7: Efficient transient transfection of PLAGL2 in HEK293 cells. Panel A and B: HEK293 cells were transiently transfected with AcGFP-tagged PLAGL2 using Lipofectamine 2000 (Invitrogen). After 24 hours cells were visualized by both bright field (Panel A) and fluorescent microscope (Panel B) to acertain AcGFP-PLAGL2 expression.

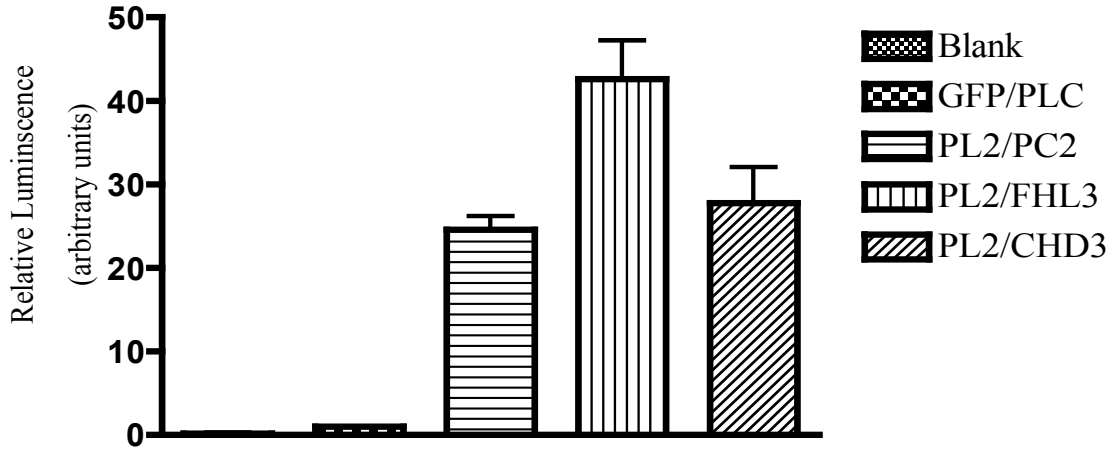

Figure 4.8: Efficient transient transfection of putative interactors $PC2_{434-784}$, FHL3, and $CHD3_{1585-1966}$. HEK293 cells were transiently transfected with either empty vector (GFP/PLC), AcGFP-PLAGL2 and ProLabel-$PC2_{434-784}$ (PL2/PC2), AcGFP-PLAGL2 and ProLabel-FHL3 (PL2/FHL3), or AcGFP-PLAGL2 and ProLabel-$CHD3_{1585-1966}$ (PL2/CHD3). After 24 hours, transfected cells were lysed and cell lysate was assayed for ProLabel activity as described in Materials and Methods. Statistically significant differences in luminescence compared to the empty vector control are indicated (#, $P<0.01$; ##, $P<0.001$).

When AcGFP-PLAGL2 was transiently transfected into HEK293 cells, we observed a distinct localization pattern. Because PLAGL2 is a zinc finger transcription factor, it seemed likely that exogenously expressed PLAGL2 was localizing to the nucleus. Therefore, we utilized dyes to identify localization of PLAGL2. HEK293 cells were transiently transfected with either empty vector (pAcGFP) or AcGFP-PLAGL2 and allowed to grow twenty-four hours in microscope slide tissue culture plates. As shown in Figure 4.9, AcGFP alone did not localize to the nucleus (Figure 4.9, left panels). In contrast, exogenously expressed AcGFP-PLAGL2 localized to the nucleus, and fluorescence overlay of GFP and nucleus staining DRAQ5 clearly demonstrated the PLAGL2 localizes to the nucleus in HEK293 cells (Figure 4.9, right panels).

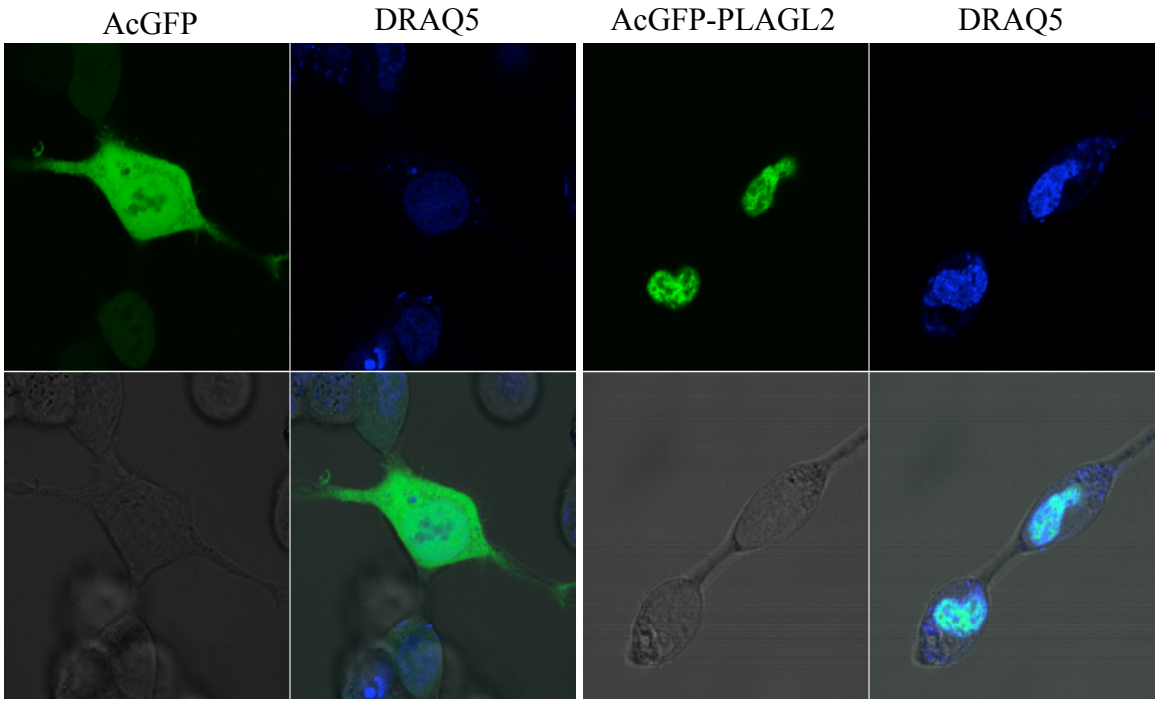

Figure 4.9: PLAGL2 is localized to the nucleus in HEK293 cells. HEK293 cells were transiently transfected with either empty vector (AcGFP) or AcGFP-tagged PLAGL2 (AcGFP-PLAGL2) in microscope slide tissue culture plates with Lipofectamine 2000 (Invitrogen) and allowed to grow 24 hrs. Live cell cultures were then treated with 10 μM DRAQ5 and allowed to incubate 30 minutes at 37^{o}C. Cells were visualized and images merged using fluorescence confocal microscopy.

Putative PLAGL2 Interactors $PC2_{434-784}$, FHL3, and $CHD3_{1585-1966}$ Bind PLAGL2 *In Vivo*

Transient transfections in HEK293 cells established that HEK293 cells can tolerate exogenously expressed PLAGL2. Additionally, we established that ProLabel tagged $PC2_{434-784}$, FHL3, and $CHD3_{1585-1966}$ were efficiently expressed when co-transfected with PLAGL2. Finally, confocal microsopy indicated that exogenously expressed PLAGL2 localized to the nucleus. These data indicate that PLAGL2 and its

putative interactors $PC2_{434-784}$, FHL3, and $CHD3_{1585-1966}$ are properly expressed in HEK293 cells and can be used for *in vivo* co-immunoprecipitations.

For *in vivo* co-immunoprecipitations, HEK293 cells were transiently transfected with either empty vectors, combinations of empty vectors with tagged expression vectors, or with both expression vectors. For example, to assay for *in vivo* interaction between $CHD3_{1595-1966}$ and PLAGL2, HEK293 cells were transfected with both AcGFP-PLAGL2 and ProLabel-$CHD3_{1585-1966}$. To control for nonspecific effects from transfection, HEK293 cells were also transfected with empty pAcGFP vector and empty pProLabel C vector. To control for background ProLabel expression, HEK293 cells were transfected with AcGFP-PLAGL2 and empty pProLabel C vector. Finally, to control for interaction specificity for PLAGL2 and $CHD3_{1585-1966}$ direct interaction, HEK293 cells were transiently transfected with empty pAcGFP vector and ProLabel-$CHD3_{1585-1966}$.

Forty-eight hours post transfection, the cells were visualized by fluorescent microscopy to check for PLAGL2 expression, harvested, and PLAGL2 protein-protein complexes were immunoprecipitated with an antibody to the AcGFP tag of PLAGL2. Cells transfected in parallel were also assayed for ProLabel expression and transfection efficiency of the PLAGL2 interactors. Immunoprecipitates were then analyzed for chemiluminescence, which specifically results from the presence of the ProLabel tag on the putative PLAGL2 interactors. As shown in Figure 4.10, Panels A-C, all three PLAGL2 putative interactors co-immunoprecipitated with PLAGL2, as shown by statistically significant enhancement of ProLabel signal in the expression vector transfections verses the empty vector controls. Taken together, these data indicate that PLAGL2 interacts directly with $PC2_{434-784}$, $CHD3_{1585-1966}$.

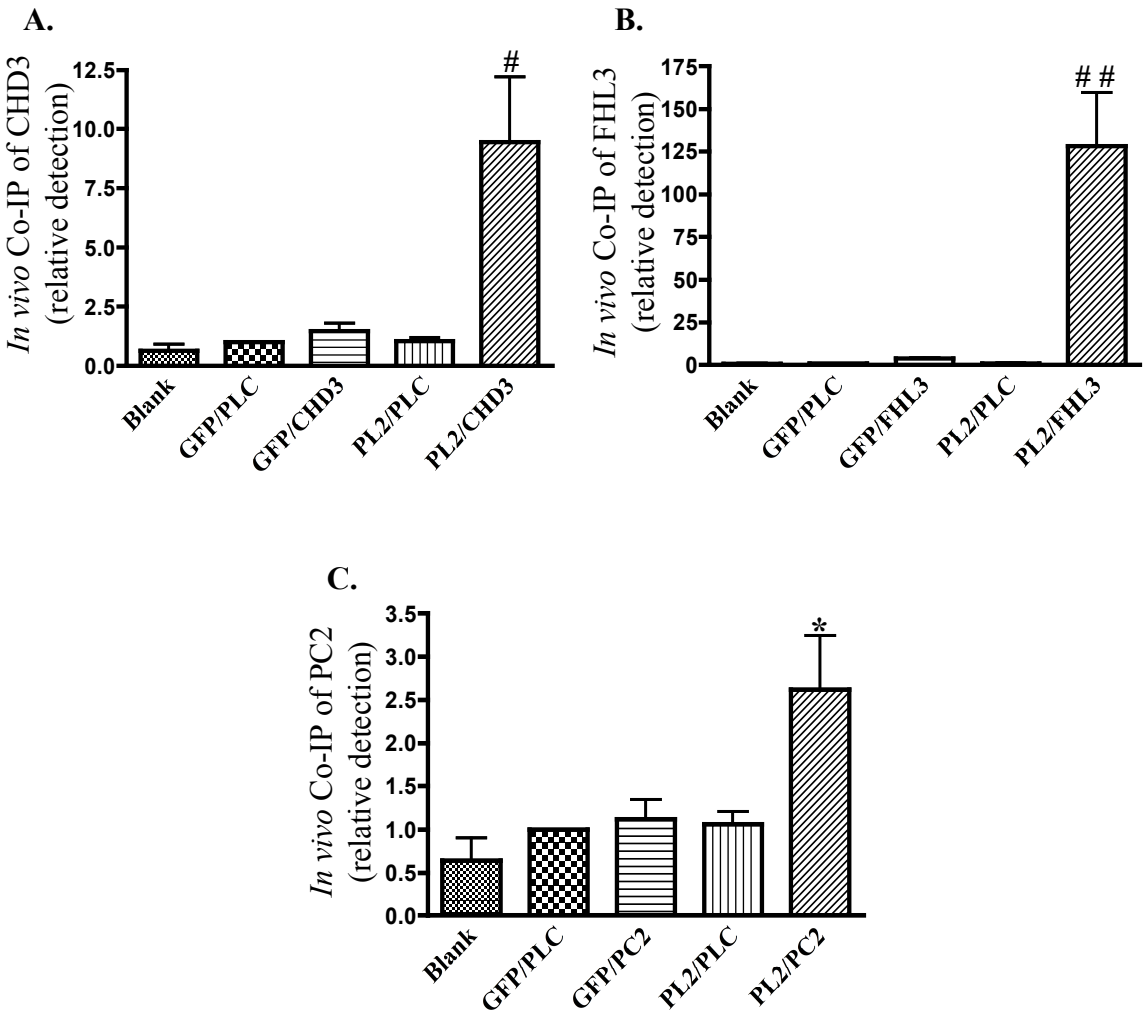

Figure 4.10: Putative PLAGL2 interactors $PC2_{434-784}$, FHL3, and $CHD3_{1585-1966}$ bind PLAGL2 *in vivo*. HEK293 cells were transiently transfected with the indicated vectors using Lipofectamine 2000. Cells were grown 48 hrs before cell lysate was harvested and immunoprecipitated with an antibody to AcGFP. Bead bound complexes were then subjected to substrate activation. ProLabel activity was detected using a 96 well luminometer for an hour and a half. Relative ProLabel activity was determined from data points taken during linear amplification and is presented as fold change relative to the AcGFP/interactor control transfection. Statisitcally significant immunoprecipitation of PLAGL2 interactors as determined by ProLabel activity was indicated for $CHD3_{1585-1966}$ (Panel A), FHL3 (Panel B), and $PC2_{434-784}$ (Panel C). Statistically significant differences relative to the empty AcGFP/putative interactor are indicated (*, $P<0.05$; #, $P<0.01$; ##, $P<0.001$).

PLAGL2 Zinc Fingers Show Unique and
Overlapping Binding Patterns With $PC2_{434-784}$, FHL3, and $CHD3_{1585-1966}$

Previously, zinc fingers six and seven of PLAGL2 were found to modulate DNA sequence recognition and binding to the *NCF2* TNF-α responsive region (TRR, see Chapter 3); however, the *in vitro* co-immunoprecipitations indicated that, while $PC2_{434-784}$ appears to weakly bind both the N-terminal and C-terminal domains of PLAGL2, $CHD3_{1585-1966}$ only bound the zinc finger N-terminal domain of PLAGL2 (Figure 4.6). Although FHL3 did not radiolabel heavily enough to determine specific domain binding, FHL3 does contain zinc fingers, and the enhanced immunoprecipitation with co-translation suggests that, like CHD3, FHL3 interaction with PLAGL2 is mediated via the zinc fingers. To determine which zinc fingers are necessary for protein-protein interactions, each PLAGL2 zinc finger was consecutively eliminated, as described in Chapter 3, by disrupting the zinc-binding domain via site-directed mutagenesis of the first histidine of each zinc finger. Using pAcGFP-PLAGL2 as template for the site directed mutagenesis meant that each PLAGL2 zinc finger still had the AcGFP tag and could be used for *in vivo* co-immunoprecipitation.

As before, HEK293 cells were transiently transfected with either wild-type PLAGL2 (WT) or one of the PLAGL2 zinc finger mutants (ZNF1-ZNF7), along with the putative PLAGL2 interactor ($PC2_{434-784}$, FHL3, or $CHD3_{1585-1966}$). Cells were allowed to grow forty-eight hours before harvest. All cells were observed for efficient transfection and expression of PLAGL2 constructs using a fluorescent microscope to visualize the AcGFP tag. Cells were then lysed, immunoprecipitated with an antibody to AcGFP, and

complex formation with the putative interactor was detected through ProLabel tag activation.

As shown in Figure 4.11, PLAGL2 zinc finger mutation resulted in a differential loss of complex formation, depending on the interactor. For $CHD3_{1585\text{-}1966}$, mutation of zinc finger two resulted in the only statistically significant loss in complex formation and accounted for about sixty-five percent of the capacity for PLAGL2 to bind $CHD3_{1585\text{-}1966}$. The remaining thirty-five percent of binding capacity is likely the result of a combination of zinc fingers three and four, as mutation to these zinc fingers resulted in a slight loss of complex formation (Figure 4.11, Panel A). These data agree with our previous *in vitro* co-immunoprecipitaions, which indicated that $CHD3_{1585\text{-}1966}$ binds PLAGL2 at the zinc finger N-terminal. Complex formation with FHL3 showed a pattern of zinc finger binding distinct from that of $CHD3_{1585\text{-}1966}$. As shown in Figure 4.11, Panel B, mutation of zinc fingers two, three, four, and six resulted in a statistically significant loss of complex formation between PLAGL2 and FHL3. These date indicate that FHL3 binds PLAGL2 at the zinc finger N-terminus. Finally, mutation of zinc fingers in PLAGL2 did not significantly impair complex formation between $PC2_{434\text{-}784}$ and PLAGL2, although the trend suggests that zinc finger three and perhaps zinc finger two may contribute to $PC2_{434\text{-}784}$ binding to PLAGL2. As suggested by the *in vitro* co-immunoprecipitations, $PC2_{434\text{-}784}$ complex formation with PLAGL2 is likely mediated by a combination of both the N-terminal and C-terminal PLAGL2 domains. Although PLAGL2 zinc finger one is a degenerate zinc finger (see Chapter 3), mutation of this zinc finger acted as a good control to show that point mutations in the zinc fingers did not interfere with global tertiary structure, since there was no loss of complex formation with any of the

interactors when zinc finger one was mutated. Taken together, these preliminary data indicate that PLAGL2 binds interacting proteins in unique and overlapping patterns.

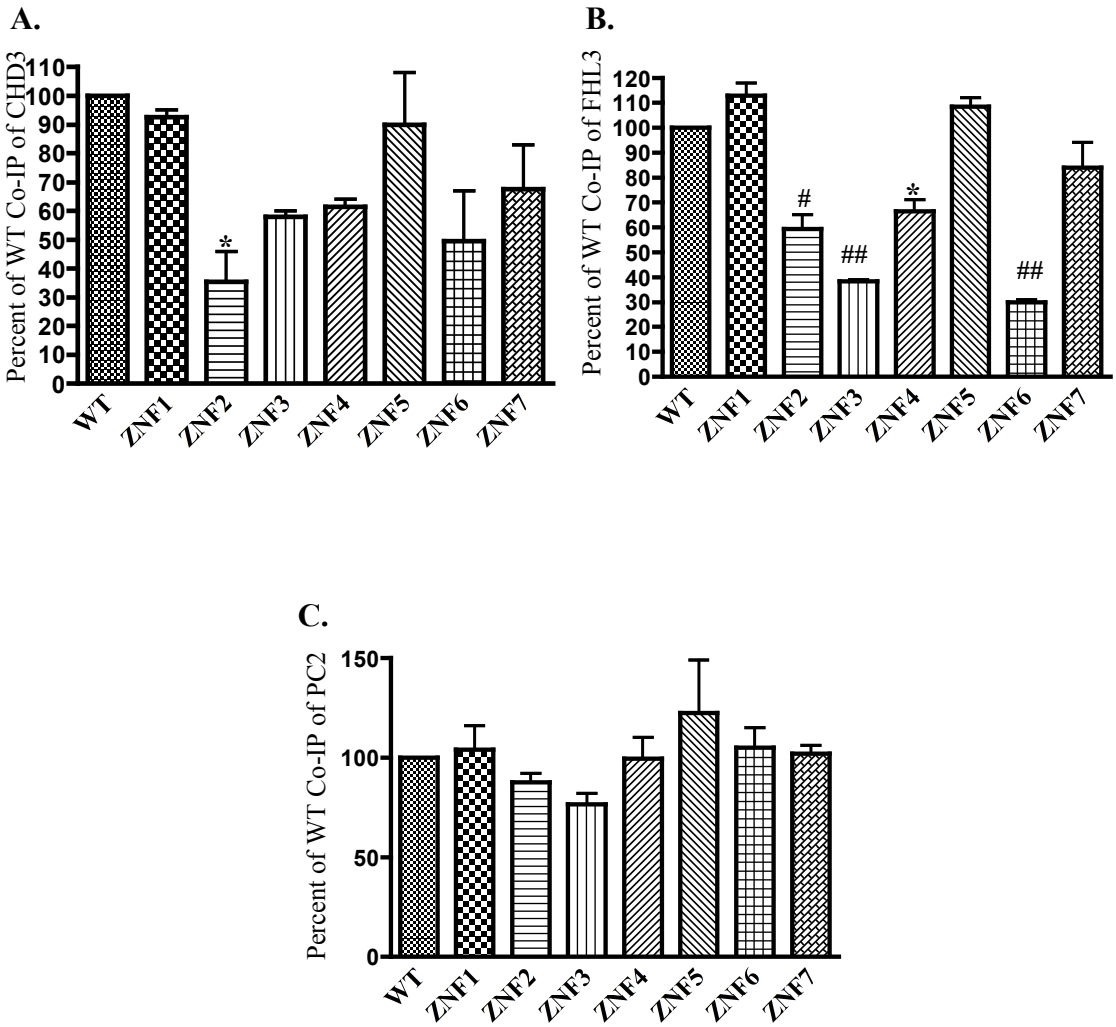

Figure 4.11: PLAGL2 forms a complex with the putative interactors $PC2_{434-784}$, FHL3, and $CHD3_{1585-1966}$ via both unique and overlapping binding patterns. PLAGL2 zinc finger mutants were generated by site directed mutagenesis of the first histidine of each zinc finger using AcGFP-PLAGL2 as template. Wild-type (WT) and zinc finger mutants (ZNF1-ZNF7) were co-transfected into HEK293 cells with each PLAGL2 putative interactor $CHD3_{1585-1966}$ (Panel A), FHL3 (Panel B), or $PC2_{434-784}$ (Panel C), respectively. Cells were allowed to grow 48 hrs before being assayed for AcGFP expression, harvested, and lysed. Cell lysate was immunoprecipitated and assayed for ProLabel activity using a 96 well luminometer. Data is presented as percent of wild-type PLAGL2 complex immunoprecipitation of the ProLabel tagged interactor. Statistically significant inhibition of complex formation is indicated (*, $P<0.05$; #, $P<0.01$; ##, $P<0.001$).

Discussion

Although there is a growing body of evidence addressing PLAGL2 regulation and transactivation, there remains little known about how PLAGL2 functions as a transcription factor. Even less explored are the potential protein-protein interactions that mediate PLAGL2 transcription activity. Studies that have looked at transactivation by PLAGL2 have identified possible protein-protein interactions between PLAGL2 and HIF1-α [226] and PLAGL2 and TTF-1 [190]. While these studies demonstrate that PLAGL2 may work in conjunction with other transcription factors, these studies failed to show that these proteins interact directly with PLAGL2. Direct interaction with PLAGL2 has been demonstrated for Tip60 [238] and Pirh2 [235]. We identified PLAGL2 as a *NCF2* intragenic region binding transcription factor [227]; however, EMSA analysis and DNase footprinting suggested that multiple factors may bind to and regulate the *NCF2* intragenic region [131] in conjunction with PLAGL2. Additionally, the relatively weak affinity PLAGL2 has for the TRR in the *NCF2* intragenic region [227] suggests that other factors may work to enhance PLAGL2 affinity at this sequence *in vivo*. Therefore, we hypothesized that PLAGL2 likely interacts with other transcription regulating factors to mediate activity at the *NCF2* intragenic region.

To address this hypothesis, we first utilized a yeast two-hybrid screen with PLAGL2 as bait and a human leukocyte cDNA library as prey. The yeast two-hybrid strategy identified four putative interacting proteins of interest. The vast majority of interacting clones sequenced as the ubiquitin conjugating enzyme E2I, the human homolog to the yeast E2 ligase UBC9. E2I is a recently identified essential component of

the SUMO-1 ligase pathway (reviewed in [244]). E2I has previously been identified as a putative PLAGL2 interactor in a yeast two-hybrid screen with murine PLAGL2 [204]. Subsequent work has identified PLAGL2 as a SUMO-1 modifed transcription factor [193]. While sumoylation appears to repress PLAGL2 transcription activation, the mechanisms responsible remain undetermined. Sumoylation can repress transcription factor activity either by recruiting respressive factors or by interfering with activating factors, as discussed above. The *in vitro* co-immunoprecipitation data presented here suggest that the effects of SUMO1-modification may be context-dependent, as sumoylation of $CHD3_{1585-1966}$ interfered with complex formation. Further characterization of how E2I and sumoylation regulate PLAGL2 transcription activity may certainly prove revealing.

Another putative PLAGL2 protein identified in the yeast two-hybrid assay was positive cofactor 2 (PC2), also known as TIG1 or ARC105. PC2 is a key component of the activator-mediated cofactor complex (ARC) that mediates TGF-β transcriptional activation [245]. While binding to PLAGL2 both *in vitro* and *in vivo* was relatively weak, $PC2_{434-784}$ consistently bound to PLAGL2. Because PC2 is a component of a larger activator complex, it is likely that $PC2_{434-784}$ makes direct contact with PLAGL2, but that strong affinity requires the full activator complex. Interestingly, $PC2_{434-784}$ contains conserved putative SUMO-1 recognizing motifs. These are not motifs that are SUMO-modified, as are present in PLAGL2. Rather, these are motifs that appear to recognize SUMO-modification on other proteins [243]. Whether these motifs mediate either binding to PLAGL2 or PLAGL2 activity remains to be determined.

A third putative PLAGL2 interactor identified via the yeast two-hybrid assay was homo sapien four and a half lim domain 3 (FHL3). FHL3 contains four zinc finger domains, known as LIM domains that are essential for both promoter transactivation and protein-protein interaction [246]. Whereas FHL3 acts as a transcriptional co-repressor in myeloid cells [247] as part of a complex recruiting histone deacetylases (HDACs) [248], FHL3 can also act as a co-activator in association with members of the CREB family of transcription factors [246]. While recent work suggests that sumoylation of PLAGL2 inhibits promoter transactivation, acetylation appears to enhance PLAGL2 transcription factor activity. Indeed deacetylation and therefore deactivation of PLAGL2 appears to be mediated through HDACs [193]. The present work indicates that FHL3 directly binds PLAGL2 both *in vitro* and *in vivo*. Together these data suggest an interesting model in which FHL3 may regulate PLAGL2 transcriptional activity through the recruitment of HDACs. Verification of this model remains to be determined; however, recent data has shown that the PLAGL2 interacting protein Tip60 recruits HDAC7 [237] and therefore may mediate PLAGL2 activity through protein-protein interactions.

The final putative PLAGL2 interactor identified in the yeast two-hybrid assay was the chromodomain helicase DNA binding protein 3 (CHD3), also known as Mi2-α. CHD3 is characterized by chromatin organization domains and helicase/ATPase domains and is part of a histone deacetylase complex called Mi2/NuRD [249]. CHD3 can act either as a co-repressor or a co-activator. CHD3 interaction with the transcription factors p73 and p53 results in repression of transcription, likely through recognition of transcription factor SUMO-1 modification [243]. On the other hand, CHD3 can activate c-myb in myeloid cells [250]. It remains to be determined whether CHD3 can act as a co-

repressor, a co-activator, or some context-dependent combination of both with PLAGL2; however, $CHD3_{1585-1966}$ clearly binds directly to PLAGL2 both *in vitro* and *in vivo*.

Besides E2I, other published protein-protein interaction with PLAGL2 include the histone acetyltransferase Tip60 [238] and the E3 ubiquitin ligase Pirh2 [235]. Although Tip60 is a histone acetyltransferase, it can also acetylate binding partners independently of histone [251]. Whereas the acetyltransferase p300 associates endogenously with Tip60 [252] and p300 has been shown to positively regulate PLAGL2 [193], a model emerges in which Tip60 acts as a co-activator of PLAGL2 through acetylation [238]. On the other hand, Tip60 can act as a co-repressor of STAT3 by recruiting HDAC7 [237], and HDAC7 has been shown to significantly decrease acetylation (and thus activation) of PLAGL2 [193], suggesting that Tip60 might also have the capacity to act as a co-repressor of PLAGL2 through recruitment of HDAC7. Again, regulation may be context dependent, and the mechanisms of regulation remain to be determined. Hoewever, between the data presented here and previous work with PLAGL2 cited above, a model for PLAGL2 is emerging in which protein-protein interactions mediate PLAGL2 activity in a context-dependent manner through the recruitment of co-repressors and co-activators that, in turn, post-translationally modify PLAGL2.

PLAGL2 contains six classical C_2H_2 zinc finger domains, if one does not consider the first zinc finger as functional since it contains degenerate sequence [188]. Previously, we have shown that PLAGL2 zinc fingers six and seven are required for binding to the TRR in the *NCF2* intragenic region and, in conjunction with zinc finger three, are required for binding to the PLAG family consensus sequence (see Chapter 3). Classic C_2H_2 zinc fingers can also mediate protein-protein interaction and whereas multiple zinc

fingers are typically required to bind DNA, a single zinc finger can mediate protein-protein interactions [253]. In the current chapter, we identified a number of putative PLAGL2 interactors and, with the exception of $PC2_{434-784}$, all of these interactors contain some type of zinc finger domain. The enhanced complex formation observed for FHL3 and $CHD3_{1585-1966}$ when these proteins were co-translated with PLAGL2 suggests that correct tertiary structure at the zinc finger domains is essential for PLAGL2 complex formation with these proteins. Furthermore, mapping of the PLAGL2 domain to which $CHD3_{1585-1966}$ bound identified the N-terminal, zinc finger-containing domain as essential for complex formation between $CHD3_{1585-1966}$ and PLAGL2. In contrast, $PC2_{434-784}$, which does not contain a zinc finger domain and whose complex formation with PLAGL2 was not enhanced by co-translation, appeared to interact with both the N-terminal and C-terminal domains of PLAGL2. This model of protein-protein interaction with PLAGL2, mediated by zinc finger domains, has recently been supported, since Tip60-PLAGL2 interaction requires the zinc finger domain of Tip60 [238]. On the other hand, PLAGL2 interaction with Pirh2 is independent of zinc finger domain in Pirh2 [235].

Taken together, these data suggest that the PLAGL2 zinc fingers might mediate protein-protein interactions. As reported in this chapter, our preliminary data identified the zinc fingers of PLAGL2 required to mediate protein-protein interactions between PLAGL2 and the putative interactors identified in the yeast two-hybrid assay. While complex formation with FHL3 required zinc fingers two, three, four, and six of PLAGL2, complex formation with $CHD3_{1585-1966}$ required only zinc finger two; although, binding may also utilize zinc fingers three, four, and six. Both CHD3 and FHL3 contain zinc

finger domains. FHL3 has multiple LIM domains that mediate protein-protein interactions [254]. Proteins that contain multiple LIM domains, such as FHL3, often act as molecular bridges [255]. For example, LIM domain proteins often mediate cell signaling pathways, such as integrin signaling [256] and Protein Kinase C signaling [257]. Although the LIM protein PINCH mediates Nck2 interaction through recognition of a SH3 domain [258] and PLAGL2 contains multiple SH3 domains (MiniMotif Miner [259]), it is demonstrated here that FHL3 mediates PLAGL2 complex formation through zinc finger interactions. CHD3 contains a PHD/RING finger domain. Ring finger domains can mediate the assembly of mutli-protein complexes that control a multitude of cellular functions, such as ubiquitin ligation and protein degredation, signal transduction, immunoglobulin gene rearrangement, and DNA repair [260]. Although chromodomains, such as that found in CHD3, can recognize methylated lysine residues in protein-protein interactions [261], it is demonstrated here that $CHD3_{1585\text{-}1966}$ mediates PLAGL2 complex formation, at least in part, through zinc finger interactions. Finally, $PC2_{434\text{-}784}$ does not contain a zinc finger domain and was found to interact *in vitro* with both the N-terminal and C-terminal domains of PLAGL2, therefore it was not surprising to find that PLAGL2 zinc finger mutation did not significantly affect $PC2_{434\text{-}784}$ complex formation with PLAGL2.

Zinc finger mutation in PLAGL2 suggests that while zinc fingers six and seven are required for binding to the TRR DNA element (see Chapter 3), zinc finger six also mediates interaction with FHL3. Furthermore, zinc finger three is also required for binding to the PLAG consensus DNA element (see Chapter 3) and for FHL3 complex formation. While it seems confusing for the same zinc finger to mediate both DNA

binding and protein-protein complex formation, there is a precedent for transcription factor zinc finger bimodal control of regulatory regions [210]. Bimodal control suggests that complex formation at the regulatory region is initiated by a pioneer transcription factor that binds the DNA, followed by some sort of enzymatic machinery, and finally followed by a histone acetyltransferase. The classic bimodal control example is promoters regulated by nuclear hormone receptors [262]. Zinc finger mutational analysis with the homologous PLAG family member PLAGL1 (also known as Zac), demonstrates that while zinc fingers six and seven bind DNA elements [263], these same zinc fingers mediate PLAGL1 binding to the CH3 and KIX domains of p300 in a DNA-bound protein complex [264]. These data suggest a bimodular model for PLAGL2 in which zinc fingers six, seven, and three can mediate DNA-binding while zinc fingers two, three, four, and six can simultaneously mediate protein-protein interactions. Finally, it is likely that the zinc fingers of PLAGL2 mediate nuclear localization, since PLAGL2 lacks a nuclear localization signal found on the other PLAG family member [239]. Nevertheless, we have shown that PLAGL2 does localize to the nucleus when expressed in HEK293 cells.

From recent work and the data presented here, a general model of PLAGL2 regulation is emerging in which PLAGL2 protein-protein complex formation creates an environment of context dependent transcriptional regulation. However, there remains a great deal of work that must be done to tease out the fine intricacies of PLAGL2 transcription regulation at the intragenic region. Here we present three novel PLAGL2 binding proteins that all contain the capacity for complex formation and transcriptional regulation and likely mediate PLAGL2 transactivation at the *NCF2* intragenic region using distinct and overlapping strategies. Because of the transformining capacity of

PLAGL2 in acute myeloid leukemia [231] and the aberrant expression of putative PLAGL2 interactors FHL3 and CHD3 in acute myeloid leukemia [265, 266], decifering the mechanisms of protein-protein interaction and regulation of PLAGL2 transactivation may prove to have significant therapeutic value.

SUMMARY AND CONCLUSIONS

The innate immune system is highly conserved and is essential for defense against a wide array of bacterial, fungal, and viral pathogens [1]. Phagocytes are especially critical to the acute inflammatory response, due to their ability to phagocytose and destroy a variety of pathogens, as well as their importance to tissue remodeling and wound healing. These cells are also known as professional phagocytes and are comprised of neutrophils, monocytes, macrophages, and eosinophils. Phagocytes utilize an extraordinary array of oxygen-dependent and oxygen-independent microbicidal weapons to destroy and remove infectious agents [3]. Oxygen-dependent mechanisms involve the production of microbicidal reactive oxygen species (ROS) via NADPH oxidase activation [66], while oxygen-independent mechanisms include chemotaxis, phagocytosis, degranulation, and release of lytic enzymes and bactericidal peptides (reviewed in [3]).

As demonstrated in chronic granulomatous disease (CGD), the production of reactive oxygen species by the NADPH oxidase is essential to the microbicidal capacity of professional phagocytes [21]. Additionally, a growing body of evidence indicates that aberrant NADPH oxidase activity may also contribute to a host of chronic inflammatory pathologies [100]. Although research into transcriptional regulation of the NADPH oxidase components is still a nascent field, recent work with the activation-limiting component $p67^{phox}$ suggests that transcriptional regulation of *NCF2*, the gene coding for $p67^{phox}$, by TNF-α plays an important role in NADPH oxidase regulation. The recent characterization of a TNF-α responsive region (TRR) in the *NCF2* intragenic region showed that this region lacked recognizable putative binding elements for known

transcription factors and suggested that transcriptional regulation of this essential component of the oxidase may be regulated in a distinct and novel way [131]. Certainly, identification of the regulatory mechanisms behind the TNF-α responsive transcriptional regulation of *NCF2* would not only enhance basic understanding of NADPH oxidase regulation, but could also have significant therapeutic value.

To address this issue, we hypothesized that the TRR was regulated by transcription factor(s) responsible for transcriptional regulation of the *NCF2* intragenic region. Thus, the goal of the work described in Chapter 2 was to identify the factor(s) that bind the TRR in the *NCF2* intragenic region. Using a yeast one-hybrid screening approach, the zinc finger transcription factor PLAGL2 was identified as a putative TRR-binding factor. Gel shift analysis confirmed that PLAGL2 bound to the TRR *in vitro*, although with relatively low affinity when compared to the PLAG family consensus sequence. Using nuclear extracts, both native and SUMO1-modified endogenous PLAGL2 were confirmed to bind the TRR *in vitro*. *In vivo* binding of endogenous PLAGL2 was enhanced by treatment of cells with TNF-α, and knock-down of endogenous PLAGL2 interfered with the TNF-α-mediated activation of the NADPH oxidase by inhibiting transcriptional upregulation of *NCF2*. Since PLAGL2 transcription and translation do not appear to be responsive to TNF-α treatment, it is likely that TNF-α mediates PLAGL2 transcriptional activity via regulation of post-translational modifications. Indeed, PLAGL2 protein modifications were observed in both primary and tissue culture immune cells treated with TNF-α.

Other essential components of the NADPH oxidase are also transcriptionally responsive to TNF-α, suggesting a coordinated mechanism of transcriptional regulation

[134]. Because the *NCF2* TRR sequence does not contain the PLAG family consensus-binding site, in chapter three site directed mutation and gel shift analysis were used to identify the sequences within the *NCF2* TRR recognized and bound by PLAGL2. Although containing some deviations, a sequence with similarity to the core element of the PLAG family consensus family sequence was identified to which PLAGL2 bound. Mutation of conserved nucleotides with the PLAGL2-binding domain inhibited luciferase expression in reporter assays. Although zinc fingers six, seven, and three were identified as important for PLAGL2 recognition of the PLAG family consensus sequence, only zinc fingers six and seven appeared important for PLAGL2 recognition of the *NCF2* TRR. Comparison of the predicted sequence recognition pattern of zinc fingers six and seven with the binding sequence identified in the *NCF2* TRR further supported these nucleotides as essential to PLAGL2 DNA recognition and intragenic region binding.

Although PLAGL2 can independently bind the *NCF2* TRR *in vitro*, gel shift analysis with nuclear extracts resulted in a complex binding pattern, suggesting that other endogenous factors interact at the *NCF2* intragenic region. PLAGL2 bound to a specific and identifiable sequence in the *NCF2* TRR; however, binding was at a relatively low affinity compared to the PLAG family consensus sequence. Finally, TNF-α treatment enhanced the binding of endogenous PLAGL2 to the *NCF2* TRR *in vivo*; although, neither *PLAGL2* gene expression nor PLAGL2 protein expression appear to be modulated by TNF-α treatment. These data suggest that PLAGL2 binding and regulation of the *NCF2* intragenic region via the TRR may require context dependent protein-protein interactions. Therefore, the goal of chapter four was to identify putative PLAGL2 binding proteins using a yeast two-hybrid screen. From this assay, E2I, $PC2_{434-784}$, FHL3,

and $CHD3_{1585-1966}$ were identified as putative PLAGL2 interactors *in vivo*. $PC2_{434-784}$, FHL3, and $CHD3_{1585-1966}$ interaction with PLAGL2 was confirmed using *in vitro* and *in vivo* co-immunoprecipitation. PLAGL2, FHL3, and CHD3 all contain zinc finger domains. Correct and functional tertiary conformation often requires that zinc finger proteins are co-translated; therefore, it is not surprising that *in vitro* co-translation of PLAGL2 with FHL3 or $CHD3_{1585-1966}$ enhanced complex formation. Further mapping of complex formation between PLAGL2 and the putative interactors identified both unique and overlapping patterns of binding. As PC2 was the only non-zinc finger protein identified to interact with PLAGL2, it was not surprising that $PC2_{4343-784}$ binding appeared to require both PLAGL2 domains and was not zinc finger dependent. On the other hand, FHL3 and $CHD3_{1585-1966}$ were found to bind the PLAGL2 zinc finger domain. While $CHD3_{1585-1966}$ mainly interacted with PLAGL2 zinc finger two, FHL3 interacted with zinc fingers two, three, four, and six.

In summary, this report demonstrates a novel mechanism of NADPH oxidase regulation. Through regulation of the *NCF2* intragenic region at the TRR, PLAGL2 is now shown to regulate NADPH oxidase activity in response to TNF-α. Our characterization of PLAGL2 binding to the TRR and the identification of putative interacting proteins suggests a model in which *NCF2* transcription regulation by PLAGL2 in response to TNF-α treatment is dependent upon post-translational modifications and protein-protein interactions at the *NCF2* intragenic region (Figure 5.1). Altogether, these results further elucidate the mechanisms regulating the NADPH oxidase in response to TNF-α likely contributing to both acute and chronic pathologies.

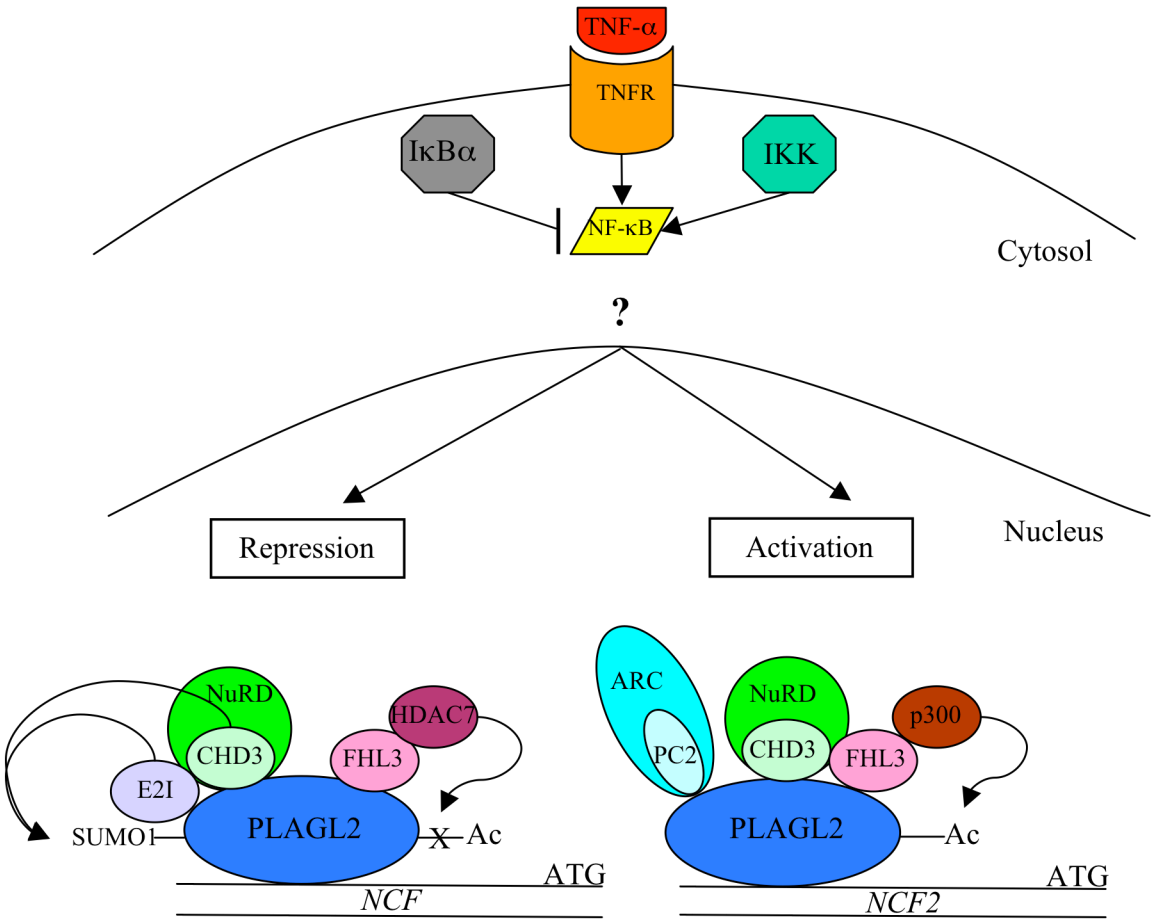

Figure 5.1: Theoretical model of PLAGL2 regulation at the intragenic region of *NCF2*. TNF-α signaling through the TNF-α receptor is transduced via NF-κB. At the intragenic region PLAGL2 transactivation is activated by acetylation and repressed by sumoylation. While E2I may repress by sumoylating PLAGL2 directly, CHD3 may act either as a repressor or enhancer as part of the NuRD complex. FHL3 likely acts as a bridge mediating deacetylation through HDAC7 or actylation via p300. Finally, PC2 likely acts as a transcriptional enhancer as part of the ARC complex.

FUTURE STUDIES

In this dissertation data have suggested a model in which PLAGL2 regulation of transcription is context dependent and relies on post-translational modifications and protein-protein mediated activity. Acetylation and sumoylation can mediate PLAGL2 transactivation and in chapter two TNF-α treatment resulted in post-translational modifications of PLAGL2. It would be interesting to further explore how TNF-α modifies PLAGL2 protein. This could be addressed a couple of ways. Development of post-translational modification specific antibodies such as antibodies to acetylated PLAGL2 could be used to monitor PLAGL2 modifications *in vivo* with TNF-α treatment. If specific antibodies to modified PLAGL2 could not be developed, immunoprecipitation of PLAGL2 from TNF-α treated cells could be analyzed for acetylated lysines, sumoylated lysines, and/or phosphorylated tryrosines or serines. Finally, physiological relevance could be established *in vivo* using the dominant negative UBC9 (E2I, in humans) expression vector to eliminate PLAGL2 sumoylation and to ascertain the effect on TNF-α mediated regulation of the NADPH oxidase.

In chapter three, PLAGL2 was shown to bind the *NCF2* TRR with slight sequence differences and significantly impaired affinity, however the characteristics of PLAGL2 binding were confirmed and specific. Since other NADPH oxidase components are transcriptionally regulated by TNF-α, it would be of interest to determine whether PLAGL2 mediates a coordinated transcriptional induction of multiple NADPH oxidase components. Careful analysis of the five prime untranslated regions (5'UTR) of *CYBB* and *NCF1* might identify sequences similar to that identified as the sequence to which

PLAGL2 binds in the *NCF2* TRR. Once identified, PLAGL2 binding could be confirmed *in vitro* and *in vivo* utilizing the same or similar methods as used to identify PLAGL2 binding and regulation of the *NCF2* intragenic region.

Chapter four presented preliminary data identifing three proteins as interacting with PLAGL2 both *in vivo* and *in vitro*, however the physiological relevance of these interactions remains to be determined. Therefore, it would be of great interest to establish the physiological effect of PLAGL2 interaction with full length PC2, FHL3, and CHD3. In context of the *NCF2* TRR, determining whether PC2, FHL3, and/or CHD3 act as binding partners to PLAGL2 at the intragenic region could be determined both *in vitro* and *in vivo*. EMSA analysis with *in vitro* translated protein could determine whether the proteins can bind the *NCF2* TRR in a complex or independently. Using nuclear extracts in EMSA analysis with antibodies specific to the PLAGL2 interacting proteins could resolve whether endogenous complexes bind the *NCF2* TRR. Finally, chromatin immunoprecipitation with antibodies specific to the PLAGL2 interacting proteins could determine whether the proteins bind the *NCF2* TRR *in vivo*. Of particular interest, would be determining whether PLAGL2 complex formation effects *NCF2* transcription. Although exogenous PLAGL2 expression has proved detrimental in TNF-α luciferase-reporter assays, exogenous expression of the PLAGL2 interacting proteins might indicate whether these interactors act as enhancers or repressors of *NCF2* transactivation in a system that contains endogenous PLAGL2.

Finally, PLAGL2 is a ubiquitously expressed oncogenic transcription factor. Emerging evidence suggests that damage mediated by reactive oxygen species produced by the NADPH oxidase is a contributing factor to the development of cancer. Trying to

bridge the gap between innate immune cell activation and neoplastic transformation presents a challenge with a great deal of potential reward. PLAGL2 is presented here as a TNF-α responsive transcription factor and in other contexts has been identified as a regulator of growth cycle, differentiation, and metabolism; however very little is known about the function of endogenous PLAGL2. Therefore, it would be of great interest to determine what roles PLAGL2 might play endogenously. PLAGL2 knock-out in mice is highly lethal, however some mice survive. It might be interesting to treat these mice with TNF-α and determine by microarray changes in inflammatory gene expression. PLAGL2 DNA binding could be universally assayed by performing a ChIP-on-chip in which chromatin immunoprecipitated from cells treated with TNF-α with antibody specific to PLAGL2 is then subjected to microarray analysis.

These studies would not only enhance understanding of the mechanisms of NADPH oxidase activation, but PLAGL2 could act as a model transcription factor to identify bridges between innate immune cell activation and malignancy. Significant therapeutic value may emerge from a greater understanding of the mechanisms by which PLAGL2 regulates the NADPH oxidase and application of this knowledge to other regulatory regions that may be controlled by PLAGL2 might contribute significantly to the understanding of pathologies associated with chronic immune activation.

REFERENCES

1. Janeway, C.A., Jr. and R. Medzhitov, *Innate immune recognition.* Annu Rev Immunol, 2002. **20**: p. 197-216.
2. Moulder, J.W., *Interaction of chlamydiae and host cells in vitro.* Microbiol Rev, 1991. **55**(1): p. 143-90.
3. Witko-Sarsat, V., et al., *Neutrophils: molecules, functions and pathophysiological aspects.* Lab Invest, 2000. **80**(5): p. 617-53.
4. Akgul, C. and S.W. Edwards, *Regulation of neutrophil apoptosis via death receptors.* Cell Mol Life Sci, 2003. **60**(11): p. 2402-8.
5. Stark, M.A., et al., *Phagocytosis of apoptotic neutrophils regulates granulopoiesis via IL-23 and IL-17.* Immunity, 2005. **22**(3): p. 285-94.
6. van Zandbergen, G., W. Solbach, and T. Laskay, *Apoptosis driven infection.* Autoimmunity, 2007. **40**(4): p. 349-52.
7. Brinkmann, V. and A. Zychlinsky, *Beneficial suicide: why neutrophils die to make NETs.* Nat Rev Microbiol, 2007. **5**(8): p. 577-82.
8. Borregaard, N., O.E. Sorensen, and K. Theilgaard-Monch, *Neutrophil granules: a library of innate immunity proteins.* Trends Immunol, 2007. **28**(8): p. 340-5.
9. Lee, W.L., R.E. Harrison, and S. Grinstein, *Phagocytosis by neutrophils.* Microbes Infect, 2003. **5**(14): p. 1299-306.
10. Volkman, A. and J.L. Gowans, *The Origin of Macrophages from Bone Marrow in the Rat.* Br J Exp Pathol, 1965. **46**: p. 62-70.
11. Gordon, S. and P.R. Taylor, *Monocyte and macrophage heterogeneity.* Nat Rev Immunol, 2005. **5**(12): p. 953-64.
12. Van Furth, R., M.C. Diesselhoff-den Dulk, and H. Mattie, *Quantitative study on the production and kinetics of mononuclear phagocytes during an acute inflammatory reaction.* J Exp Med, 1973. **138**(6): p. 1314-30.
13. Quinn, J.M. and M.T. Gillespie, *Modulation of osteoclast formation.* Biochem Biophys Res Commun, 2005. **328**(3): p. 739-45.
14. McCusker, K. and J. Hoidal, *Characterization of scavenger receptor activity in resident human lung macrophages.* Exp Lung Res, 1989. **15**(4): p. 651-61.
15. Palecanda, A., et al., *Role of the scavenger receptor MARCO in alveolar macrophage binding of unopsonized environmental particles.* J Exp Med, 1999. **189**(9): p. 1497-506.
16. Taylor, P.R., et al., *The beta-glucan receptor, dectin-1, is predominantly expressed on the surface of cells of the monocyte/macrophage and neutrophil lineages.* J Immunol, 2002. **169**(7): p. 3876-82.
17. Surh, C.D. and J. Sprent, *T-cell apoptosis detected in situ during positive and negative selection in the thymus.* Nature, 1994. **372**(6501): p. 100-3.
18. Weston, B., et al., *Severe congenital neutropenia: clinical effects and neutrophil function during treatment with granulocyte colony-stimulating factor.* J Lab Clin Med, 1991. **117**(4): p. 282-90.
19. Barbosa, M.D., et al., *Identification of the homologous beige and Chediak-Higashi syndrome genes.* Nature, 1996. **382**(6588): p. 262-5.

20. Di Rocco, M., et al., *Neutropenia and impaired neutrophil function in glycogenosis type Ib.* J Inherit Metab Dis, 1984. **7**(4): p. 151-4.
21. Heyworth, P.G., A.R. Cross, and J.T. Curnutte, *Chronic granulomatous disease.* Curr Opin Immunol, 2003. **15**(5): p. 578-84.
22. Andrews, T. and K.E. Sullivan, *Infections in patients with inherited defects in phagocytic function.* Clin Microbiol Rev, 2003. **16**(4): p. 597-621.
23. Curnutte, J.T. and B.M. Babior, *Chronic granulomatous disease.* Adv Hum Genet, 1987. **16**: p. 229-97.
24. Morgenstern, D.E., et al., *Absence of respiratory burst in X-linked chronic granulomatous disease mice leads to abnormalities in both host defense and inflammatory response to Aspergillus fumigatus.* J Exp Med, 1997. **185**(2): p. 207-18.
25. Hampton, M.B., et al., *Oxidant-mediated phosphatidylserine exposure and macrophage uptake of activated neutrophils: possible impairment in chronic granulomatous disease.* J Leukoc Biol, 2002. **71**(5): p. 775-81.
26. Brown, J.R., et al., *Diminished production of anti-inflammatory mediators during neutrophil apoptosis and macrophage phagocytosis in chronic granulomatous disease (CGD).* J Leukoc Biol, 2003. **73**(5): p. 591-9.
27. Schappi, M.G., et al., *Colitis in chronic granulomatous disease.* Arch Dis Child, 2001. **84**(2): p. 147-51.
28. Imhof, B.A. and M. Aurrand-Lions, *Adhesion mechanisms regulating the migration of monocytes.* Nat Rev Immunol, 2004. **4**(6): p. 432-44.
29. Katschke, K.J., Jr., et al., *Differential expression of chemokine receptors on peripheral blood, synovial fluid, and synovial tissue monocytes/macrophages in rheumatoid arthritis.* Arthritis Rheum, 2001. **44**(5): p. 1022-32.
30. Vey, E., D. Burger, and J.M. Dayer, *Expression and cleavage of tumor necrosis factor-alpha and tumor necrosis factor receptors by human monocytic cell lines upon direct contact with stimulated T cells.* Eur J Immunol, 1996. **26**(10): p. 2404-9.
31. Vey, E., J.M. Dayer, and D. Burger, *Direct contact with stimulated T cells induces the expression of IL-1beta and IL-1 receptor antagonist in human monocytes. Involvement of serine/threonine phosphatases in differential regulation.* Cytokine, 1997. **9**(7): p. 480-7.
32. Szekanecz, Z. and A.E. Koch, *Chemokines and angiogenesis.* Curr Opin Rheumatol, 2001. **13**(3): p. 202-8.
33. Veale, D.J. and U. Fearon, *Inhibition of angiogenic pathways in rheumatoid arthritis: potential for therapeutic targeting.* Best Pract Res Clin Rheumatol, 2006. **20**(5): p. 941-7.
34. Szekanecz, Z., L. Gaspar, and A.E. Koch, *Angiogenesis in rheumatoid arthritis.* Front Biosci, 2005. **10**: p. 1739-53.
35. Sato, K. and H. Takayanagi, *Osteoclasts, rheumatoid arthritis, and osteoimmunology.* Curr Opin Rheumatol, 2006. **18**(4): p. 419-26.
36. Robinson, J., et al., *Activation of neutrophil reactive-oxidant production by synovial fluid from patients with inflammatory joint disease. Soluble and*

insoluble immunoglobulin aggregates activate different pathways in primed and unprimed cells. Biochem J, 1992. **286 (Pt 2)**: p. 345-51.

37. Edwards, S.W. and M.B. Hallett, *Seeing the wood for the trees: the forgotten role of neutrophils in rheumatoid arthritis.* Immunol Today, 1997. **18**(7): p. 320-4.
38. Kowanko, I.C., E.J. Bates, and A. Ferrante, *Neutrophil-mediated cartilage injury in vitro is enhanced by tumour necrosis factor alpha.* Rheumatol Int, 1990. **10**(2): p. 85-90.
39. Olofsson, P., et al., *Positional identification of Ncf1 as a gene that regulates arthritis severity in rats.* Nat Genet, 2003. **33**(1): p. 25-32.
40. Cowburn, A.S., et al., *Role of PI3-kinase-dependent Bad phosphorylation and altered transcription in cytokine-mediated neutrophil survival.* Blood, 2002. **100**(7): p. 2607-16.
41. Dunican, A.L., et al., *TNFalpha-induced suppression of PMN apoptosis is mediated through interleukin-8 production.* Shock, 2000. **14**(3): p. 284-8; discussion 288-9.
42. Cowburn, A.S., et al., *The survival effect of TNF-alpha in human neutrophils is mediated via NF-kappa B-dependent IL-8 release.* Eur J Immunol, 2004. **34**(6): p. 1733-43.
43. van Lent, P.L., et al., *Uptake of apoptotic leukocytes by synovial lining macrophages inhibits immune complex-mediated arthritis.* J Leukoc Biol, 2001. **70**(5): p. 708-14.
44. Bosma, K.J. and J.F. Lewis, *Emerging therapies for treatment of acute lung injury and acute respiratory distress syndrome.* Expert Opin Emerg Drugs, 2007. **12**(3): p. 461-77.
45. Britschgi, M. and T. Wyss-Coray, *Systemic and acquired immune responses in Alzheimer's disease.* Int Rev Neurobiol, 2007. **82**: p. 205-33.
46. Griffiths, M., J.W. Neal, and P. Gasque, *Innate immunity and protective neuroinflammation: new emphasis on the role of neuroimmune regulatory proteins.* Int Rev Neurobiol, 2007. **82**: p. 29-55.
47. Rajala, M.W. and P.E. Scherer, *Minireview: The adipocyte--at the crossroads of energy homeostasis, inflammation, and atherosclerosis.* Endocrinology, 2003. **144**(9): p. 3765-73.
48. Weisberg, S.P., et al., *Obesity is associated with macrophage accumulation in adipose tissue.* J Clin Invest, 2003. **112**(12): p. 1796-808.
49. Xu, H., et al., *Chronic inflammation in fat plays a crucial role in the development of obesity-related insulin resistance.* J Clin Invest, 2003. **112**(12): p. 1821-30.
50. Lehrke, M., et al., *An inflammatory cascade leading to hyperresistinemia in humans.* PLoS Med, 2004. **1**(2): p. e45.
51. Brandacher, G., et al., *Chronic immune activation underlies morbid obesity: is IDO a key player?* Curr Drug Metab, 2007. **8**(3): p. 289-95.
52. Stern, N. and Y. Marcus, *Perivascular fat: innocent bystander or active player in vascular disease?* J Cardiometab Syndr, 2006. **1**(2): p. 115-20.
53. Liang, C.P., et al., *The macrophage at the crossroads of insulin resistance and atherosclerosis.* Circ Res, 2007. **100**(11): p. 1546-55.

54. Cathcart, M.K., D.W. Morel, and G.M. Chisolm, 3rd, *Monocytes and neutrophils oxidize low density lipoprotein making it cytotoxic.* J Leukoc Biol, 1985. **38**(2): p. 341-50.
55. Aviram, M., et al., *Activation of NADPH oxidase required for macrophage-mediated oxidation of low-density lipoprotein.* Metabolism, 1996. **45**(9): p. 1069-79.
56. Chisolm, G.M. and D. Steinberg, *The oxidative modification hypothesis of atherogenesis: an overview.* Free Radic Biol Med, 2000. **28**(12): p. 1815-26.
57. Csernok, E., A. Muller, and W.L. Gross, *Immunopathology of ANCA-associated vasculitis.* Intern Med, 1999. **38**(10): p. 759-65.
58. Walport, M.J., *Lupus, DNase and defective disposal of cellular debris.* Nat Genet, 2000. **25**(2): p. 135-6.
59. Patel, V.A., et al., *The affirmative response of the innate immune system to apoptotic cells.* Autoimmunity, 2007. **40**(4): p. 274-80.
60. Knowles, H.J. and A.L. Harris, *Macrophages and the hypoxic tumour microenvironment.* Front Biosci, 2007. **12**: p. 4298-314.
61. Sica, A., et al., *Targeting tumour-associated macrophages.* Expert Opin Ther Targets, 2007. **11**(9): p. 1219-29.
62. Porta, C., et al., *Tumor promotion by tumor-associated macrophages.* Adv Exp Med Biol, 2007. **604**: p. 67-86.
63. Reiter, I., B. Krammer, and G. Schwamberger, *Cutting edge: differential effect of apoptotic versus necrotic tumor cells on macrophage antitumor activities.* J Immunol, 1999. **163**(4): p. 1730-2.
64. Djaldetti, M., et al., *Phagocytosis--the mighty weapon of the silent warriors.* Microsc Res Tech, 2002. **57**(6): p. 421-31.
65. Chanock, S.J., et al., *The respiratory burst oxidase.* J Biol Chem, 1994. **269**(40): p. 24519-22.
66. Roos, D., R. van Bruggen, and C. Meischl, *Oxidative killing of microbes by neutrophils.* Microbes Infect, 2003. **5**(14): p. 1307-15.
67. Babior, B.M., *NADPH oxidase.* Curr Opin Immunol, 2004. **16**(1): p. 42-7.
68. Segal, A.W. and O.T. Jones, *Novel cytochrome b system in phagocytic vacuoles of human granulocytes.* Nature, 1978. **276**(5687): p. 515-7.
69. Parkos, C.A., et al., *Primary structure and unique expression of the 22-kilodalton light chain of human neutrophil cytochrome b.* Proc Natl Acad Sci U S A, 1988. **85**(10): p. 3319-23.
70. DeLeo, F.R., et al., *Processing and maturation of flavocytochrome b558 include incorporation of heme as a prerequisite for heterodimer assembly.* J Biol Chem, 2000. **275**(18): p. 13986-93.
71. Rotrosen, D., et al., *Cytochrome b558: the flavin-binding component of the phagocyte NADPH oxidase.* Science, 1992. **256**(5062): p. 1459-62.
72. Sumimoto, H., et al., *Cytochrome b558, a component of the phagocyte NADPH oxidase, is a flavoprotein.* Biochem Biophys Res Commun, 1992. **186**(3): p. 1368-75.
73. Bokoch, G.M. and B.A. Diebold, *Current molecular models for NADPH oxidase regulation by Rac GTPase.* Blood, 2002. **100**(8): p. 2692-6.

74. Price, M.O., et al., *Rac activation induces NADPH oxidase activity in transgenic COSphox cells, and the level of superoxide production is exchange factor-dependent.* J Biol Chem, 2002. **277**(21): p. 19220-8.
75. Knaus, U.G., et al., *Regulation of human leukocyte p21-activated kinases through G protein--coupled receptors.* Science, 1995. **269**(5221): p. 221-3.
76. Diekmann, D., et al., *Rac GTPase interacts with GAPs and target proteins through multiple effector sites.* Embo J, 1995. **14**(21): p. 5297-305.
77. Heyworth, P.G., et al., *Rac translocates independently of the neutrophil NADPH oxidase components p47phox and p67phox. Evidence for its interaction with flavocytochrome b558.* J Biol Chem, 1994. **269**(49): p. 30749-52.
78. Lapouge, K., et al., *Architecture of the p40-p47-p67phox complex in the resting state of the NADPH oxidase. A central role for p67phox.* J Biol Chem, 2002. **277**(12): p. 10121-8.
79. Iyer, S.S., et al., *Evidence for a readily dissociable complex of p47phox and p67phox in cytosol of unstimulated human neutrophils.* J Biol Chem, 1994. **269**(35): p. 22405-11.
80. Quinn, M.T. and K.A. Gauss, *Structure and regulation of the neutrophil respiratory burst oxidase: comparison with nonphagocyte oxidases.* J Leukoc Biol, 2004. **76**(4): p. 760-81.
81. Cross, A.R. and J.T. Curnutte, *The cytosolic activating factors p47phox and p67phox have distinct roles in the regulation of electron flow in NADPH oxidase.* J Biol Chem, 1995. **270**(12): p. 6543-8.
82. Nakamura, R., et al., *The PC motif: a novel and evolutionarily conserved sequence involved in interaction between p40phox and p67phox, SH3 domain-containing cytosolic factors of the phagocyte NADPH oxidase.* Eur J Biochem, 1998. **251**(3): p. 583-9.
83. Kuribayashi, F., et al., *The adaptor protein p40(phox) as a positive regulator of the superoxide-producing phagocyte oxidase.* Embo J, 2002. **21**(23): p. 6312-20.
84. Smith, R.M., et al., *The cytosolic subunit p67phox contains an NADPH-binding site that participates in catalysis by the leukocyte NADPH oxidase.* J Clin Invest, 1996. **98**(4): p. 977-83.
85. de Mendez, I., et al., *Role of p67-phox SH3 domains in assembly of the NADPH oxidase system.* J Biol Chem, 1994. **269**(23): p. 16326-32.
86. Paclet, M.H., et al., *P67-phox-mediated NADPH oxidase assembly: imaging of cytochrome b558 liposomes by atomic force microscopy.* Biochemistry, 2000. **39**(31): p. 9302-10.
87. Clark, R.A., *Activation of the neutrophil respiratory burst oxidase.* J Infect Dis, 1999. **179 Suppl 2**: p. S309-17.
88. Foubert, T.R., et al., *Structural changes are induced in human neutrophil cytochrome b by NADPH oxidase activators, LDS, SDS, and arachidonate: intermolecular resonance energy transfer between trisulfopyrenyl-wheat germ agglutinin and cytochrome b(558).* Biochim Biophys Acta, 2002. **1567**(1-2): p. 221-31.
89. Groemping, Y., et al., *Molecular basis of phosphorylation-induced activation of the NADPH oxidase.* Cell, 2003. **113**(3): p. 343-55.

90. Uhlinger, D.J., K.L. Taylor, and J.D. Lambeth, *p67-phox enhances the binding of p47-phox to the human neutrophil respiratory burst oxidase complex.* J Biol Chem, 1994. **269**(35): p. 22095-8.
91. De Leo, F.R., et al., *Assembly of the human neutrophil NADPH oxidase involves binding of p67phox and flavocytochrome b to a common functional domain in p47phox.* J Biol Chem, 1996. **271**(29): p. 17013-20.
92. Koga, H., et al., *Tetratricopeptide repeat (TPR) motifs of p67(phox) participate in interaction with the small GTPase Rac and activation of the phagocyte NADPH oxidase.* J Biol Chem, 1999. **274**(35): p. 25051-60.
93. Rinckel, L.A., et al., *Rac1 disrupts p67phox/p40phox binding: a novel role for Rac in NADPH oxidase activation.* Biochem Biophys Res Commun, 1999. **263**(1): p. 118-22.
94. Vaissiere, C., V. Le Cabec, and I. Maridonneau-Parini, *NADPH oxidase is functionally assembled in specific granules during activation of human neutrophils.* J Leukoc Biol, 1999. **65**(5): p. 629-34.
95. de Boer, M., et al., *Cytochrome b558-negative, autosomal recessive chronic granulomatous disease: two new mutations in the cytochrome b558 light chain of the NADPH oxidase (p22-phox).* Am J Hum Genet, 1992. **51**(5): p. 1127-35.
96. Segal, A.W., et al., *Stimulated neutrophils from patients with autosomal recessive chronic granulomatous disease fail to phosphorylate a Mr-44,000 protein.* Nature, 1985. **316**(6028): p. 547-9.
97. Volpp, B.D., W.M. Nauseef, and R.A. Clark, *Two cytosolic neutrophil oxidase components absent in autosomal chronic granulomatous disease.* Science, 1988. **242**(4883): p. 1295-7.
98. Schneider, S.D., et al., *Adenovirus-mediated gene transfer into monocyte-derived macrophages of patients with X-linked chronic granulomatous disease: ex vivo correction of deficient respiratory burst.* Gene Ther, 1997. **4**(6): p. 524-32.
99. Jendrossek, V., et al., *Improvement of superoxide production in monocytes from patients with chronic granulomatous disease by recombinant cytokines.* Blood, 1993. **81**(8): p. 2131-6.
100. Quinn, M.T., M.C. Ammons, and F.R. Deleo, *The expanding role of NADPH oxidases in health and disease: no longer just agents of death and destruction.* Clin Sci (Lond), 2006. **111**(1): p. 1-20.
101. Rojkind, M., et al., *Role of hydrogen peroxide and oxidative stress in healing responses.* Cell Mol Life Sci, 2002. **59**(11): p. 1872-91.
102. Chen, E.Y., et al., *Age-related decreases in GTP-cyclohydrolase-I immunoreactive neurons in the monkey and human substantia nigra.* J Comp Neurol, 2000. **426**(4): p. 534-48.
103. Jobsis, Q., et al., *Hydrogen peroxide and nitric oxide in exhaled air of children with cystic fibrosis during antibiotic treatment.* Eur Respir J, 2000. **16**(1): p. 95-100.
104. Tamiya, S., et al., *Induction of matrix metalloproteinases 2 and 9 following stress to the lens.* Exp Eye Res, 2000. **71**(6): p. 591-7.

105. Sato, K., et al., *In vivo lipid-derived free radical formation by NADPH oxidase in acute lung injury induced by lipopolysaccharide: a model for ARDS.* Faseb J, 2002. **16**(13): p. 1713-20.
106. Wu, D.C., et al., *NADPH oxidase mediates oxidative stress in the 1-methyl-4-phenyl-1,2,3,6-tetrahydropyridine model of Parkinson's disease.* Proc Natl Acad Sci U S A, 2003. **100**(10): p. 6145-50.
107. Ridker, P.M., et al., *Elevation of tumor necrosis factor-alpha and increased risk of recurrent coronary events after myocardial infarction.* Circulation, 2000. **101**(18): p. 2149-53.
108. Omar, B.A., et al., *Ischemic preconditioning is not mediated by free radicals in the isolated rabbit heart.* Free Radic Biol Med, 1991. **11**(5): p. 517-20.
109. Tesfamariam, B. and R.A. Cohen, *Role of superoxide anion and endothelium in vasoconstrictor action of prostaglandin endoperoxide.* Am J Physiol, 1992. **262**(6 Pt 2): p. H1915-9.
110. Kumar, K.V. and U.N. Das, *Are free radicals involved in the pathobiology of human essential hypertension?* Free Radic Res Commun, 1993. **19**(1): p. 59-66.
111. Rey, F.E., et al., *Novel competitive inhibitor of NAD(P)H oxidase assembly attenuates vascular O(2)(-) and systolic blood pressure in mice.* Circ Res, 2001. **89**(5): p. 408-14.
112. Bokoch, G.M. and U.G. Knaus, *NADPH oxidases: not just for leukocytes anymore!* Trends Biochem Sci, 2003. **28**(9): p. 502-8.
113. Arnold, R.S., et al., *Hydrogen peroxide mediates the cell growth and transformation caused by the mitogenic oxidase Nox1.* Proc Natl Acad Sci U S A, 2001. **98**(10): p. 5550-5.
114. Warzocha, K., et al., *Genetic polymorphisms in the tumor necrosis factor locus influence non-Hodgkin's lymphoma outcome.* Blood, 1998. **91**(10): p. 3574-81.
115. Cathcart, M.K., *Regulation of superoxide anion production by NADPH oxidase in monocytes/macrophages: contributions to atherosclerosis.* Arterioscler Thromb Vasc Biol, 2004. **24**(1): p. 23-8.
116. Maranchie, J.K. and Y. Zhan, *Nox4 is critical for hypoxia-inducible factor 2-alpha transcriptional activity in von Hippel-Lindau-deficient renal cell carcinoma.* Cancer Res, 2005. **65**(20): p. 9190-3.
117. Wendt, M.C., et al., *Differential effects of diabetes on the expression of the gp91phox homologues nox1 and nox4.* Free Radic Biol Med, 2005. **39**(3): p. 381-91.
118. Sorescu, D., et al., *Superoxide production and expression of nox family proteins in human atherosclerosis.* Circulation, 2002. **105**(12): p. 1429-35.
119. Guzik, T.J., et al., *Coronary artery superoxide production and nox isoform expression in human coronary artery disease.* Arterioscler Thromb Vasc Biol, 2006. **26**(2): p. 333-9.
120. Eid, N.S., R.E. Kravath, and K.W. Lanks, *Heat-shock protein synthesis by human polymorphonuclear cells.* J Exp Med, 1987. **165**(5): p. 1448-52.
121. Jack, R.M. and D.T. Fearon, *Selective synthesis of mRNA and proteins by human peripheral blood neutrophils.* J Immunol, 1988. **140**(12): p. 4286-93.

122. Newburger, P.E., Q. Dai, and C. Whitney, *In vitro regulation of human phagocyte cytochrome b heavy and light chain gene expression by bacterial lipopolysaccharide and recombinant human cytokines.* J Biol Chem, 1991. **266**(24): p. 16171-7.
123. Newburger, P.E., et al., *Induction of phagocyte cytochrome b heavy chain gene expression by interferon gamma.* Proc Natl Acad Sci U S A, 1988. **85**(14): p. 5215-9.
124. Dubravec, D.B., et al., *Circulating human peripheral blood granulocytes synthesize and secrete tumor necrosis factor alpha.* Proc Natl Acad Sci U S A, 1990. **87**(17): p. 6758-61.
125. Zhang, X., et al., *Gene expression in mature neutrophils: early responses to inflammatory stimuli.* J Leukoc Biol, 2004. **75**(2): p. 358-72.
126. Kobayashi, S.D., et al., *Global changes in gene expression by human polymorphonuclear leukocytes during receptor-mediated phagocytosis: cell fate is regulated at the level of gene expression.* Proc Natl Acad Sci U S A, 2002. **99**(10): p. 6901-6.
127. Subrahmanyam, Y.V., et al., *RNA expression patterns change dramatically in human neutrophils exposed to bacteria.* Blood, 2001. **97**(8): p. 2457-68.
128. Hua, J., et al., *Evaluation of the expression of NADPH oxidase components during maturation of HL-60 cells to neutrophil lineage.* J Leukoc Biol, 2000. **68**(2): p. 216-24.
129. Skalnik, D.G., *Transcriptional mechanisms regulating myeloid-specific genes.* Gene, 2002. **284**(1-2): p. 1-21.
130. Eklund, E.A. and R. Kakar, *Recruitment of CREB-binding protein by PU.1, IFN-regulatory factor-1, and the IFN consensus sequence-binding protein is necessary for IFN-gamma-induced p67phox and gp91phox expression.* J Immunol, 1999. **163**(11): p. 6095-105.
131. Gauss, K.A., et al., *Identification of a novel tumor necrosis factor alpha-responsive region in the NCF2 promoter.* J Leukoc Biol, 2005. **77**(2): p. 267-78.
132. Marden, C.M., et al., *Differentiation-dependent up-regulation of p47(phox) gene transcription is associated with changes in PU.1 phosphorylation and increased binding affinity.* Biochem Biophys Res Commun, 2003. **305**(1): p. 193-202.
133. Moriwaki, K., et al., *Interferon-gamma enhances superoxide production in human mesangial cells via the JAK-STAT pathway.* Kidney Int, 2006. **70**(4): p. 788-93.
134. Gauss, K.A., et al., *Role of NF-kappaB in transcriptional regulation of the phagocyte NADPH oxidase by tumor necrosis factor-alpha.* J Leukoc Biol, 2007. **82**(3): p. 729-41.
135. Voo, K.S. and D.G. Skalnik, *Elf-1 and PU.1 induce expression of gp91(phox) via a promoter element mutated in a subset of chronic granulomatous disease patients.* Blood, 1999. **93**(10): p. 3512-20.
136. Eklund, E.A. and D.G. Skalnik, *Characterization of a gp91-phox promoter element that is required for interferon gamma-induced transcription.* J Biol Chem, 1995. **270**(14): p. 8267-73.
137. Li, S.L., et al., *PU.1 is essential for p47(phox) promoter activity in myeloid cells.* J Biol Chem, 1997. **272**(28): p. 17802-9.

138. Li, S.L., et al., *Multiple PU.1 sites cooperate in the regulation of p40(phox) transcription during granulocytic differentiation of myeloid cells.* Blood, 2002. **99**(12): p. 4578-87.
139. Li, S.L., et al., *Transcriptional regulation of the p67phox gene: role of AP-1 in concert with myeloid-specific transcription factors.* J Biol Chem, 2001. **276**(42): p. 39368-78.
140. Gauss, K.A., P.L. Bunger, and M.T. Quinn, *AP-1 is essential for p67(phox) promoter activity.* J Leukoc Biol, 2002. **71**(1): p. 163-72.
141. Skalnik, D.G., E.C. Strauss, and S.H. Orkin, *CCAAT displacement protein as a repressor of the myelomonocytic-specific gp91-phox gene promoter.* J Biol Chem, 1991. **266**(25): p. 16736-44.
142. Hawkins, S.M., T. Kohwi-Shigematsu, and D.G. Skalnik, *The matrix attachment region-binding protein SATB1 interacts with multiple elements within the gp91phox promoter and is down-regulated during myeloid differentiation.* J Biol Chem, 2001. **276**(48): p. 44472-80.
143. Lu, Y., et al., *HoxA10 represses gene transcription in undifferentiated myeloid cells by interaction with histone deacetylase 2.* J Biol Chem, 2003. **278**(48): p. 47792-802.
144. Lindsey, S., et al., *HoxA10 represses transcription of the gene encoding p67phox in phagocytic cells.* J Immunol, 2005. **175**(8): p. 5269-79.
145. Bei, L., et al., *Identification of a HoxA10 activation domain necessary for transcription of the gene encoding beta3 integrin during myeloid differentiation.* J Biol Chem, 2007. **282**(23): p. 16846-59.
146. Hensley, K., et al., *Reactive oxygen species, cell signaling, and cell injury.* Free Radic Biol Med, 2000. **28**(10): p. 1456-62.
147. Gabbita, S.P., et al., *Redox regulatory mechanisms of cellular signal transduction.* Arch Biochem Biophys, 2000. **376**(1): p. 1-13.
148. Banerjee, R., et al., *Cutting edge: infection by the agent of human granulocytic ehrlichiosis prevents the respiratory burst by down-regulating gp91phox.* J Immunol, 2000. **164**(8): p. 3946-9.
149. Carlyon, J.A., et al., *Repression of rac2 mRNA expression by Anaplasma phagocytophila is essential to the inhibition of superoxide production and bacterial proliferation.* J Immunol, 2002. **169**(12): p. 7009-18.
150. Allen, J.F., *Superoxide as an obligatory, catalytic intermediate in photosynthetic reduction of oxygen by adrenaline and dopamine.* Antioxid Redox Signal, 2003. **5**(1): p. 7-14.
151. Malech, H.L., T.R. Bauer, Jr., and D.D. Hickstein, *Prospects for gene therapy of neutrophil defects.* Semin Hematol, 1997. **34**(4): p. 355-61.
152. Lekstrom-Himes, J.A., et al., *Neutrophil-specific granule deficiency results from a novel mutation with loss of function of the transcription factor CCAAT/enhancer binding protein epsilon.* J Exp Med, 1999. **189**(11): p. 1847-52.
153. *A candidate gene for familial Mediterranean fever. The French FMF Consortium.* Nat Genet, 1997. **17**(1): p. 25-31.

154. Chabrashvili, T., et al., *Expression and cellular localization of classic NADPH oxidase subunits in the spontaneously hypertensive rat kidney.* Hypertension, 2002. **39**(2): p. 269-74.
155. Szocs, K., et al., *Upregulation of Nox-based NAD(P)H oxidases in restenosis after carotid injury.* Arterioscler Thromb Vasc Biol, 2002. **22**(1): p. 21-7.
156. McColl, A., et al., *Effects of glucocorticoids on apoptosis and clearance of apoptotic cells.* ScientificWorldJournal, 2007. **7**: p. 1165-81.
157. Baud, V. and M. Karin, *Signal transduction by tumor necrosis factor and its relatives.* Trends Cell Biol, 2001. **11**(9): p. 372-7.
158. Swain, S.D., T.T. Rohn, and M.T. Quinn, *Neutrophil priming in host defense: role of oxidants as priming agents.* Antioxid Redox Signal, 2002. **4**(1): p. 69-83.
159. Chang, H.Y. and X. Yang, *Proteases for cell suicide: functions and regulation of caspases.* Microbiol Mol Biol Rev, 2000. **64**(4): p. 821-46.
160. Tracey, K.J. and A. Cerami, *Tumor necrosis factor: an updated review of its biology.* Crit Care Med, 1993. **21**(10 Suppl): p. S415-22.
161. Vazquez-Torres, A. and F.C. Fang, *Oxygen-dependent anti-Salmonella activity of macrophages.* Trends Microbiol, 2001. **9**(1): p. 29-33.
162. Bouwmeester, T., et al., *A physical and functional map of the human TNF-alpha/NF-kappa B signal transduction pathway.* Nat Cell Biol, 2004. **6**(2): p. 97-105.
163. Green, S.P., et al., *Expression of p47-phox and p67-phox proteins in murine bone marrow-derived macrophages: enhancement by lipopolysaccharide and tumor necrosis factor alpha but not colony stimulating factor 1.* J Leukoc Biol, 1994. **55**(4): p. 530-5.
164. Gupta, J.W., et al., *Induction of expression of genes encoding components of the respiratory burst oxidase during differentiation of human myeloid cell lines induced by tumor necrosis factor and gamma-interferon.* Cancer Res, 1992. **52**(9): p. 2530-7.
165. Leto, T.L., et al., *Cloning of a 67-kD neutrophil oxidase factor with similarity to a noncatalytic region of p60c-src.* Science, 1990. **248**(4956): p. 727-30.
166. Kenney, R.T., et al., *Characterization of the p67phox gene: genomic organization and restriction fragment length polymorphism analysis for prenatal diagnosis in chronic granulomatous disease.* Blood, 1993. **82**(12): p. 3739-44.
167. Gauss, K.A., et al., *Variants of the 5'-untranslated region of human NCF2: expression and translational efficiency.* Gene, 2006. **366**(1): p. 169-79.
168. Wisdom, R., *AP-1: one switch for many signals.* Exp Cell Res, 1999. **253**(1): p. 180-5.
169. Barnes, P.J. and M. Karin, *Nuclear factor-kappaB: a pivotal transcription factor in chronic inflammatory diseases.* N Engl J Med, 1997. **336**(15): p. 1066-71.
170. Karin, M., Z. Liu, and E. Zandi, *AP-1 function and regulation.* Curr Opin Cell Biol, 1997. **9**(2): p. 240-6.
171. Monaco, C. and E. Paleolog, *Nuclear factor kappaB: a potential therapeutic target in atherosclerosis and thrombosis.* Cardiovasc Res, 2004. **61**(4): p. 671-82.
172. Clark, R.A. and A.J. Valente, *Nuclear factor kappa B activation by NADPH oxidases.* Mech Ageing Dev, 2004. **125**(10-11): p. 799-810.

173. Wajant, H., K. Pfizenmaier, and P. Scheurich, *Tumor necrosis factor signaling.* Cell Death Differ, 2003. **10**(1): p. 45-65.
174. Anrather, J., G. Racchumi, and C. Iadecola, *NF-kappaB regulates phagocytic NADPH oxidase by inducing the expression of gp91phox.* J Biol Chem, 2006. **281**(9): p. 5657-67.
175. Cross, A.R. and A.W. Segal, *The NADPH oxidase of professional phagocytes--prototype of the NOX electron transport chain systems.* Biochim Biophys Acta, 2004. **1657**(1): p. 1-22.
176. Bokoch, G.M., *Regulation of innate immunity by Rho GTPases.* Trends Cell Biol, 2005. **15**(3): p. 163-71.
177. Mizrahi, A., et al., *Assembly of the phagocyte NADPH oxidase complex: chimeric constructs derived from the cytosolic components as tools for exploring structure-function relationships.* J Leukoc Biol, 2006. **79**(5): p. 881-95.
178. Dang, P.M., J.L. Johnson, and B.M. Babior, *Binding of nicotinamide adenine dinucleotide phosphate to the tetratricopeptide repeat domains at the N-terminus of p67PHOX, a subunit of the leukocyte nicotinamide adenine dinucleotide phosphate oxidase.* Biochemistry, 2000. **39**(11): p. 3069-75.
179. Nisimoto, Y., et al., *The p67(phox) activation domain regulates electron flow from NADPH to flavin in flavocytochrome b(558).* J Biol Chem, 1999. **274**(33): p. 22999-3005.
180. Gorzalczany, Y., et al., *A prenylated p67phox-Rac1 chimera elicits NADPH-dependent superoxide production by phagocyte membranes in the absence of an activator and of p47phox: conversion of a pagan NADPH oxidase to monotheism.* J Biol Chem, 2002. **277**(21): p. 18605-10.
181. Bylund, J., D. Goldblatt, and D.P. Speert, *Chronic granulomatous disease: from genetic defect to clinical presentation.* Adv Exp Med Biol, 2005. **568**: p. 67-87.
182. Koshkin, V., O. Lotan, and E. Pick, *The cytosolic component p47(phox) is not a sine qua non participant in the activation of NADPH oxidase but is required for optimal superoxide production.* J Biol Chem, 1996. **271**(48): p. 30326-9.
183. Freeman, J.L. and J.D. Lambeth, *NADPH oxidase activity is independent of p47phox in vitro.* J Biol Chem, 1996. **271**(37): p. 22578-82.
184. Levy, R. and H.L. Malech, *Effect of 1,25-dihydroxyvitamin D3, lipopolysaccharide, or lipoteichoic acid on the expression of NADPH oxidase components in cultured human monocytes.* J Immunol, 1991. **147**(9): p. 3066-71.
185. Cassatella, M.A., et al., *Interferon-gamma transcriptionally modulates the expression of the genes for the high affinity IgG-Fc receptor and the 47-kDa cytosolic component of NADPH oxidase in human polymorphonuclear leukocytes.* J Biol Chem, 1991. **266**(33): p. 22079-82.
186. Graziani-Bowering, G.M., J.M. Graham, and L.G. Filion, *A quick, easy and inexpensive method for the isolation of human peripheral blood monocytes.* J Immunol Methods, 1997. **207**(2): p. 157-68.
187. Jutila, M.A., et al., *Characterization of a functionally important and evolutionarily well-conserved epitope mapped to the short consensus repeats of E-selectin and L-selectin.* J Exp Med, 1992. **175**(6): p. 1565-73.

188. Kas, K., et al., *Transcriptional activation capacity of the novel PLAG family of zinc finger proteins.* J Biol Chem, 1998. **273**(36): p. 23026-32.
189. Furukawa, T., et al., *Involvement of PLAGL2 in activation of iron deficient- and hypoxia-induced gene expression in mouse cell lines.* Oncogene, 2001. **20**(34): p. 4718-27.
190. Yang, M.C., et al., *Pleiomorphic adenoma gene-like-2, a zinc finger protein, transactivates the surfactant protein-C promoter.* Am J Respir Cell Mol Biol, 2005. **32**(1): p. 35-43.
191. Hensen, K., et al., *The tumorigenic diversity of the three PLAG family members is associated with different DNA binding capacities.* Cancer Res, 2002. **62**(5): p. 1510-7.
192. Voz, M.L., et al., *PLAG1, the main translocation target in pleomorphic adenoma of the salivary glands, is a positive regulator of IGF-II.* Cancer Res, 2000. **60**(1): p. 106-13.
193. Zheng, G. and Y.C. Yang, *Sumoylation and acetylation play opposite roles in the transactivation of PLAG1 and PLAGL2.* J Biol Chem, 2005. **280**(49): p. 40773-81.
194. Summerton, J. and D. Weller, *Morpholino antisense oligomers: design, preparation, and properties.* Antisense Nucleic Acid Drug Dev, 1997. **7**(3): p. 187-95.
195. Baugh, J.A. and R. Bucala, *Mechanisms for modulating TNF alpha in immune and inflammatory disease.* Curr Opin Drug Discov Devel, 2001. **4**(5): p. 635-50.
196. Beutler, B., *TNF, immunity and inflammatory disease: lessons of the past decade.* J Investig Med, 1995. **43**(3): p. 227-35.
197. Hilgarth, R.S. and K.D. Sarge, *Detection of sumoylated proteins.* Methods Mol Biol, 2005. **301**: p. 329-38.
198. Weissmann, G., *Pathogenesis of rheumatoid arthritis.* J Clin Rheumatol, 2004. **10**(3 Suppl): p. S26-31.
199. Liu, H. and R.M. Pope, *Phagocytes: mechanisms of inflammation and tissue destruction.* Rheum Dis Clin North Am, 2004. **30**(1): p. 19-39, v.
200. Landrette, S.F., et al., *Plag1 and Plagl2 are oncogenes that induce acute myeloid leukemia in cooperation with Cbfb-MYH11.* Blood, 2005. **105**(7): p. 2900-7.
201. Abdollahi, A., *LOT1 (ZAC1/PLAGL1) and its family members: mechanisms and functions.* J Cell Physiol, 2007. **210**(1): p. 16-25.
202. Muller, S., M.J. Matunis, and A. Dejean, *Conjugation with the ubiquitin-related modifier SUMO-1 regulates the partitioning of PML within the nucleus.* Embo J, 1998. **17**(1): p. 61-70.
203. Yang, S.H., et al., *Dynamic interplay of the SUMO and ERK pathways in regulating Elk-1 transcriptional activity.* Mol Cell, 2003. **12**(1): p. 63-74.
204. Van Dyck, F., et al., *Repression of the Transactivating Capacity of the Oncoprotein PLAG1 by SUMOylation.* J Biol Chem, 2004. **279**(34): p. 36121-31.
205. Kim, J., et al., *Transcriptional activity of CCAAT/enhancer-binding proteins is controlled by a conserved inhibitory domain that is a target for sumoylation.* J Biol Chem, 2002. **277**(41): p. 38037-44.

206. Desterro, J.M., M.S. Rodriguez, and R.T. Hay, *SUMO-1 modification of IkappaBalpha inhibits NF-kappaB activation.* Mol Cell, 1998. **2**(2): p. 233-9.
207. Hietakangas, V., et al., *Phosphorylation of serine 303 is a prerequisite for the stress-inducible SUMO modification of heat shock factor 1.* Mol Cell Biol, 2003. **23**(8): p. 2953-68.
208. Comerford, K.M., et al., *Small ubiquitin-related modifier-1 modification mediates resolution of CREB-dependent responses to hypoxia.* Proc Natl Acad Sci U S A, 2003. **100**(3): p. 986-91.
209. Van Dyck, F., et al., *PLAG1, the prototype of the PLAG gene family: versatility in tumour development (review).* Int J Oncol, 2007. **30**(4): p. 765-74.
210. Urnov, F.D., *A feel for the template: zinc finger protein transcription factors and chromatin.* Biochem Cell Biol, 2002. **80**(3): p. 321-33.
211. Cook, W.J., et al., *Mutations in the zinc-finger region of the yeast regulatory protein ADR1 affect both DNA binding and transcriptional activation.* J Biol Chem, 1994. **269**(12): p. 9374-9.
212. Freyd, G., S.K. Kim, and H.R. Horvitz, *Novel cysteine-rich motif and homeodomain in the product of the Caenorhabditis elegans cell lineage gene lin-11.* Nature, 1990. **344**(6269): p. 876-9.
213. Gamsjaeger, R., et al., *Sticky fingers: zinc-fingers as protein-recognition motifs.* Trends Biochem Sci, 2007. **32**(2): p. 63-70.
214. Mackay, J.P. and M. Crossley, *Zinc fingers are sticking together.* Trends Biochem Sci, 1998. **23**(1): p. 1-4.
215. Shastry, B.S., *Transcription factor IIIA (TFIIIA) in the second decade.* J Cell Sci, 1996. **109 (Pt 3)**: p. 535-9.
216. Wolfe, S.A., L. Nekludova, and C.O. Pabo, *DNA recognition by Cys2His2 zinc finger proteins.* Annu Rev Biophys Biomol Struct, 2000. **29**: p. 183-212.
217. Bowers, P.M., L.E. Schaufler, and R.E. Klevit, *A folding transition and novel zinc finger accessory domain in the transcription factor ADR1.* Nat Struct Biol, 1999. **6**(5): p. 478-85.
218. Elrod-Erickson, M. and C.O. Pabo, *Binding studies with mutants of Zif268. Contribution of individual side chains to binding affinity and specificity in the Zif268 zinc finger-DNA complex.* J Biol Chem, 1999. **274**(27): p. 19281-5.
219. Pavletich, N.P. and C.O. Pabo, *Zinc finger-DNA recognition: crystal structure of a Zif268-DNA complex at 2.1 A.* Science, 1991. **252**(5007): p. 809-17.
220. Corbi, N., et al., *Synthesis of a new zinc finger peptide; comparison of its 'code' deduced and 'CASTing' derived binding sites.* FEBS Lett, 1997. **417**(1): p. 71-4.
221. Choo, Y. and A. Klug, *A role in DNA binding for the linker sequences of the first three zinc fingers of TFIIIA.* Nucleic Acids Res, 1993. **21**(15): p. 3341-6.
222. Foster, M.P., et al., *Domain packing and dynamics in the DNA complex of the N-terminal zinc fingers of TFIIIA.* Nat Struct Biol, 1997. **4**(8): p. 605-8.
223. Aurora, R. and G.D. Rose, *Helix capping.* Protein Sci, 1998. **7**(1): p. 21-38.
224. Varrault, A., et al., *hZAC encodes a zinc finger protein with antiproliferative properties and maps to a chromosomal region frequently lost in cancer.* Proc Natl Acad Sci U S A, 1998. **95**(15): p. 8835-40.

225. Guo, Y., et al., *PLAGL2 translocation and SP-C promoter activity--a cellular response of lung cells to hypoxia.* Biochem Biophys Res Commun, 2007. **360**(3): p. 659-65.
226. Mizutani, A., et al., *A zinc-finger protein, PLAGL2, induces the expression of a proapoptotic protein Nip3, leading to cellular apoptosis.* J Biol Chem, 2002. **277**(18): p. 15851-8.
227. Ammons, M.C., et al., *Binding of pleomorphic adenoma gene-like 2 to the tumor necrosis factor (TNF)-alpha-responsive region of the NCF2 promoter regulates p67(phox) expression and NADPH oxidase activity.* J Biol Chem, 2007. **282**(24): p. 17941-52.
228. Ikeda, K. and K. Kawakami, *DNA binding through distinct domains of zinc-finger-homeodomain protein AREB6 has different effects on gene transcription.* Eur J Biochem, 1995. **233**(1): p. 73-82.
229. Morita, E.H., et al., *Implications of the zinc-finger motif found in the DNA-binding domain of the human XPA protein.* Genes Cells, 1996. **1**(5): p. 437-42.
230. Nagaoka, M. and Y. Sugiura, *Distinct phosphate backbone contacts revealed by some mutant peptides of zinc finger protein Spl: effect of protein-induced bending on DNA recognition.* Biochemistry, 1996. **35**(26): p. 8761-8.
231. Castilla, L.H., et al., *Identification of genes that synergize with Cbfb-MYH11 in the pathogenesis of acute myeloid leukemia.* Proc Natl Acad Sci U S A, 2004. **101**(14): p. 4924-9.
232. Pendeville, H., et al., *Cloning and embryonic expression of zebrafish PLAG genes.* Gene Expr Patterns, 2006. **6**(3): p. 267-76.
233. Van Dyck, F., et al., *Loss of the PlagL2 Transcription Factor Affects Lacteal Uptake of Chylomicrons.* Cell Metab, 2007. **6**(5): p. 406-13.
234. Alam, S., et al., *Members of the Plag gene family are expressed in complementary and overlapping regions in the developing murine nervous system.* Dev Dyn, 2005. **234**(3): p. 772-82.
235. Zheng, G., J. Ning, and Y.C. Yang, *PLAGL2 controls the stability of Pirh2, an E3 ubiquitin ligase for p53.* Biochem Biophys Res Commun, 2007. **364**(2): p. 344-50.
236. Gaughan, L., et al., *Tip60 and histone deacetylase 1 regulate androgen receptor activity through changes to the acetylation status of the receptor.* J Biol Chem, 2002. **277**(29): p. 25904-13.
237. Xiao, H., et al., *Tip60 is a co-repressor for STAT3.* J Biol Chem, 2003. **278**(13): p. 11197-204.
238. Ning, J., G. Zheng, and Y.C. Yang, *Tip60 modulates PLAGL2-mediated transactivation by acetylation.* J Cell Biochem, 2007.
239. Braem, C.V., et al., *Identification of a karyopherin alpha 2 recognition site in PLAG1, which functions as a nuclear localization signal.* J Biol Chem, 2002. **277**(22): p. 19673-8.
240. Zheng, G. and Y.C. Yang, *ZNF76, a novel transcriptional repressor targeting TATA-binding protein, is modulated by sumoylation.* J Biol Chem, 2004. **279**(41): p. 42410-21.

241. Girdwood, D., et al., *P300 transcriptional repression is mediated by SUMO modification.* Mol Cell, 2003. **11**(4): p. 1043-54.
242. Jaenicke, R. and R. Rudolph, *Refolding and association of oligomeric proteins.* Methods Enzymol, 1986. **131**: p. 218-50.
243. Minty, A., et al., *Covalent modification of p73alpha by SUMO-1. Two-hybrid screening with p73 identifies novel SUMO-1-interacting proteins and a SUMO-1 interaction motif.* J Biol Chem, 2000. **275**(46): p. 36316-23.
244. Winn, P.J., et al., *Structural and electrostatic properties of ubiquitination and related pathways.* Front Biosci, 2007. **12**: p. 3419-30.
245. Ishikawa, H., et al., *TRIM11 binds to and destabilizes a key component of the activator-mediated cofactor complex (ARC105) through the ubiquitin-proteasome system.* FEBS Lett, 2006. **580**(20): p. 4784-92.
246. Fimia, G.M., D. De Cesare, and P. Sassone-Corsi, *A family of LIM-only transcriptional coactivators: tissue-specific expression and selective activation of CREB and CREM.* Mol Cell Biol, 2000. **20**(22): p. 8613-22.
247. Takahashi, K., C. Matsumoto, and C. Ra, *FHL3 negatively regulates human high-affinity IgE receptor beta-chain gene expression by acting as a transcriptional co-repressor of MZF-1.* Biochem J, 2005. **386**(Pt 1): p. 191-200.
248. Takahashi, K., et al., *Molecular mechanisms for transcriptional regulation of human high-affinity IgE receptor beta-chain gene induced by GM-CSF.* J Immunol, 2006. **177**(7): p. 4605-11.
249. Bowen, N.J., et al., *Mi-2/NuRD: multiple complexes for many purposes.* Biochim Biophys Acta, 2004. **1677**(1-3): p. 52-7.
250. Saether, T., et al., *The chromatin remodeling factor Mi-2alpha acts as a novel co-activator for human c-Myb.* J Biol Chem, 2007. **282**(19): p. 13994-4005.
251. Sapountzi, V., I.R. Logan, and C.N. Robson, *Cellular functions of TIP60.* Int J Biochem Cell Biol, 2006. **38**(9): p. 1496-509.
252. Col, E., et al., *HIV-1 Tat targets Tip60 to impair the apoptotic cell response to genotoxic stresses.* Embo J, 2005. **24**(14): p. 2634-45.
253. Matthews, J.M. and M. Sunde, *Zinc fingers--folds for many occasions.* IUBMB Life, 2002. **54**(6): p. 351-5.
254. Brown, S., et al., *Role of LIM domains in mediating signaling protein interactions.* IUBMB Life, 2001. **51**(6): p. 359-64.
255. Kadrmas, J.L. and M.C. Beckerle, *The LIM domain: from the cytoskeleton to the nucleus.* Nat Rev Mol Cell Biol, 2004. **5**(11): p. 920-31.
256. Tu, Y., F. Li, and C. Wu, *Nck-2, a novel Src homology2/3-containing adaptor protein that interacts with the LIM-only protein PINCH and components of growth factor receptor kinase-signaling pathways.* Mol Biol Cell, 1998. **9**(12): p. 3367-82.
257. Mochly-Rosen, D., *Localization of protein kinases by anchoring proteins: a theme in signal transduction.* Science, 1995. **268**(5208): p. 247-51.
258. Vaynberg, J., et al., *Structure of an ultraweak protein-protein complex and its crucial role in regulation of cell morphology and motility.* Mol Cell, 2005. **17**(4): p. 513-23.

259. Balla, S., et al., *Minimotif Miner: a tool for investigating protein function.* Nat Methods, 2006. **3**(3): p. 175-7.
260. Saurin, A.J., et al., *Does this have a familiar RING?* Trends Biochem Sci, 1996. **21**(6): p. 208-14.
261. Seet, B.T., et al., *Reading protein modifications with interaction domains.* Nat Rev Mol Cell Biol, 2006. **7**(7): p. 473-83.
262. Urnov, F.D. and A.P. Wolffe, *A necessary good: nuclear hormone receptors and their chromatin templates.* Mol Endocrinol, 2001. **15**(1): p. 1-16.
263. Hoffmann, A., et al., *Transcriptional activities of the zinc finger protein Zac are differentially controlled by DNA binding.* Mol Cell Biol, 2003. **23**(3): p. 988-1003.
264. Hoffmann, A., T. Barz, and D. Spengler, *Multitasking C2H2 zinc fingers link Zac DNA binding to coordinated regulation of p300-histone acetyltransferase activity.* Mol Cell Biol, 2006. **26**(14): p. 5544-57.
265. Morgan, M.J. and S.A. Whawell, *The structure of the human LIM protein ACT gene and its expression in tumor cell lines.* Biochem Biophys Res Commun, 2000. **273**(2): p. 776-83.
266. Camos, M., et al., *Gene expression profiling of acute myeloid leukemia with translocation t(8;16)(p11;p13) and MYST3-CREBBP rearrangement reveals a distinctive signature with a specific pattern of HOX gene expression.* Cancer Res, 2006. **66**(14): p. 6947-54.